9-10-2018 9:00 AM

Spraying Slurries: Impact of Slurry Properties on Spray Characteristics and Agglomerate Formation in Fluidized Beds

Joshua Idowu
The University of Western Ontario

Supervisor
Briens, Cedric
The University of Western Ontario Co-Supervisor
Pjontek, Dominic
The University of Western Ontario

Graduate Program in Chemical and Biochemical Engineering
A thesis submitted in partial fulfillment of the requirements for the degree in Master of Engineering Science

Abstract

Fluid Coking™ is a process that upgrades Alberta's heavy oil. The recycle stream in the process contains unwanted fines which could affect the interaction between the liquid feed and the bed particles and the tendency to form agglomerates. Agglomeration leads to lower product yields and vessel damage.

The impacts of slurry solids on spray stability and angle were measured in open air while the impacts on agglomerate stability and liquid distribution were studied in a fluidized bed. Particle properties were varied to understand the impact of the solids on agglomerates.

In open air, it was observed that the presence of solids had a negligible impact on spray behavior. Within the fluidized bed, changing the concentration of injected solids produced significant effect on agglomerate stability and liquid distribution.

By changing the properties of the slurry fines, it was determined that the injection of solids resulted in a filler effect within the agglomerates: the fines strengthened the agglomerates.

Keywords

Fluidized bed, slurry injection, formation and breakage of agglomerates, liquid distribution, agglomerate stability, filler effect, Fluid Coking™.

Acknowledgments

I would like to thank my supervisors, Dr. Cedric Briens and Dr. Dominic Pjontek for providing this opportunity and for their continual guidance and advice that has enabled me to successfully complete this project

I am grateful to Syncrude for the financial support that made this research possible and Jennifer McMillan for providing guidance and industrial advice for my research project.

Special thanks go to Francisco Sanchez, Thomas Johnston, Cody Ruthman and Jake for all the technical assistance that was provided with regards to my equipment and research experiments. I am also grateful to my friends at ICFAR: Yohann, Tim, Aaron, Erfan, Cher, Connie, Mohammed and everyone who has helped me during my program.

I am most grateful to my parents and siblings and to the Haig family who have provided priceless support for me during my time at Western University. I am also, grateful to Demi and Nadia for their words of advice and inspiration.

Finally, I am especially grateful for wonderful friends like Hillary, Nick, Lexi, Laura, Charles, John Wayne, Caitie, Nigel, Carlos and Hanesa who provided, encouragement, assistance and support when it was needed.

Table of Contents

List of Tables

List of Figures

List of Symbols

d_{aggl}: Agglomerate diameter (μm)

d_{psm}: Sauter-mean diameter (μm)

$m_{<600}$: Bed mass after recovery of macro-agglomerates (g)

m_{bed}: Initial bed mass (g)

m_d: Mass of dye (g)

m_{GA}: Mass of Gum Arabic (g)

m_{macro}: Mass of macro-agglomerates (g)

m_{micro,R_i}: mass of micro-agglomerates in a size cut sample (g)

m_p: mass of fine particles (g)

m_{sand} : mass of washed and dried sand particles (g)

$m_{micro,i}$: Total mass of agglomerates in the bed for each size cut (g)

F_L: Liquid mass flux in ($g/s/mm^2$)

Fs_L: Slurry mass flux in ($g/s/mm^2$)

GLR: Gas-liquid ratio

P_A: Picture frame area (m^2)

P_{ATO}: Atomization pressure (psig)

P_{BTK}: Mixing tank pressure (psig)

P_{PM}: Pre-mixer pressure (psig)

Q_{SL}: Slurry volumetric flux in ($cm^3/s/mm^2$)

S_A: Spray area, (m^2)

V_{gd}: Fluidization velocity during drying (m/s)

V_{gi}: Fluidization velocity during injection (m/s)

x_f: Weight fraction of fines in sample

x_{bed}: Weight fraction of fines in bed

Θ: Spray angle (degrees)

φ: Volumetric fraction of slurry

λ_c: Characteristic wavelength (nm)

Chapter 1

1 Introduction

In a Fluid Coking™ system, a fraction of the product is recycled back into the reactor to improve the yield of valuable liquid products. Because the recycle stream comes from a scrubber located downstream of the coker reactor, it contains fine coke and clay particles. The work and research presented in this thesis investigates the effects of these fines on open-air spray characteristics and liquid distribution within a fluidized bed.

1.1 Fluid Coking™

1.1.1 General Description and Background

According to Alberta Energy, Alberta`s oil sands have the third largest oil reserves in the world and as of 2016, production of bitumen was at least 2.5 million barrels per day (Alberta Energy Regulator 2018). According to Natural Resources Canada, the oil and gas industry produces up to 77% of Canada`s total energy production (NRCan 2016). This oil and gas industry have been a huge investor in the Canadian economy contributing over $13 billion to the country`s revenue with over 228,000 jobs supported/ created by the oil sands industry in Alberta (Canadian Association of Petroleum Producers (CAPP) 2017). The oil sands are thus a proven source of economic growth for Canada. The oil sands reserve available in Alberta produces heavy grade oil which is much more viscous and heavier than conventional crude oil. Due to these characteristics, heavy oil is difficult to transport by conventional methods and cannot be processed in regular refineries (Nares et al. 2007)

Heavy oil from the oil sands can, however, be upgraded to synthetic crude oil. The first stage of the upgrading process separates the heavy oil to different fractions of lighter oil and residue that are easier to convert to useful end products. This is done using both vacuum and atmospheric distillation processes. The upgrading process will then have two more stages; primary upgrading and secondary upgrading. Primary upgrading involves the conversion of residue from the vacuum distillation process to produce lighter oil fractions. Fluid Coking™ is one of the several methods of primary upgrading which is currently being employed by ExxonMobil and Syncrude Canada. Other systems for primary upgrading include delayed coking, flexi-coking, thermal and catalytic cracking, and other hydroconversion processes (Gray 2015). The products then go through secondary upgrading processes such as hydrotreating or hydrocracking before being sent to the refineries (Gray 2015).

Fluid Coking™ is a continuous process that is used to convert vacuum residue by thermally cracking the hydrocarbons to produce lighter products such as naphtha, gas oil and reactor gas with coke as a by-product (Paul Kamienski 2009, Gray 2015). A schematic diagram of the Fluid Coking™ process is shown in **Figure 1.1**. The reactor unit consists of three main sections: the scrubber, the reactor and the burner. The vacuum residue (feed) stream is split and fed into both the scrubber and the reactor. The feed injection is done using gas-liquid spray nozzles. In the reactor, the vacuum residue is thermally cracked to produce coke and product vapors; coking occurs on the surface of the particles at 510 to 550 °C (Gray 2015). The vacuum residue introduced into the scrubber contacts the product vapors and gets heated up. In the scrubber, the lighter feed components vaporize and the heavier components in the product vapors condense. In

addition, particles escaping from the reactor cyclones with the product vapors are captured by the liquid. Stream 1 in the **Figure 1.1** is the recycle stream that contains the solid particles. The reactor vessel also has a stripping section, at the bottom, where the coke flowing from the reactor zone is stripped using steam to remove hydrocarbon vapors. The resulting cold coke is conveyed to a burner where it is burnt and heated up to 630 degrees Celsius (Gray 2015), and a fraction is then returned to the reactor to provide heat for the continuous coking process.

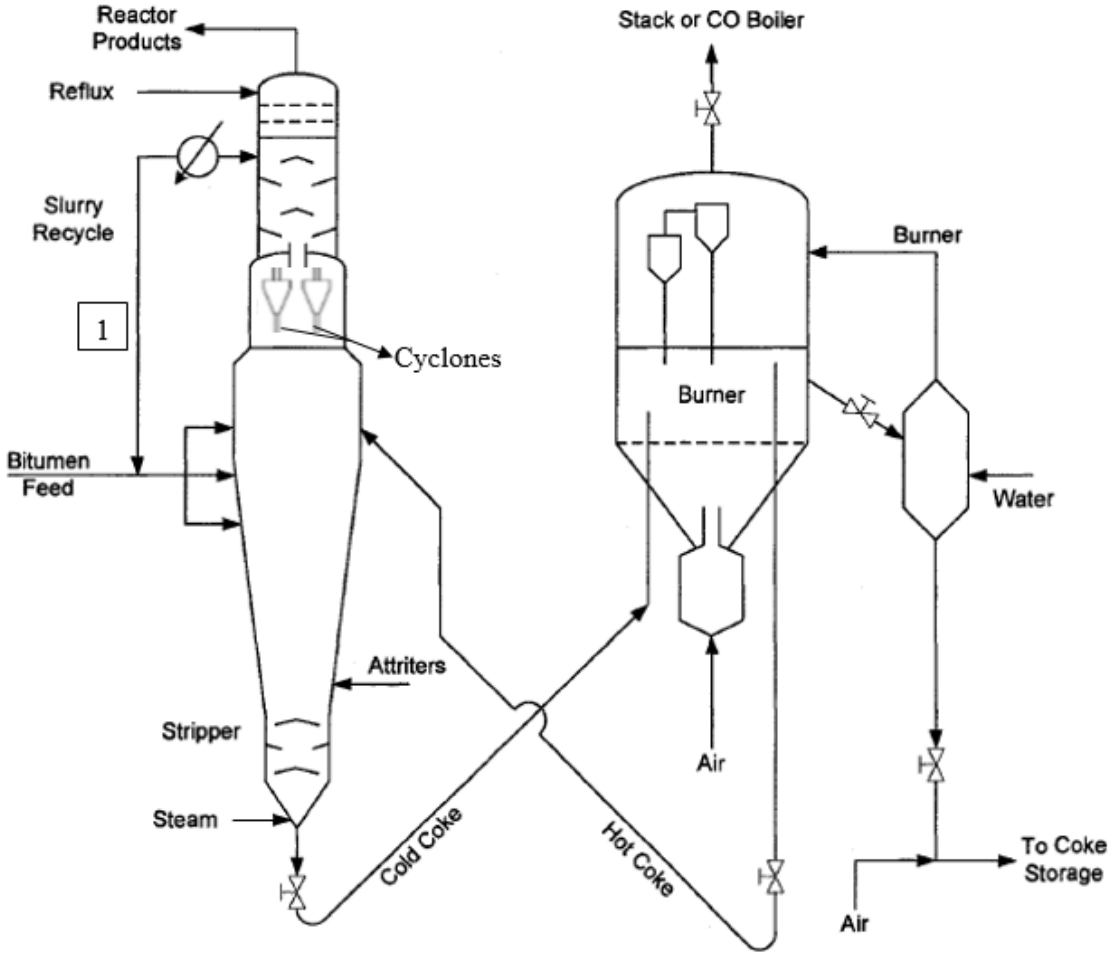

Figure 1.1: Schematic diagram of a Fluid Coker™ (Adapted from (House 2008))

As a continuous system, Fluid Coking™ is very useful in heavy oil upgrading, however, the biggest problems encountered with this technology is the agglomeration of coke particles and production of sulfur and metallic oxides which are environmentally undesirable (Bi et al. 2007, Nares et al. 2007).

1.1.2 Sources of recycled solid particles

In the Fluid Coker™, product vapors flow from the reactor to the scrubber through parallel cyclones as shown in **Figure 1.1**. Particles escaping the cyclones, enter the scrubber and contaminate the recycle stream that is fed to the reactor spray nozzles (McDonald and Rhys 1959).

There are different sources for these solid particles. The products from the cyclone consist mostly of vapor products, with some liquid and fine coke particles (Jankovic 2005). Another important note is that, over time, cyclone fouling leads to lower cyclone efficiency, resulting in more and possibly larger particles entering the scrubber. Also, the liquid fed to the scrubber could react prematurely, resulting in coke formation in the scrubber (Subudhi 2006). There could also be other types of fine particles being injected into the reactor based on the feed composition. Some of these solids could include, but are not limited to, clay particles, silica sand, and trace metals with an average particle size of about 10 μm (Wangen et al. 2007). It is important for this work to establish the effect of injecting fine particles on liquid distribution in the reactor bed and agglomeration of bed coke particles.

1.2 Spray Behavior

1.2.1 Spray Performance and Characterization

A good understanding of the spray behavior is necessary to optimize the mixing process in a fluidized bed. The spray behavior affects the formation and breakage of agglomerates by impacting the heat and mass transfer processes in the bed (House 2008). The liquid distribution in the bed depends on the spray performance, i.e. the size of the liquid droplets, the liquid-solid contact in the bed and the flowrate of particles entrained within the spray region. Any impact of particles present in the liquid on spray performance in the reactor bed can be detected indirectly by characterizing the spray properties such as the spray stability, angle and length.

The spray stability depends on the amplitude and frequency of spray fluctuations. Many studies have been conducted to understand the effects of pulsations on the spray nozzle performance. Ariyapadi (2004) compared stable and unstable sprays and found that stable sprays produce a stream of fine droplets due to uniform atomization while the droplets in pulsating sprays were likely to coalesce with each other producing larger final droplets. Hulet et al. (2003) observed that more stable sprays are likely to increase the amount of fluidized bed particles entrained in the spray. In most cases, a non-pulsating spray is considered optimal for reactor operations as it reduces the production of liquid-solid agglomerates (Briens et al. 2011). However, Leach et al. (2013) have shown that imposing spray pulsations with specific frequencies could lead to better liquid spreading in the fluidized bed, minimizing the formation of agglomerates. Important factors that affect the spray stability include but are not limited to nozzle internal configuration, atomization flowrate and pre-mixer configuration. However, current industrial practice is

to minimize spray fluctuations that occur “naturally” as they are usually associated with poor spray performance.

The spray angle affects the efficiency of fluidized bed processes as it provides information on the solid’s entrainment in the spray jet. Ariyapadi (2004) showed that the flowrate of entrained solids in the spray jet is proportional to the spray angle. Prior work has shown that the spray angle is mainly affected by the nozzle configuration, the atomization gas flowrate and liquid properties (Portoghese 2007).

The spray penetration into the bed determines where the liquid-solids contact occurs in the bed. Also, understanding the jet penetration in a system is useful in identifying the boundaries to avoid erosion of the vessel internals (Berruti et al. 2009). Bruhns and Werther (2005) found out that doubling the atomization gas flowrate resulted in a longer spray jet cavity but the mean droplet size was halved. The authors also noticed that when the spray angle increased, the jet length was reduced as there was a wider distribution of the liquid feed (Bruhns and Werther 2005). The jet length has also been observed to be affected by the nozzle geometry, the injection velocity and the density of the atomization gas (Ariyapadi 2004).

1.2.2 Impact of sprays in FCC

An FCC (Fluid Catalytic Cracking) unit converts heavy oil through catalytic and thermal cracking processes. The gas oil feed is cracked to lighter products such as distillate, gasoline and olefins while producing coke as by-product. Unlike Fluid Coking^{TM}, FCC makes use of a porous catalyst which must be constantly regenerated by burning off the coke residue forming on the catalysts. Studies have shown that the injection parameters: injection velocity, injection angle, jet length and droplet size significantly affect the

mixing hydrodynamics, heat transfer, feed vaporization and reaction product yields in the FCC risers (Chang et al. 2001). In the FCC riser, the temperature of the reactivated catalyst is usually higher than the boiling point of the feed, hence the vaporization rate is usually dependent on the heat transfer rate into the feed droplets. Quick vaporization of the feed is important because, direct contact between fed liquid and catalyst particles leads to coke formation and growth of agglomerates (Mirgain et al. 2000). Hence being able to control the droplet size and vaporization time is essential to limiting the formation and growth of agglomerates in the reactor. Also, the produced coke could damage the catalyst active sites, block the pores and hence reduce yield (Chen 2006).

1.2.3 Impact of sprays in a Fluid Coker™

Fluid Coking™, as explained earlier, converts bitumen vacuum residue to lighter and more useful hydrocarbons via thermal cracking. The feed is introduced into the system using a manifold of fluid spray injectors. The droplets introduced from the sprays interact with the fluidized bed of coke particles and affect the hydrodynamic properties (Tafreshi et al. 2002). This interaction of the droplets with bed particles is essential for the thermal cracking reactions, as the hot coke particles heat the bitumen, but it also leads to agglomeration formation within the fluidized bed. The presence of agglomerates results in reduced heat transfer with the hot bed, consequently lowering product yields (Darabi et al. 2010) and increasing fouling of the vessel and its internals (Sanchez Careaga 2013). The efficiency of the Fluid Coker™ is thus dependent on the nozzle configuration and the spray properties. A smaller liquid droplet size distribution enhances heat and mass transfer and increases solids entrainment in the spray jet leading to better liquid distribution and mass transfer, improving product yields (House 2008).

1.3 Agglomeration

Agglomeration is a process where individual particles collide and stick together to form larger agglomerates, usually in the presence of a binding agent. Agglomeration is common in industries with particulate operations such as pharmaceutical industries, food industries, biomedicine, biomass combustion and coking processes. Depending on the process and objective, agglomeration could be useful. It can be used to enhance the quality of products in food and pharmaceutical industries (Iveson et al 2001) however it reduces overall product yields in coking processes (Gray 2002).

1.3.1 Formation and Breakage of Agglomerates

This thesis focuses on the mechanism of agglomeration growth with a liquid binder. This type of agglomeration usually comprises of three major stages: wetting and nucleation, coalescence and consolidation, and finally attrition and breakage (Iveson et al. 2001). **Figure 1.2** shows a schematic representation of the steps involved during wet agglomeration with a liquid binder.

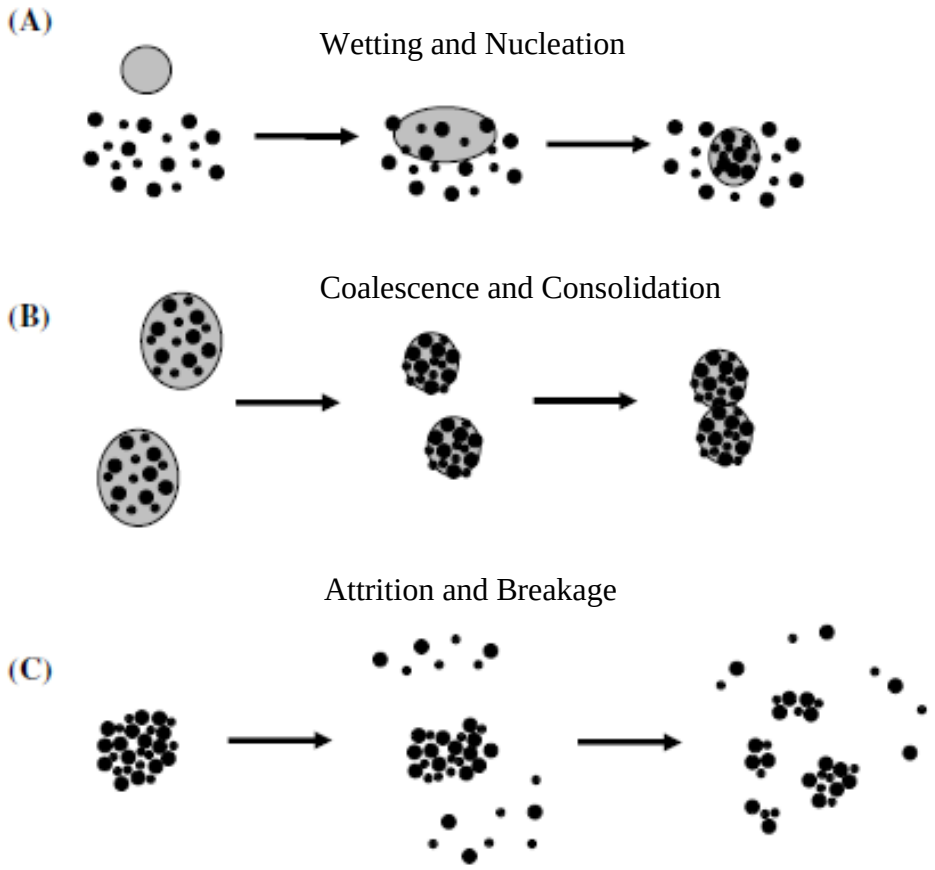

Figure 1.2: Schematic of the agglomeration process. (Adapted from (Iveson et al. 2001))

a) Wetting and Nucleation

This is a process where the liquid binder is introduced to the surface of the solid particles leading to the initial nuclei formation. This process can occur in two ways: distribution mechanism and immersion mechanism (Schæfer 2001). In the distribution method, the liquid binder sticks to and coats the surface of the smaller particles and essentially acts like a bridge that joins different particles together. In the immersion mechanism, the solid particles are immersed in the binder which

holds the particles together. The size distribution of the resulting agglomerates is usually dependent on the wetting kinetics and thermodynamics, which are affected by the binder and powder properties (Iveson et al. 2001). **Figure 1.3** shows the different mechanisms during wetting and nucleation.

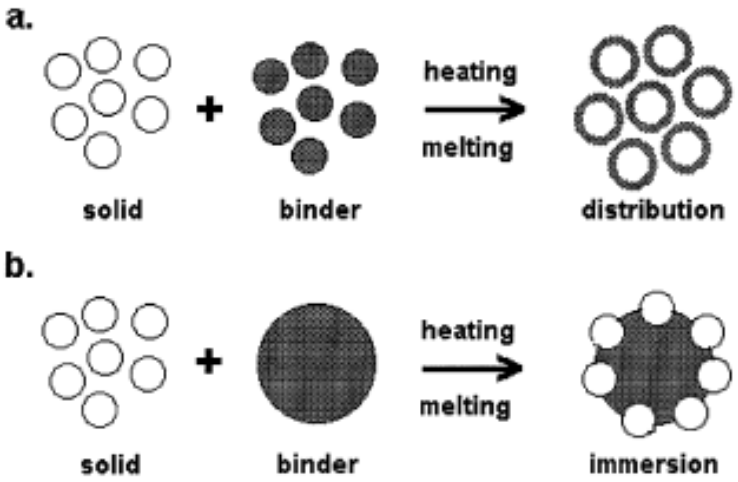

Figure 1.3: Wetting and Nucleation mechanisms. (a) Distribution mechanism, (b) Immersion mechanism. (Adapted from (Schæfer 2001))

b) Coalescence and Consolidation:

The coalescence stage leads to agglomerate growth as two or more nuclei/granules collide with each other and stick to form a larger agglomerate. This process continues with more agglomerates until a critical mass is reach beyond which the agglomerates break or deform (Ennis et al. 1991). This suggests that the final agglomerate size is determined during the coalescence and breakage stages. Agglomerate size is affected by the amount and viscosity of the liquid binder. As more liquid binder is involved in coalescence, more bridges are formed, resulting in larger and stronger agglomerates. **Figure 1.4** shows the

changes in the liquid bridging process caused by the addition of a liquid binder.

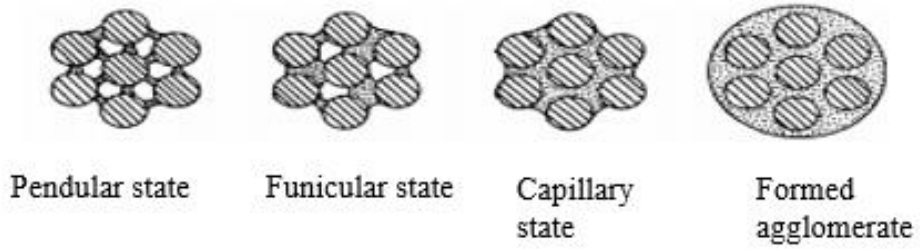

Figure 1.4: Changes in the state of liquid bridging caused by the addition of a liquid binder. (Adapted from (Schæfer 2001))

c) Attrition and Breakage:

Wet or dried agglomerates or granules break due to impact, wear or compaction (Iveson et al. 2001). As the agglomerates continue to grow and collide with each other, part of the agglomerates begins to break-off and separate. Breakage usually occurs with wet agglomerates and could determine the size of the agglomerates while attrition is more common with dried agglomerates (Weber 2009) . There are several causes of breakage or attrition such as voidage (Ennis et al. 1991), vessel walls, fluidization velocity (Li 2016), or the loading rate or unpacking system in granulation processes (Aman et al. 2010). However, the most important factors are the particles properties and the micro-bonding mechanism between the particles that make up the agglomerate (Antonyuk et al. 2005).

1.3.2 Agglomeration in food industries

Despite the various methods, the main goal of agglomeration in food industries is to improve the physical properties of food powders such as flowability, bulk density, dispersibility, shelf-life, stability and preventing dust formation (Dhanalakshmi et al. 2011). It also avoids de-mixing during transport processes (Palzer 2011). The agglomeration process here could be achieved via pressure, drying or growth with a liquid binder (Schuchmann 1995).

Agglomeration is also useful in spraying food additives to achieve a desired flavor. In food processing, smaller particles are intentionally collided and joined together to achieve a desired result. Sometimes a drying step is included to prolong the product shelf-life. This could be done by freezing or spray drying the final agglomerates. The liquid binder for growth agglomeration process improves powder properties, making it easier to transport. Examples of liquid binders include water, lecithin solution or gum solution (B.J. et al. 2009). Free flowing powders make further processing, such as tableting, much easier (Ghosal, Indira, and Bhattacharya 2010).

Agglomeration can also be used to create granulated and compacted items for cereal production, snacks coating with sugar and sweeteners, and for controlling consistency during production of cocoa powder, soymilk, soup mix, instant powder and artificial sweeteners (Dhanalakshmi et al. 2011). According to Dewettinck and Huyghebaert (1999), coating food powders enhances handling, taste masking, controlled production and product life span.

1.3.3 Agglomeration in Pharmaceutical Industries

The purpose of agglomeration in pharmaceutical industries is like that of food industries: to improve dispersibility, compressibility, homogeneity and flowability of the final product. Unlike the food industry, drug production in pharmaceuticals has been limited to mainly batch processes. New continuous technologies have nonetheless been emerging that utilize continuous agglomeration in the manufacturing process (Vervaet and Remon 2005). Pharmaceutical manufacturing industries have continued to evolve and utilize science and engineering principles, such as fluidization, to improve process efficiency and product quality (Parikh 2005). Some continuous wet agglomeration systems in the pharmaceutical industry include high shear granulation, fluid bed agglomeration, extrusion/spheronization and spray drying (Agrawal and Naveen 2011). Continuous wet agglomeration is useful in drug dosage and in optimizing the production process by reducing costs and making transport easier (Vervaet and Remon 2005). The use of co-agglomerated drug components could prevent segregation during transportation and ensures that the drugs are properly tableted (Pietsch 2008). However, unlike the food industry, segregation is harder to avoid because some drugs are hydrophobic, making it more difficult to achieve proper granulation.

1.3.4 Agglomeration in Fluid Coking

Unlike food and pharmaceutical processes, agglomeration is undesirable in the Fluid Coking^{TM} process. With this process, the formation of agglomerates leads to heat and mass transfer limitations (House 2008). Injected liquid that is trapped within the agglomerate cannot react unless the agglomerates are broken up to free the liquid. The amount of liquid that gets to react and process efficiency is thus dependent on the rate of

formation or breakage of the agglomerates. Some liquid could remain trapped in the agglomerates when the coke is sent to the burner to be reheated (Sanchez Careaga 2013), resulting in lower product yields. Agglomerates could also lead to fouling and possible damage of the vessel and its internals. Hence, it is essential to understand the agglomeration behavior during the coking process.

The formation and breakage of agglomerates is affected by different factors, including the quality of the injected spray, spray stability, viscosity and surface tension of the liquid (bitumen) and fluidized bed (coke) properties like density, size distribution and contact angle. Gray (2002) explained that agglomeration occurs mainly because the feed acts as a liquid binder. According to Dunlop et al. (1958), agglomerates are formed by granulation when the particle size is greater than 70 μm in the Fluid Coker^{TM}, but if the particle in contact with the liquid is less than 70 μm, the liquid just coats the particle. This suggests that the spray droplets size relative to the size of the bed particles is important in determining the agglomeration mechanism that takes place in the fluidized bed.

1.3.5 Agglomeration in slurry pipe flow

With the introduction of solids in the flow stream, there is a tendency for agglomeration to occur in the nozzle conduit before the slurry is sprayed. The agglomeration of the particles in slurry flow is usually affected Van der Waals forces, capillary and solid bridge forces, electrostatic, collision, net gravity and shear forces (Wang et al. 2015). Wang et al. (2015) showed that the capillary bridging forces were the dominant in forming liquid bridges and hence agglomerate formation within slurry flow while the shear-rate was the dominant separation force. As the shear rate approaches zero, more

agglomeration occurs but increasing the shear-rate reduces the maximum critical agglomeration size within the flow. Anoop et al. (2009) has also shown that deagglomeration occurs at high shear rates. This means that as velocity increases, the tendency for agglomeration to occur within the slurry flow drops. As slurry velocity increased, more particles are suspended leading to homogeneous flow (Albion et al. 2011). For homogenous flows, the solids are uniformly distributed within the pipe, particle-particle collisions are less likely, the shear forces are more dominant the agglomerating forces, thereby minimizing the tendency to form agglomerates within the slurry flow. However, for a hetergenous flow, some solids are deposited at the bottom of the pipe and the distance between the particles is less than the minimum separation distance required for collisions to occur. As a result agglomeration is more likely to occur in heterogeneous slurry flow than homogeneous flow. Therefore, to properly simulate the industrial system, it essential to obtain a homogenous flow where the solids are properly suspended.

1.3.6 Stability of Agglomerates

Agglomerate stability is important in processes that vary the strength of the product material, for example increasing the strength of concrete mix or with fillers for composites (Boyle et al. 2005). There are four groups of properties that greatly affect the stability and outcome of the final agglomerates. These include properties of the solid particles, properties of the liquid binders (e.g., viscosity and surface tension), external factors (e.g., fluidization velocity), and the interaction between the capillary/interfacial forces in the agglomerates (Benali et al. 2009). Important solid properties include average particle size, size distribution, presence of fines, particle shape, density, and wettability

with the liquid binder. According to Iveson and Page (2001), the binder viscosity and wettability are the most significant physiochemical properties that affect agglomeration. Wettability is dependent on the contact angle formed when the particle contacts the liquid. The higher the contact angle, the lower the chance of forming agglomerates (Rondeau et al. 2003). McDougall et al. (2005) has shown that with low contact angles, agglomerates will form with increasing viscosity; however, the viscosity does not affect the agglomerate formation at high contact angles.

The agglomerate stability is also affected by a balance between the hydrodynamic forces acting on an agglomerate and the individual particle-particle bonds/capillary forces within the agglomerates (Boyle et al. 2005). When particles are closely packed, a greater tensile force is required to fragment the agglomerate as the cohesive forces holding the particles are stronger. The strength of agglomerates is thus highly dependent on the properties of the particles in contact with the liquid binder during formation (Weber 2009).

1.3.7 Previous Studies on Agglomerate formation from sprayed liquid

Previous studies have examined the relationship between the agglomeration process and the liquid distribution in the fluidized bed. Liquid trapped within the final agglomerates in the Fluid Coker™ does not get the chance to react, leading to lower overall product yields. McDougall et al. (2004) have shown that a water-sand system properly simulates the bitumen coke system as there is nearly perfect wettability for the solids by the liquids in both cases.

House (2007) developed a cold simulation model where sugar was used as the binder for the experiments. The amount of glucose in the agglomerates was determined using gravimetric analysis. Using this model, he studied the effect of nozzle design on the formation of agglomerates. The author found out that improved feed dispersion nozzles would produce fewer macro-agglomerates and hence less probability for fouling in the coker. This model however only provided information about the initial agglomerates and did not consider potential formation or breakage of agglomerates after injection.

Pardo Reyes (2015) developed a cold-model to simulate and analyze the agglomeration process. A solution made up of Gum Arabic, food dye and water, was injected at a temperature of 130°C. The Gum Arabic served as the liquid binder while the food dye was the tracer. The agglomerates formed were analyzed to obtain the amount of liquid trapped based on the amount of trapped dye using a spectrometer. The author discovered that increasing the binder concentration resulted in more agglomerates as the increased viscosity led to more stable agglomerates. It was also observed that increasing viscosity led to an increased amount of liquid trapped within the agglomerates. Work was also done on pulse injection and it was concluded that one full spray produced fewer agglomerates rather than four sprays with the same total amount of injected liquid.

Li (2016) studied the effects of high gas velocity on agglomerates and liquid distribution. It was observed that increasing the fluidization velocity during injection reduced the amount of agglomerates. This phenomenon was however only significant in the bubble flow regime of the fluidized bed. Once the fluidized bed entered the turbulent regime, a further increase in fluidization velocity had a minimal effect on the amount of agglomerates produced. Higher gas velocities also led to better liquid distribution. This is

because the higher drying velocity causes breakage of the agglomerates, releasing previously trapped liquid. The effect of spray stability and liquid distribution at low gas velocities were also studied (both during injection and drying), and bed hydrodynamics were dominant while spray stability had a negligible effect. At higher superficial gas velocities (during both injection and drying), the spray stability was more significant.

1.3.8 Previous Studies on Agglomerate Stability in Fluidized Beds

Weber (2009) investigated the effect of particle and bed properties on the agglomerate stability. The agglomerates used were custom made in the laboratory and inserted into the fluidized bed and then re-examined after the experiment. Agglomerates formed from larger particles were more porous and trapped less moisture than agglomerates made from smaller particles. Agglomerates were more stable when they included particles from a wide range of particle sizes. It was also observed that different types of particles led to different rates of formation or breakage of agglomerates. Particle properties such as size, shape, porosity and abrasiveness significantly affected the outcome of the final agglomerates. The wettability of the injected agglomerates also appeared to affect the breakage rate of the agglomerates. It was also shown that increasing the fluidization velocity led to a lower mass of agglomerates.

Parveen (2011) continued the work of Weber (2009) by studying the effects of agglomerate properties, bed particle properties and fluidization velocity on agglomerate breakage. Wet agglomerates were simulated using polyurethane foam, epoxy glue and an RFID (Radio-frequency identification) tag. The RFID tag was used to detect agglomerate breakup within the bed. It was found that agglomerate stability depended not just on particle size, but also on the number of fines. Increasing the Sauter-mean diameter of the

particles also reduced agglomerate stability. Increasing the fluidization velocity led to faster breakage of the agglomerates and denser agglomerates broke up more slowly than less dense ones.

1.4 Research Objectives

Based on the previous studies, it is necessary to understand the bed hydrodynamics, liquid distribution, and the agglomerate stability within the fluidized bed. Several liquid properties were studied, such as viscosity, density and contact angle. However, the injection of a liquid-solid slurry into the fluidized bed has not been studied. This thesis focuses on the impact of injecting a slurry on the liquid distribution within the fluidized bed and the agglomerate stability. The research was conducted in three main stages, which have been separated as chapters.

Chapter 3: The impact of injected particles on spray properties in open-air. Experiments were conducted in open-air to understand the effect of the solids on spray stability and angle. Particles with varying properties were also tested to see how the open-air spray characteristics varied with particle properties.

Chapter 4: The impact of injected slurry on agglomerate formation and break-up. This chapter uses the cold simulation model developed by Pardo Reyes (Pardo Reyes 2015) to investigate the impact of the slurry injection on initial agglomerate formation and breakage. Fine silica sand particles were used as the solids for the results in this chapter at different concentrations: 0 wt.%, 10 wt.% and 20 wt.%. The impact on liquid distribution and agglomerate stability were also studied by varying the fluidization velocity during injection.

Chapter 5: Impact of different particle properties on the liquid distribution. In this chapter, particles with varying properties were tested to better understand the impact on agglomeration behavior when injecting a slurry. Particle size, shape, density and wettability were varied. The effect of these properties provided insight into the physical mechanisms responsible for the impact of slurry particles on liquid distribution and agglomerate stability in a fluidized bed.

Chapter 2

2 Experimental Set-up and Methodology

2.1 Open Air Experiments

2.1.1 Experimental Set-up

Figure 2.1 shows a schematic diagram of the open-air experimental process which starts at the mixing tank where the slurry mixture is first formed using a compressed air motor and impeller. Atomization gas was provided from the nitrogen tanks to produce a spray at the end of the TEB spray nozzle (Base et al., 1999). The desired atomization gas pressure was set using a pressure regulator which is measured by the pressure transducer at P_{ATO}. A calibrated sonic orifice was used to adjust the gas flow to the required gas mass flux. The conduit diameter of the fittings and line for the gas flow is 6.4 mm (1/4"). Nitrogen gas was also sent through the mixing tank and the pressure is measured at P_{BTK}. The flowrate of the slurry leaving the mixing tank was dependent on the pressure recorded at P_{BTK} and the size of the flow restrictor. The slurry from the mixing tank was sent through the flow restrictor and is mixed with the atomization gas at the pre-mixer. The resulting mixture was produced at the tip of the TEB spray nozzle. The TEB nozzle was specially designed to ensure proper gas-liquid mixing within the conduit. The system was able to achieve sonic flow in the sonic orifice for the experiments which were done at different atomization gas-to-liquid, (GLR) ratios: 1, 2 and 3 wt.%.

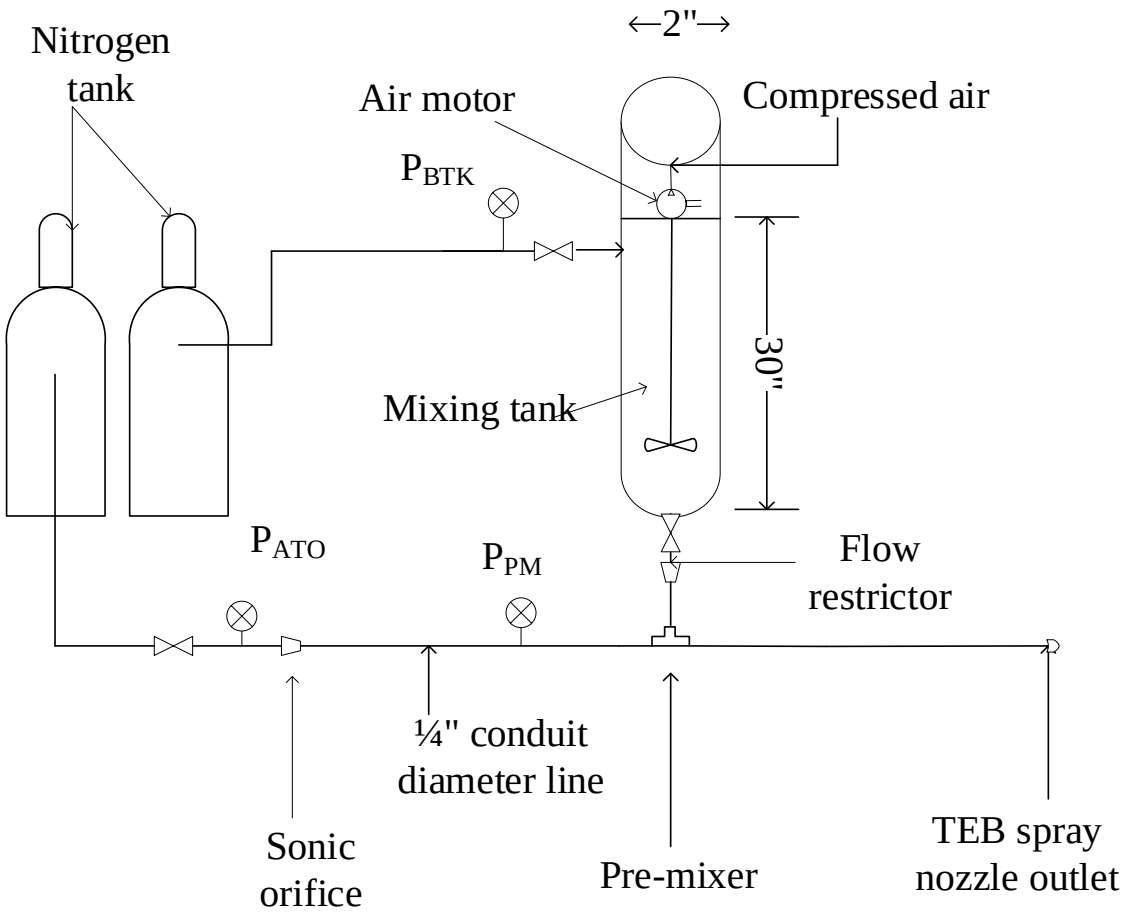

Figure 2.1: Schematic diagram of open-air injection system

Figure 2.2 shows a TEB spray nozzle which is a scaled down version of an industrial nozzle and is suitable and efficient for simulating the industrial conditions (Farkhondehkavaki 2012). In this study, the tip of the TEB spray nozzle was either 1 or 2 mm in diameter.

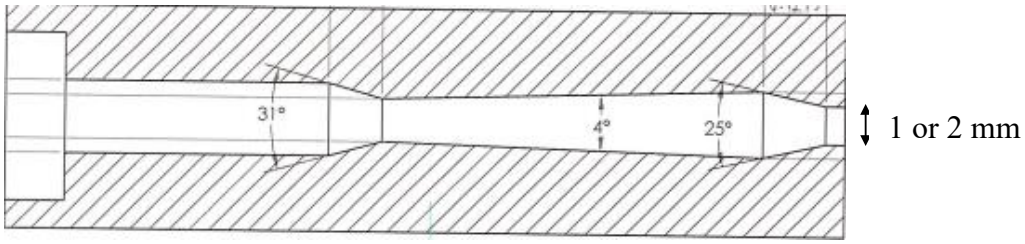

Figure 2.2: Diagram of TEB nozzle

2.1.2 Mixing tank and Solids Suspension Quality

Table 2.1 gives details about the results from the solids suspension quality test. To properly simulate the industrial slurry-recycle stream, the mixing tank was tested to ensure that the solids were properly suspended in the mixing tank. Good mixing of the slurry would prevent particle agglomeration during pipe flow as the solids should be well dispersed and properly suspended. The motor in the mixing tank was run using compressed air at 90 psig which corresponds to a maximum speed of 25 rpm.

Sand particles (d_{psm} =12.8 μm, ρ = 2650 kg/m^3) were used as the solid particles for the test because they had the highest density compared to other solids tested and should therefore be the hardest to suspend. The solid particles and liquid were introduced into mixing tank with the motor set at 25 rpm where the mixing occurs. Half of the resulting mixture was sprayed in open-air and collected in a bucket. The sprayed slurry was collected, weighed and its solids concentration obtained by letting its liquid dry off and measuring the mass of the dry particles. From **Table 2.1**, the concentration of the solids in the sprayed liquid increased relative to the initial concentration of the slurry. This shows that the mixing unit is more efficient at lower concentrations of solids which is expected.

Table 2.1: Testing suspension quality of sand particles in sand-water slurry

wt.% of slurry solids in original mix	wt.% of solids in sprayed liquid	wt.% of solids in liquid remaining in tank
5	5.05	4.95
10	11.29	8.71
20	23.5	16.5

2.1.3 Slurry mixtures and solutions

Table 2.2 shows the different injected solids and their particle properties. Most of the open-air experiments were done with a slurry mixture of sand (Sauter-mean diameter, d_{psm} = 12.8 μm) and water. However, for spray stability experiments, other solids such as hollow glass beads (d_{psm} = 9.8 μm), solid glass beads (d_{psm} = 10.2 μm) and crushed coke (d_{psm} = 9.0 μm) were used. **Figure 2.3** shows the cumulative size distribution of the solids which were measured using a Sympatec Helos particle size analyzer. Appendix A contains more details on cumulative size distribution of all the solids. Also, to simulate the industrial viscosity conditions, different base fluids were tested such as 0.05 wt.% CMC-water solutions and 30 wt.% sugar-water solutions with sand as the solid particles. The concentrations of solids tested was from 0 to 20 wt.%. The system experienced

plugging above 20 wt.% concentration of solids with d_{psm}= 12.8 μm, specifically at 30 wt.% and 40 wt.%.

Salt-water solutions were used to examine the effect of changing density on the spray properties. The concentration of salt in the solution was adjusted to achieve the desired density for each case. For example, 22.5 % salt solution would have the same density (1400 kg/m^3) as a 20 wt.% sand-water slurry.

Table 2.2: Properties of the injected solids tested. From Weber (2009) and Thermtest Inc. (2018).

Solids	Properties			
	Particle density (kg/m^3)	Sauter-mean diameter (μm)	Particle shape	Wettable with water
Sand	2650	12.8	angular	yes
Hollow Glass (H.G.) beads	1000	9.8 61.0	round	yes
Solid Glass (S.G.) beads	2450	10.2	round	yes

Coke	1450	9	angular	no

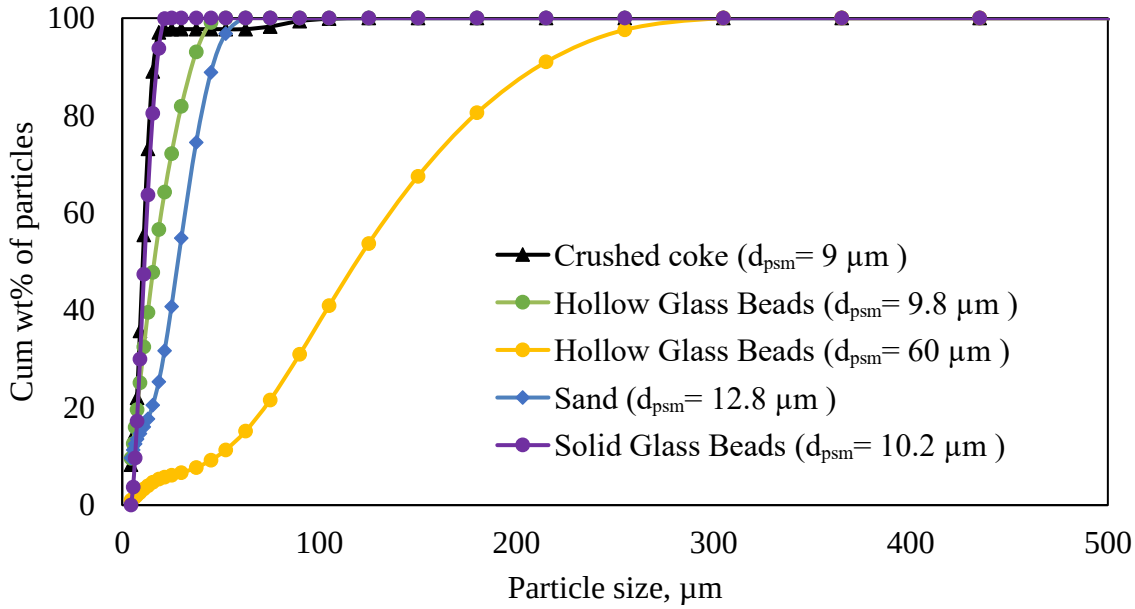

Figure 2.3: Cumulative size distribution of particles for all injected solids

2.1.4 Determining the effective viscosity of suspensions and solutions

- Einstein`s viscosity equation (for φ < 5%) (Mooney 1951)

$$\mu_{eff} = \mu_f(1 + 2.5\varphi) \qquad \textbf{2-1}$$

Where: φ is the volumetric fraction of the solids in the slurry.

This equation was only useful when the volume fraction was less than 5% (10 wt.%), hence it was not used for higher concentrations up to 20 wt.%. More robust equations were required to estimate the effective viscosity of the slurry.

- Batchelor`s correlation (Batchelor 2000),

$$\mu_{eff} = \mu_f(1 + 2.5\varphi + 6.5\varphi^2) \quad \textbf{2-2}$$

- Thomas` correlation for viscosity of mixtures, (Thomas 1965)

$$\mu_{eff} = \mu_f(1 + 2.5\varphi + k\varphi^2) \quad \textbf{2-3}$$

Where k ranges from 10.5 to 14.1

Equation 2-2 is like **equation 2-3** but with a k value of 6.5. **Equation 2-3** was used to estimate the viscosity with k = 14.1 as this would be the worst-case scenario. However, changing the value of k from 6.5 to 14.1 led to a difference of 4 % in effective viscosity, at 20 wt.% solids which is a negligible difference.

The viscosity of the CMC and salt solutions were measured using a Cannon-Fenske viscometer tube(D75).

2.1.5 Average Spray Angle

Figure 2.4 shows how the angle of the spray is measured. The average spray angle gives information about the liquid dispersion in the spray and the liquid droplet size. The video of the spray is taken using a high -speed camera (Casio Exilim EX-ZR1700SR) at 420 frames per second and analyzed using Matlab to obtain the spray angle with respect to picture frames and is then used to obtain the average spray angle for each run. The average spray angles are then plotted against concentration of solids.

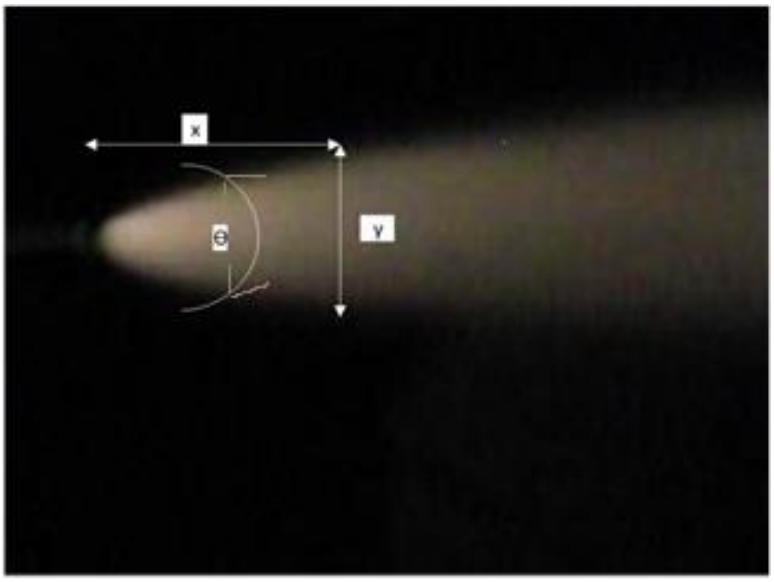

Figure 2.4: Measuring spray angle

$$Spray\ angle, \theta = 2 * \tan^{-1}(y/_{2 * x}) \quad \textbf{2-4}$$

Where x = 9 cm

2.1.6 Spray Stability

Spray stability was examined visually using a high speed camera, but it is related to the flow pattern within the conduit which is more difficult to examine physically (Li 2016). The flow pattern is affected by the effectiveness of gas-liquid mixing at the pre-mixer and within the nozzle conduit and the gas and liquid flowrates. This means that better mixing will lead to less fluctuations in the spray and a more uniform spray droplet size distribution. To obtain a stable spray, it is preferred that the flow pattern within the conduit be in dispersed bubble phase as shown in **Figure 2.5**. In this regime, there is

better gas-liquid mixing as the velocity of the flow is high enough to the counteract buoyant forces acting on the bubbles.

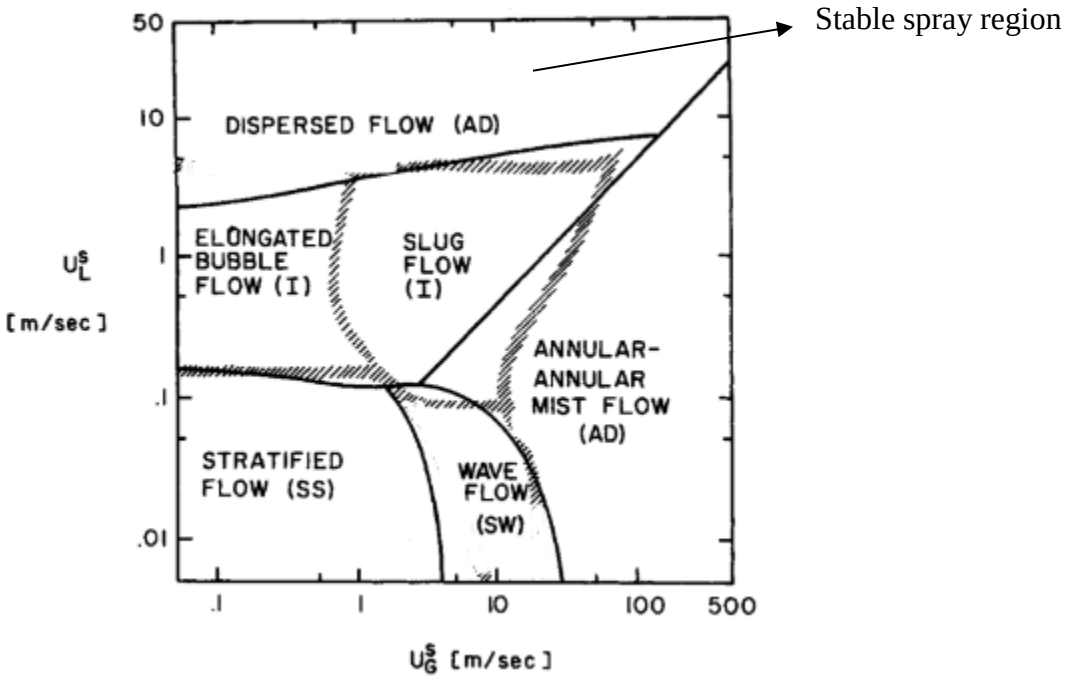

Figure 2.5: Flow regime for water-air flow at room conditions. Adapted from (Taitel and Dukler 1976)

The stability of the spray can be measured in two different ways: using the coefficient of variation (COV) based on the video properties and the change in pre-mixer pressure readings with time. Spray videos (at 420 frames per second) are taken using a high-speed camera and used to obtain the coefficient of variation based on video properties. The pre-mixer pressure readings are obtained by converting voltage readings from the pressure transducer at the pre-mixer. Joness (2018) looked at different ways of measuring stability using the coefficient of variation from spray videos obtained using a high-speed camera. The author looked at coefficient of variation of the proportion of gray-scale pixels,

average pixel intensity values and the sum of pixel intensity relative to the spray area. **Figure 2.6** shows a picture frame from a spray video. Everything within the box can be considered as the picture frame area, P_A, while the darker region is the spray area, S_A. Lower values for coefficient of variation indicate a more stable spray while higher values represent a more pulsating spray.

- Proportion of gray-scale pixels: Every frame from the color video was converted first to gray-scale and then to a binary picture with the background as 0 and the pixels of the spray as 1. The ratio of the spray area to the picture area, (S_A/P_A), was obtained as the proportion of the spray for each picture frame. This was repeated for every frame and used to obtain the coefficient of variation.

- Average pixel intensity values: This method measures the time-averaged pixel intensity values of the spray. It shows how the spray region, S_A contracts or expands with time.
- Sum of intensity/area: Here, the sum of the pixel intensity values in the spray area of a picture frame is obtained first and then divided by the spray area S_A. This calculation is then repeated for every picture frame in the spray video. The coefficient of variation of the obtained values for every frame in the video, were then used to qualify the spray stability. In this study, a value less than 0.06 indicated a non-pulsating spray. This method also takes into consideration both stability and liquid dispersion of the spray. It was

concluded that this method was most accurate compared to the other video methods.

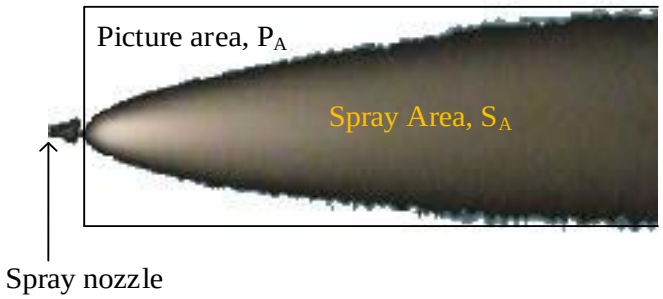

Figure 2.6: Picture frame of spray for stability analysis

2.1.7 Determining spray flowrate

Figure 2.7 andFigure **2.8** show the change in the proportion of gray-scale pixels and pre-mixer pressure with time respectively. The video of the spray taken during each run is analyzed in Matlab to produce a figure showing how the proportion of gray-scale pixels varies with time, from which the spray time can be estimated. The spray time was then used get the average flowrate for each run. Similarly, the flowrate could also be estimated from the plot of pre-mixer pressure readings with time.

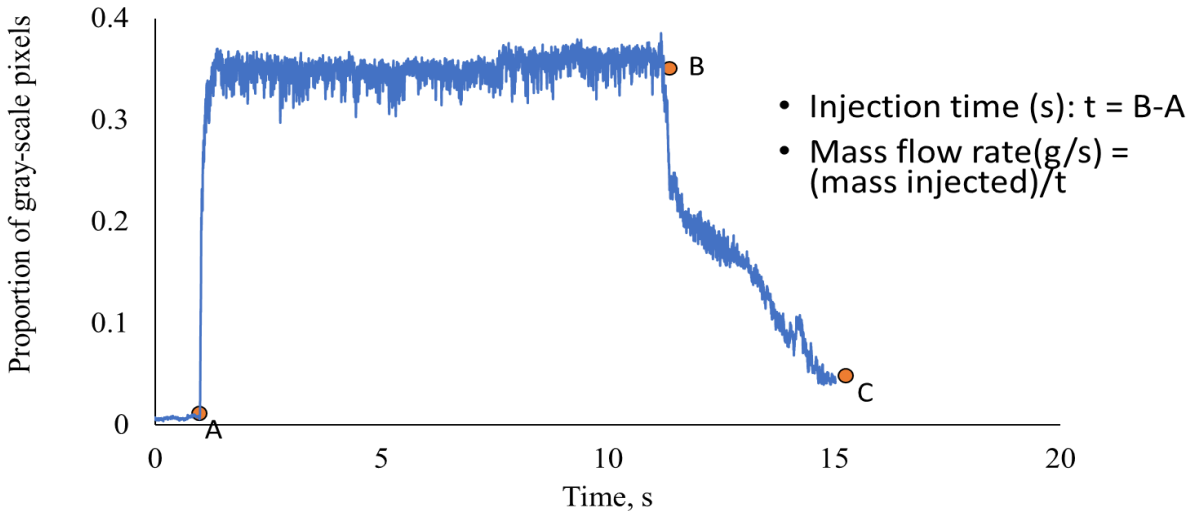

Figure 2.7: Proportion of gray-scale pixels with time

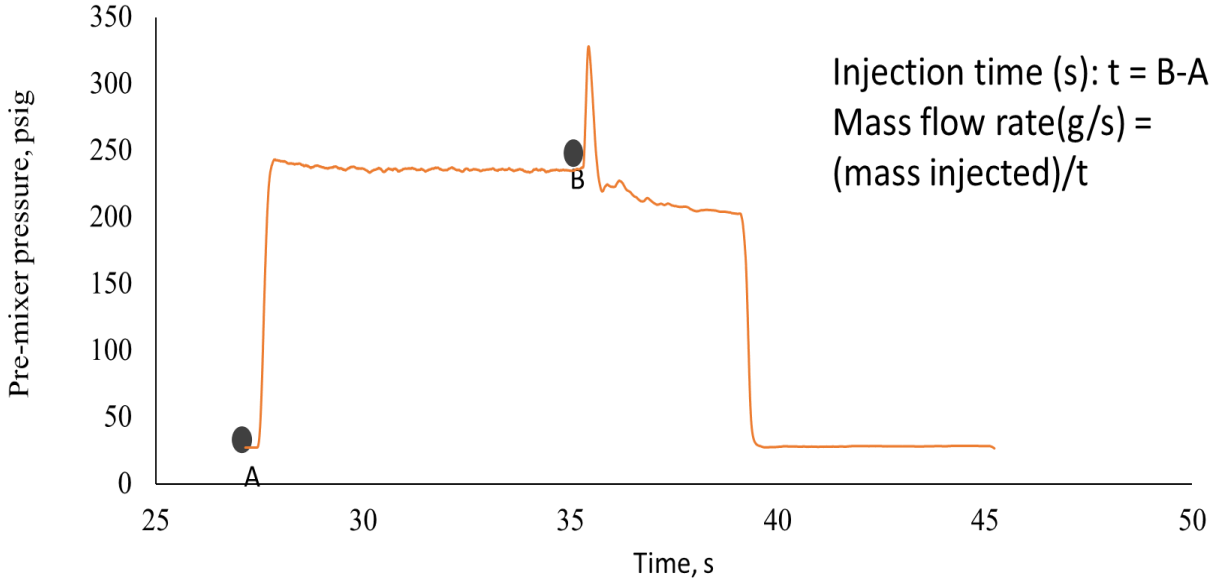

Figure 2.8: Pre-mixer pressure readings with time

From **Figure 2.9**, clearly the values of the flowrates obtained from the pressure reading and proportion of gray-scale pixels agreed with each other, with the pressure readings

resulting in slightly lower flowrate values. The average value from both cases were used as the final value for each wt.% run.

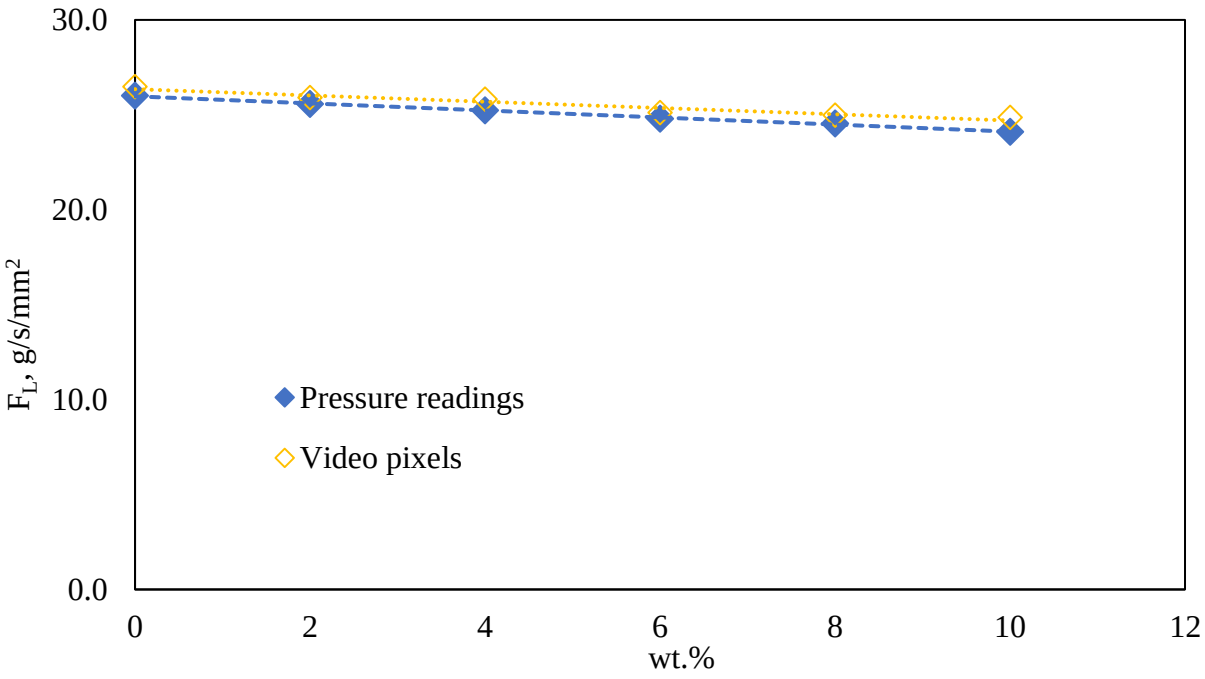

Figure 2.9: Comparing the two methods used to obtain the liquid flowrate

2.2 Fluidized Bed Experiments

2.2.1 Experimental Set-up

Figure 2.10 shows the experimental set-up for the fluidized bed experiments. The injection system is identical to that of the open-air experiments but with the spray being injected in a fluidized bed. For all fluidized bed experiments, the bed which had an approximate height of 0.45 m, was made up of 45 kg of silica sand with a Sauter-mean diameter of 190 μm and a particle density of 2650 kg/m^3. The cumulative size distribution of the bed particles is given in **Figure 2.11**. **Figure 2.12** shows a photo of the fluidized bed system. An induction heater is attached to the outside wall to heat up the

bed to 135 °C for Gum Arabic model experiments. As a result, the heating system does not interfere with the fluidization process. The spray injections were carried out with a TEB nozzle with a 1 mm throat diameter at 2 wt.% GLR as shown in **Figure 2.2**. The spray nozzle was located 0.21 m above the windbox. The temperature of the bed was measured using a thermocouple located on the opposite end of wall from the injection nozzle.

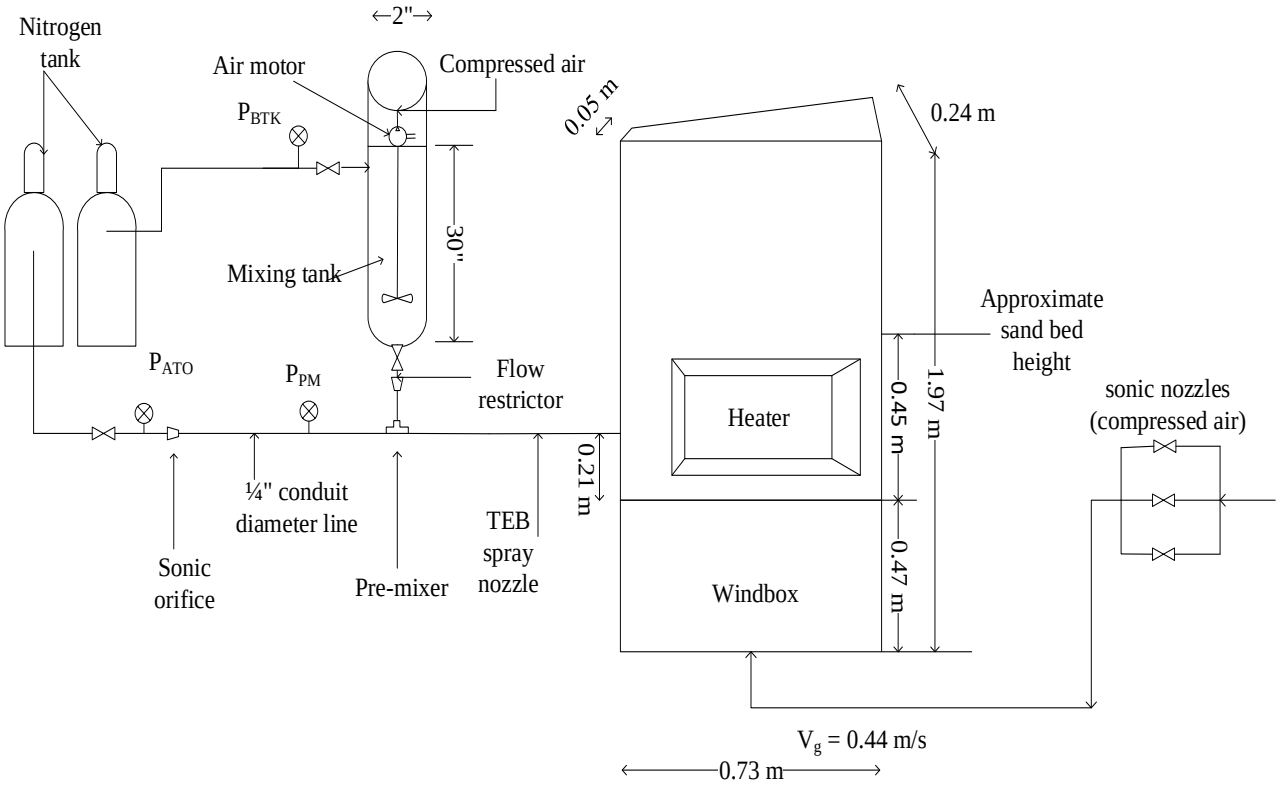

Figure 2.10: Schematic diagram of the experimental set-up for fluidized bed experiments.

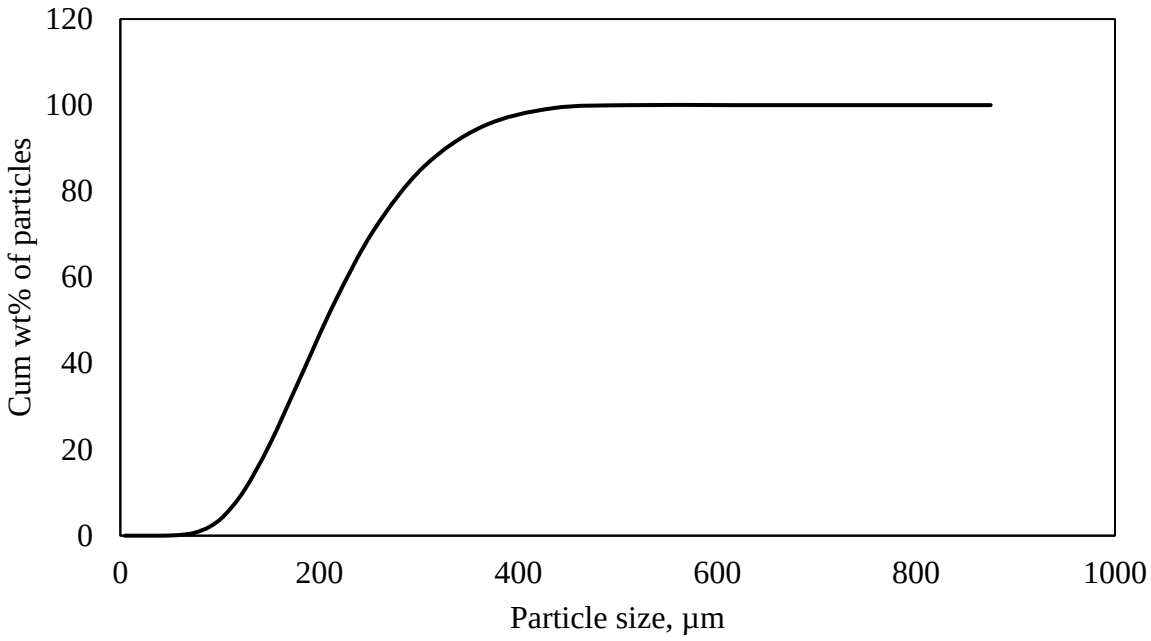

Figure 2.11: Cumulative size distribution of the bed sand particles

Figure 2.12: Photo of fluidized bed system

2.2.2 Low temperature (Gum Arabic) experimental model

Pardo Reyes`s cold simulation model (Pardo Reyes 2015) was adopted for the fluidized bed experiments. The model has been proven to effectively simulate formation and breakage of agglomerates in a Fluid Coker^{TM} from bitumen injection using pilot plant-scale equipment (Pardo Reyes 2015).

The injected mixture is made of solid particles and Gum Arabic solution. The solution is made up of 92 wt.% water, 6 wt.% Gum Arabic powder which acts as the binder and 2 wt.% blue dye which was used as the tracer. The pH of the solution was adjusted to a pH of 3.0 using a few drops of hydrochloric acid. Pardo Reyes (2015) has proven that at a pH of 3, the solution has a viscosity of 3 cP which is near the viscosity of injected bitumen in the industrial Fluid Coker^{TM}. The total mass of injected mixture was 200 g of slurry for all runs with an atomization gas flux of 0.463 g/s/mm^2 which corresponded to a GLR of 2 wt.% for 0 wt.% of solids.

2.2.3 Experimental procedure for fluidized bed experiments

- Preheat bed at low fluidization velocity (V_{g1})
- Increase to desired injection fluidization velocity, V_{gi}
- Inject 200 g of gum Arabic solution (injection time: 11 s without solids)
- Reduce V_g to desired fluidization velocity, V_{gd} during drying
- Switch off the heater and allow bed to cool to below 50° C (which took approximately 55 minutes for all cases, with or without injected solids).

- Collect bed solids with vacuum system and screen to recover the agglomerates. The agglomerates are then collected, weighed, sized and analyzed for trapped liquid content, using the method described by (Pardo Reyes 2015).

To properly investigate the effect of the slurry on agglomerate formation and breakage, a variety of fluidization velocities were tested, and a summary is given in **Table 2.3**.

Table 2.3: Summary of fluidization velocities tested during injection and drying of agglomerates

V_{gd} (m/s) / V_{gi} (m/s)	0	0.12	0.44
0.35	N/A	measured	N/A
0.44	measured	measured	measured
0.75	N/A	measured	N/A

2.2.4 Characterization of Agglomerates

2.2.4.1 Size Distribution of Agglomerates

After the experiment, the bed of sand constitutes of a mixture of macro- agglomerates, micro-agglomerates and the initial bed particles. The macro-agglomerates are the

agglomerates with a size greater than 600 μm while the micro-agglomerates range from 355 μm and 600 μm. Due to their size, the macro-agglomerates can be easily sieved into different size cuts that are weighed directly. The macro-agglomerates were divided into the following size cuts:

$$d_{aggl} \geq 9500\ \mu m$$

$$9500\ \mu m \leq d_{aggl} \geq 4000\ \mu m$$

$$4000\ \mu m \leq d_{aggl} \geq 2000\ \mu m$$

$$2000\ \mu m \leq d_{aggl} \geq 1400\ \mu m$$

$$1400\ \mu m \leq d_{aggl} \geq 850\ \mu m$$

$$850\ \mu m \leq d_{aggl} \geq 600\ \mu m$$

The remaining mass, mass of micro-agglomerates and bed particles is therefore given as

$$m_{<600\ \mu m} = m_{bed} - m_{macro} \qquad \textbf{2-5}$$

The size cut for the micro-agglomerates are divided as follow:

$$600\ \mu m \leq d_{aggl} \geq 500\ \mu m$$

$$500\ \mu m \leq d_{aggl} \geq 425\ \mu m$$

$$425\ \mu m \leq d_{aggl} \geq 355\ \mu m$$

Since the size range of the micro-agglomerates overlaps with the size range of the initial bed particles, the size cuts obtained by sieving would include bed particles, making it difficult to obtain the actual mass of the micro-agglomerates. As a result, only a 5 kg sample was taken from the bed (after the macro-agglomerates have been removed) and the trapped fines were used as a tracer to estimate the mass of the micro-agglomerates in the bed. The mass of the micro-agglomerates in the sample (m_{micro,R_i}), was calculated as:

$$m_{micro,R_i} = m_d + m_{GA} + m_p \quad \textbf{2-6}$$

Where; m_d = mass of dye; m_{GA} = mass of gum Arabic, and m_p= mass of trapped fine particles.

The mass of the dye and gum Arabic in the sample was obtained from spectral analysis for liquid trapped in the agglomerates (see section 2.2.4.2 below). Assuming the size distribution of the trapped bed fines was the same as the initial size distribution of the bed, the mass of the trapped particles (m_p) was calculated as follows (Pardo Reyes 2015):

$$m_p = m_{sand}\left(\frac{x_f}{x_{bed}}\right) \quad \textbf{2-7}$$

Once the mass of the agglomerates in the sample was known, the total amount of the micro-agglomerates for each size cut in the bed was calculated as follows (Pardo Reyes 2015):

$$m_{micro,i} = m_{micro,R_i}\left(\frac{x_f}{x_{bed}}\right) \quad \textbf{2-8}$$

2.2.4.2 Determination of liquid trapped (Pardo Reyes 2015)

The amount of liquid trapped in the agglomerates was estimated based on the mass of the blue dye in the injected solution. After the agglomerates were weighed, they were dissolved in water to extract the dye. The mass ratio of water to agglomerates is 3:1. A magnetic stirrer helps dissolve the gum Arabic and the dye and a centrifuge was used to separate the sand from the resulting dyed liquid. A sample of this final liquid was analyzed in a spectrometer to measure the absorbance at the characteristic wavelength, λ_c of blue light (630 nm). The concentration and mass of the blue dye was obtained using the absorbance and calibration shown in the **Figure 2.13** below.

Since the blue dye acts as a tracer, and the initial ratio of dye to liquid is known, the mass of the liquid trapped in the agglomerates was then obtained using the mass of the dye. For each case studied, the average of the replicates was taken to produce a line graph to show the effects produced for each case.

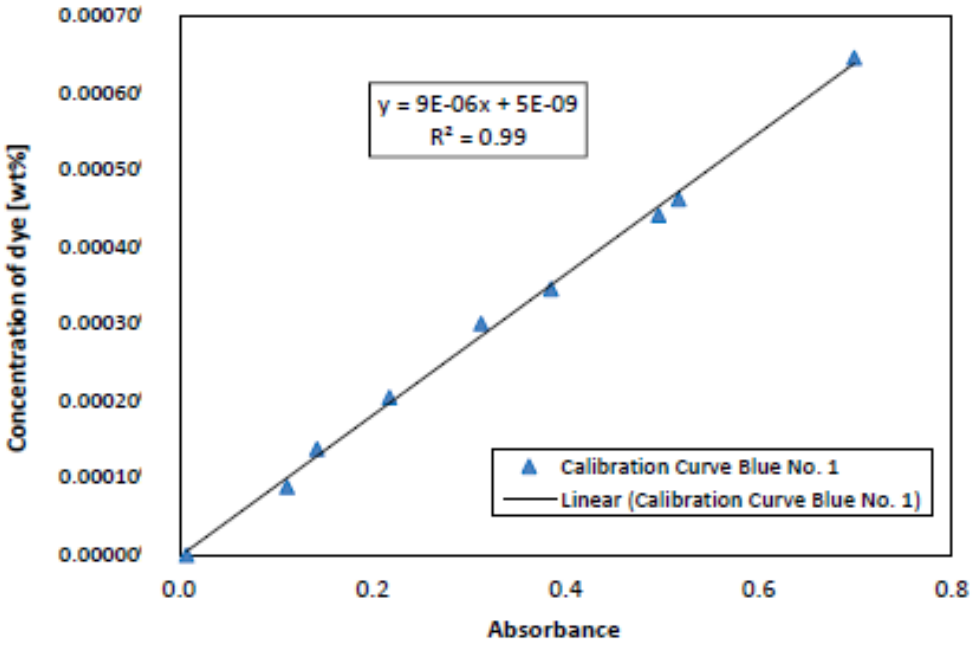

Figure 2.13: Calibration curve for absorbance of blue dye, λc = 630 nm. (Pardo Reyes 2015)

2.2.5 Jet Penetration

A method developed by Li (2017) was used to measure the length of a spray jet in the fluidized bed. The set-up (described in 2.2.1), comprised of a movable spray nozzle at one end of the fluidized bed with a thermocouple on the other end, directly opposite the spray nozzle. The thermocouple was used to measure the temperature drop caused by the sprayed liquid. For each run, the nozzle is placed at a reasonable distance away from the thermocouple and the liquid is sprayed into the bed at a temperature of 130 °C. To obtain the exact spray length, each time a run was made, the nozzle was moved closer to the thermocouple until a significant change in the temperature drop was observed. The resulting distance from the spray tip to the thermocouple is measured as the jet length.

Chapter 3

3 Effect of slurry concentration on open-air spray properties

3.1 Introduction

Many fluidized bed processes, including Fluid Coking™ make use of a horizontal spray system. The behavior of the spray jet into the Fluid Coker™ is important as it significantly affects the agglomeration process and hence the overall efficiency of the process. Agglomeration of the fluidized bed particles with the sprayed liquid can lead to yield losses and fouling in the bed (Stanlick 2014, Sanchez Careaga 2013). Changes to spray behavior due to the solids present in the injected liquid could enhance or adversely affect the liquid distribution within the Fluid Coker™. As mentioned in chapter 1, relevant spray characteristics that could affect the agglomeration include the spray stability, angle and length. Open-air experiments can measure the effect of the recycled solids on these spray properties. Past studies have shown that spray stability in open-air and in a fluidized bed are directly related (Ariyapadi 2004). Although the spray angle is quite different in open-air than in the fluidized bed (Berruti et al. 2009), if the slurry solids affect the spray angle in open-air, they will also affect it in the fluidized bed.

This work analyzes the spray stability, and spray angle to investigate the effect of the injected solid particles. Experiments were also carried out to examine how the liquid flowrate might be affected by changing the concentration of injected solids. Because the mass flowrate of atomization gas was kept constant in the experiments, any change in liquid flowrate would result in a change in the gas-to-liquid mass ratio (GLR).

Improving the spray stability usually enhances the efficiency of the process as it improves liquid distribution in the bed. However, Leach et. al (2008) has shown that introducing specific pulsations could enhance jet-bed interactions. There have been a lot of studies on the effects spray stability and pulsations on agglomeration in a fluidized bed. Ariyapadi (2003) observed that unstable sprays tend to reduce the amount of solids entrained in the spray jet and affect solids mixing. House (2008) also suggested that improving spray stability enhances the liquid-solid contact, thus increasing liquid distribution within the fluidized bed. Since the concentration of the solids affect the effective viscosity and density, it is relevant to examine how these factors affect the spray stability. Change in the viscosity can affect the stability of the spray. Ariyapadi (2004) conducted experiments to show that increasing viscosity would results in a less stable spray.

The spray angle can be used to obtain information on stability and liquid dispersion. Measuring the change in spray angle with time can be used as a measure of stability. Increasing spray angle would also lead to an increase in solids entrainment in the spray jet and further enhance product yield (House 2008). The average spray angle could be used to estimate the average droplet size. With respect to gas-liquid ratio (GLR), House (2008) concluded that increasing GLR from 1.5 wt.% to 2.75 wt.% should increase the spray angle as there is a higher gas flow.

The jet penetration was not considered in open-air experiments, because within the fluidized bed, it is bound to be different than it would be for open-air experiments as the bed solids will affect it.

The objective of this chapter is to examine, if any, the effect of the injected solid particles on spray properties such as stability and spray angle, liquid mass flowrate and gas-liquid ratio (GLR) and the significance of the effects.

3.2 Experimental Set-up and methodology

The experimental set-up, materials and methodology for the open-air experiments and data analysis is available in chapter 2 of this thesis. The experiments were done in open-air using the set-up shown in **Figure 2.1**. A high-speed camera was used to take a video of the sprays at a frame rate of 420 frames per second while a data acquisition system was used to record the change in pre-mixer pressure with time.

3.3 Results and Discussion

3.3.1 Impact of slurry Concentration on flowrate

Figure 3.1, Figure 3.2 and **Figure** 3.3 show the relationships between the concentration of the injected solids and liquid mass flux, total slurry mass flux and slurry volumetric flux of the spray, respectively. The pre-mixer pressure was kept constant for the duration of all the runs. From **Figure 3.1**, the liquid mass flow drops when there is a higher concentration of solids. Since, the total mass of the slurry was kept constant at 200 g, it is expected that the liquid flowrate drops with an increase in weight fraction (wt.%) of solids as the amount of liquid (water) in the slurry is reduced. The liquid flowrate corresponds to the amount of liquid available in the slurry. From **Figure 3.2**, the total slurry mass flowrate increases with an increase in concentration for all the different solids. Hence, the spray time is reduced when more solids are injected due to the reduced mass of liquid. From **Figure 3.3**, the slurry volumetric flux remains almost constant across the solids' concentrations suggesting that the solids have no significant effect on

the volumetric flowrate of the slurry. This confirms that the effect produced on total slurry mass flux and liquid mass flux is just due to the change in the volume of liquid in the slurry.

Figure 3.1: Impact of slurry concentration on liquid mass flux (water) at 2 wt.% GLR at 0 wt.% of solids. P_{ATO}: 558 psig; P_{BTK}: 285 psig; P_{PM}: 235 psig

Figure 3.2: Impact of slurry concentration on total slurry mass flux at 2 wt.% GLR at 0 wt.% of solids. P_{ATO}: 558 psig; P_{BTK}: 285 psig; P_{PM}: 235 psig

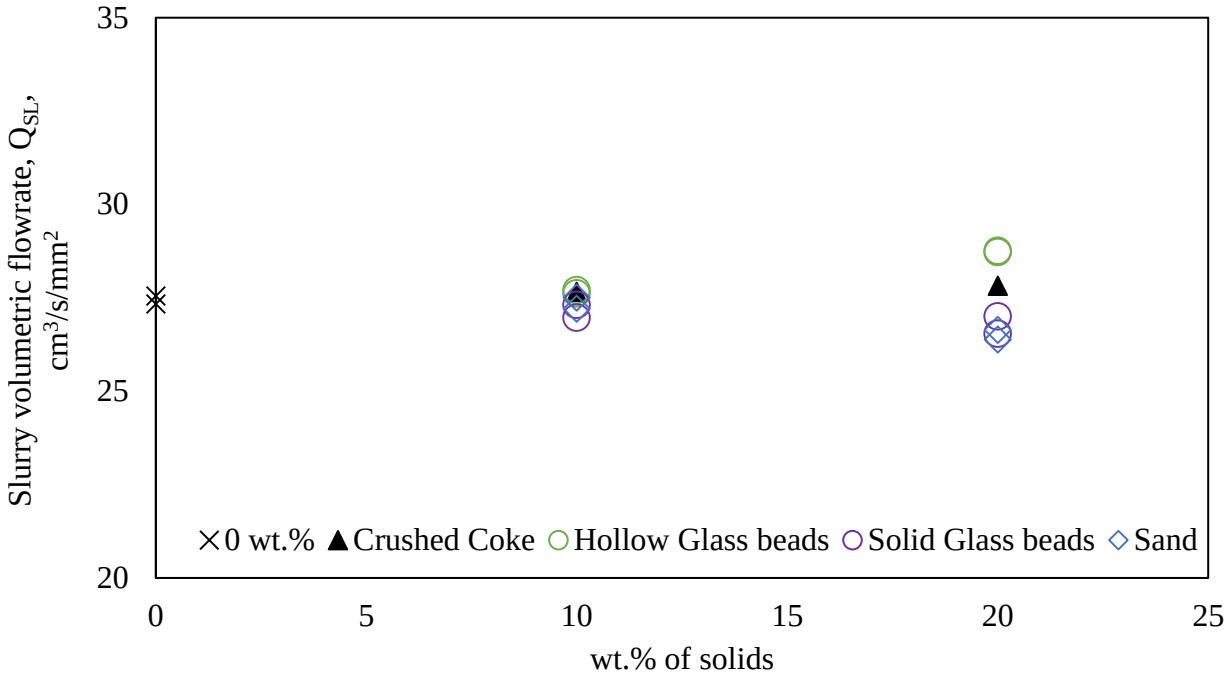

Figure 3.3: Impact of slurry concentration on total slurry mass flux at 2 wt.% GLR at 0 wt.% of solids. P_{ATO}: 558 psig; P_{BTK}: 285 psig; P_{PM}: 235 psig

3.3.2 Impact of slurry concentration on liquid flux at different GLRs

Figure 3.4 shows the impact of sand slurry concentration on liquid mass flux at different GLRs using a 2 mm nozzle. Across the different gas flowrates, the same trend is observed, the liquid flowrate drops with increasing concentration. Changing the GLR did not change the effect of the solids on the mass flowrates. **Table 3.1** shows the pressure conditions set for each GLR.

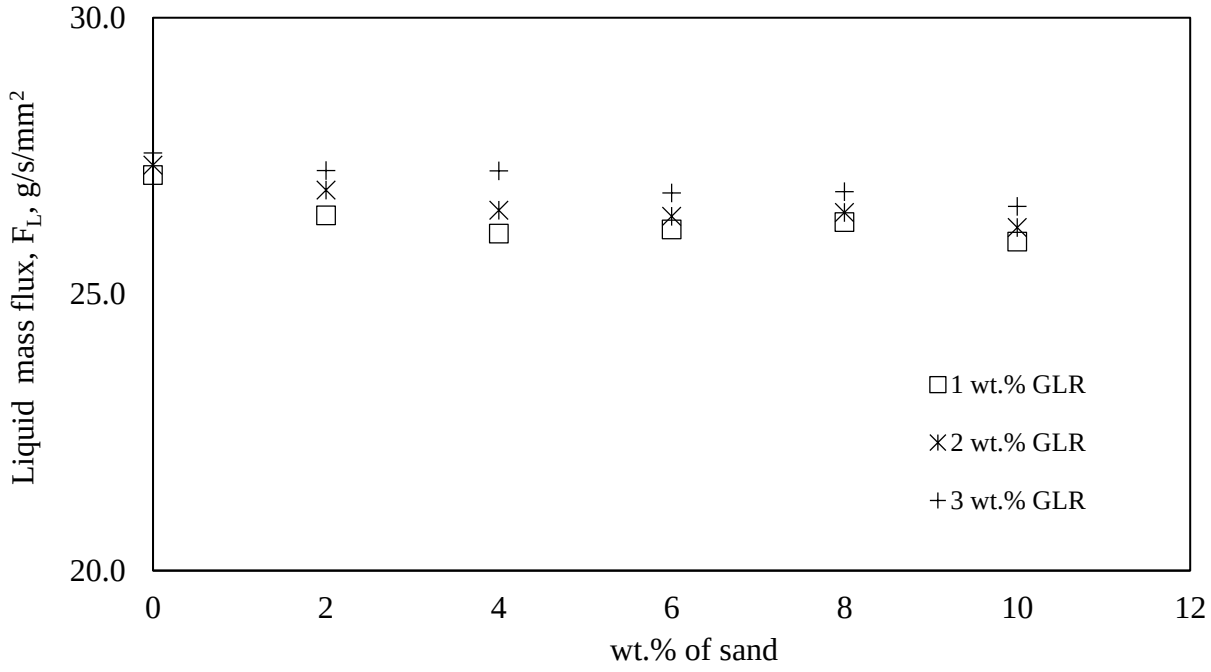

Figure 3.4: Impact of slurry concentration on liquid mass flux (water) at different GLRs

Table 3.1: The experimental pressure conditions for each GLR

GLR	1 wt.%	2 wt.%	3 wt.%
P_{ATO} (psig)	420	588	595
P_{BTK} (psig)	280	377	380
Pre-mixer pressure (psig)	177	240	283

3.3.3 Relevance of effective density and viscosity of the slurry

Since the concentration of the injected solids had some impact on the flowrate, the effective viscosity and effective density of the mixture were therefore examined to determine which had a more significant effect. Tests were done using solids free solutions: CMC solution (constant density and changing effective viscosity) and salt-solution (changing density and constant viscosity). **Table 3.2** shows the recorded conditions used for the experiments. The pressure conditions were kept constant for every run. The recorded values are similar and are essentially equal. The solids used for these experiments were sand particles (d_{psm}= 12.8 microns).

Table 3.2: The pressure conditions used for the different runs with different solvents

Solvent	Sand-water slurry	CMC solution	Salt solution
P_{ATO} (psig)	597	597	597
P_{BTK} (psig)	379	381	381
Pre-mixer pressure (psig)	283	281	284

All experiments were done at 3 wt.% GLR at 0 wt. solids (based on previous results, it is expected that both 1 wt.% and 2 wt. % GLR would have the same trend with 3 wt.% GLR). The range of viscosities considered was from 1 cp to 1.12 cP (for 0 to 0.25 wt.% CMC solution) which corresponds to 0 wt.% and 10 wt.% sand slurry, respectively. The viscosity of the CMC and salt solutions were measured using a Cannon-Fenske

viscometer (D75) while the effective viscosity of the slurry was estimated using **equation 2-3** from chapter 2. The densities ranged from 1 g/cm^3 to 1.07 g/cm^3 which correspond to 0 wt.% to 11.5 wt.% salt solution and 0 wt.% to 10 wt.% sand slurry.

Figure 3.5 shows a comparison between the results obtained from sand-water slurry mixture and the CMC solution. The total slurry mass flow increases with increase in the concentration of the solids. If the viscosity had a strong effect on the flowrate, the CMC graph would produce a similar trend as the slurry graph which is not the case. Changing the effective viscosity from 1 to 1.17 cP resulted in a negligible change in the total mass flowrate of the solution.

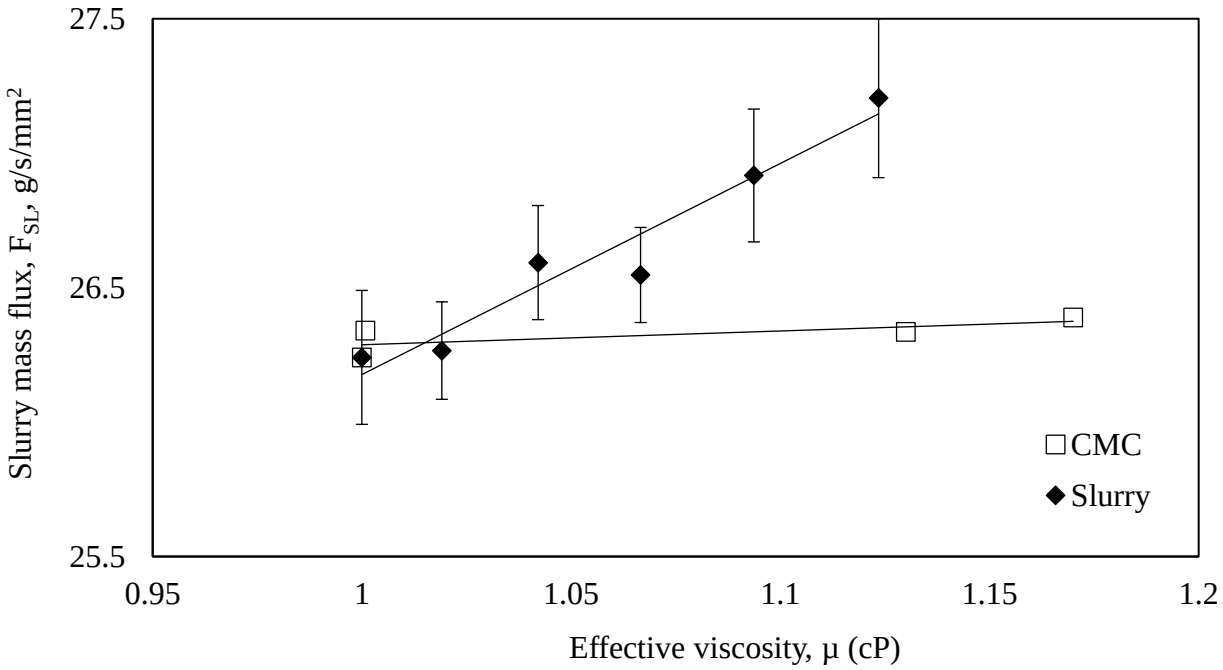

Figure 3.5: Effect of changing viscosity with changing concentration using equivalent CMC solution. (error bars show the estimate of the standard deviation of the replicates)

Figure 3.6 shows a comparison between the sand-water mixture and the salt solution results. An increased effective density resulted in higher mass flowrates for the solution. The values from the salt solution also agree with the slurry results, suggesting that the effective density affects the total slurry flowrate. The results show that the effective density has a stronger agreement with the slurry mass flowrate than the effective viscosity. This can be explained by recognizing that the fluid dynamics of the flow is more dependent on the inertial forces than the frictional viscous forces in the nozzle conduit. Hence for a homogenous flow in the turbulent regime, the effective viscosity of the flow at different concentrations is bound to be approximately the same as the viscosity of water (Vibeke and Steinar 2000). Therefore, it can be concluded, that the flowrate is most likely dependent on the effective density of the slurry than the effective viscosity.

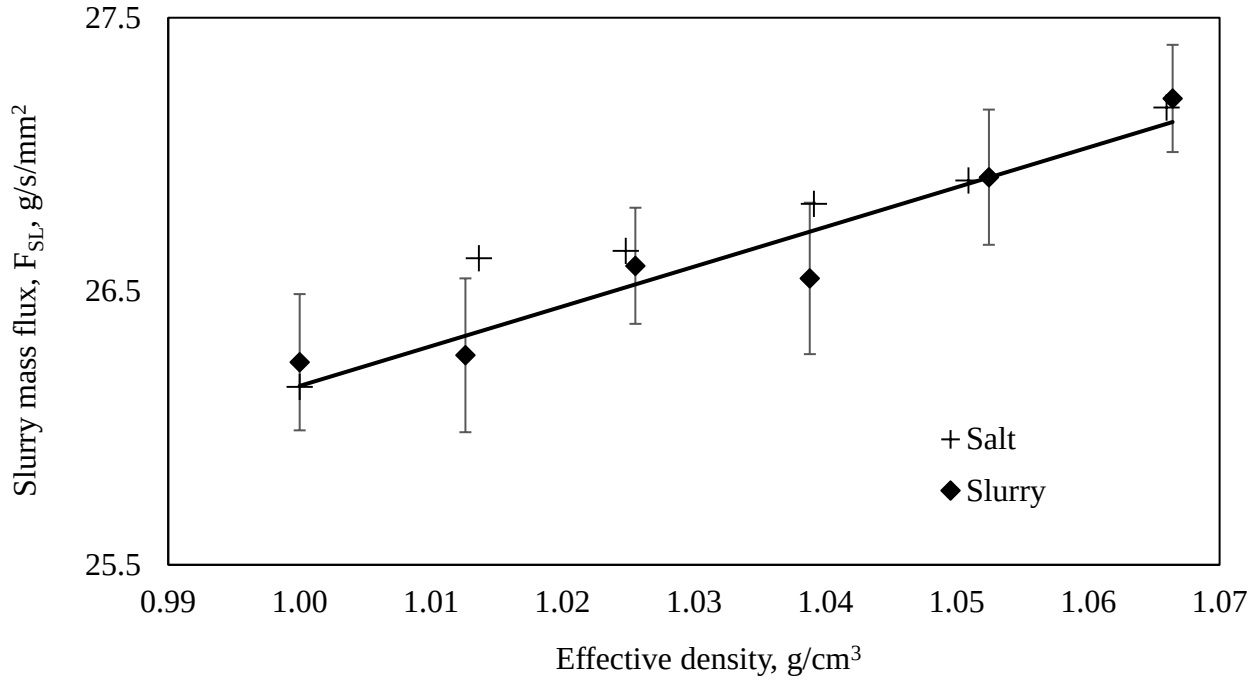

Figure 3.6: Effect of changing density with changing slurry concentration using equivalent salt solution. (error bars show the estimate standard deviation)

3.3.4 Effect of slurry concentration on the average spray angle

Figure 3.7 shows the relationship between average spray angle (in degrees) with a change in concentration from 0 to 10 wt.% of sand slurry with a 2 mm spray nozzle. **Figure 3.8** shows the effect of different injected solids on the spray angle for 0 to 20 wt.% solids with a 1 mm TEB nozzle. From **Figure 3.7,** between 0 wt.% and 10 wt.%, at 1 wt.%, 2 wt.% and 3 wt.% GLR, there was no significant change in the spray angle. Across the GLRs, there is a bit of a trend in the average spray angle. As the GLR increases from 1 wt.% to 2 wt.% to 3 wt.%, the average spray angle increases. The larger amount of gas could lead to the increase in the spray angle from 1 wt.% to 3 wt.% GLR. From **Figure 3.8**, the results show that even with changing the properties of the solids, there was still a negligible effect of the solids on the average spray angle.

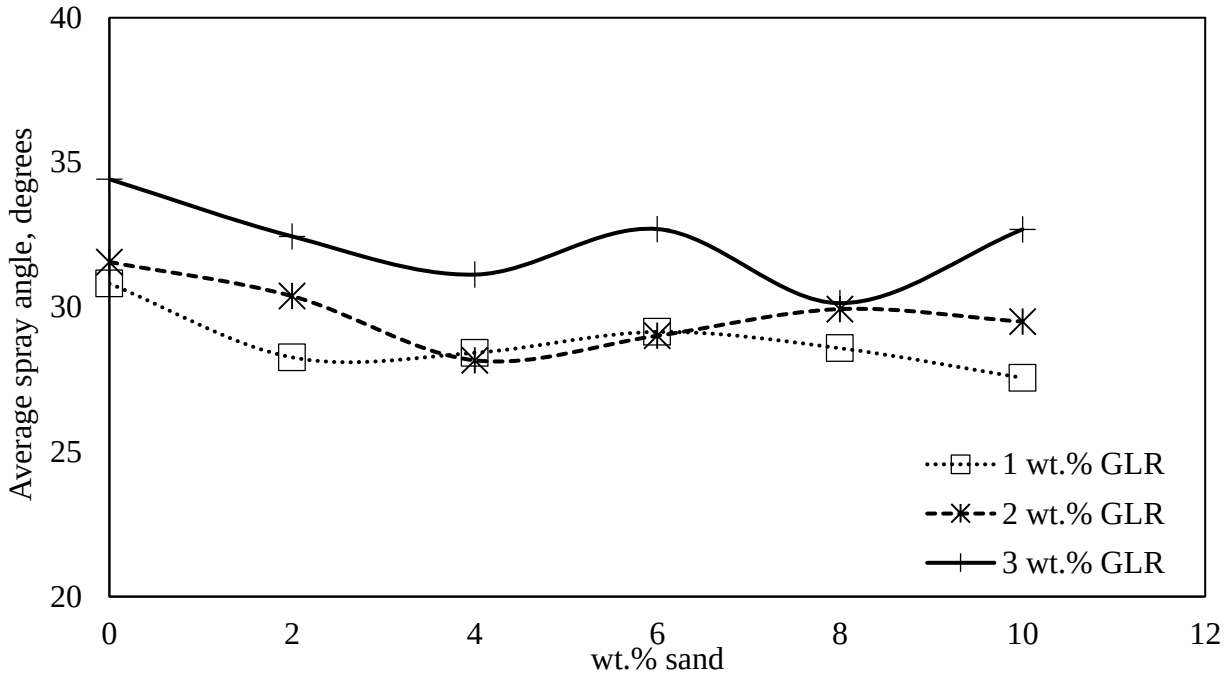

Figure 3.7: Average spray angle vs wt.% of sand at different GLR

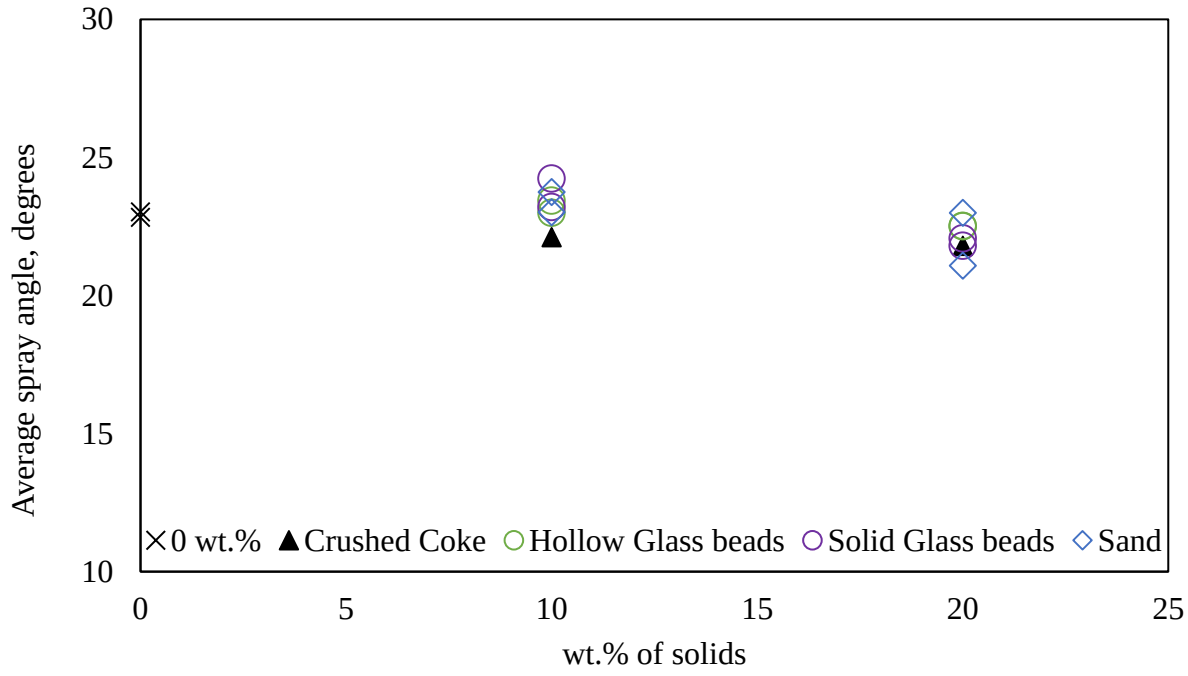

Figure 3.8: Average spray Angle vs wt.% of solids

3.3.5 Effect of slurry concentration on the stability of the spray

Figure 3.9 and **Figure** 3.10 show the stability of the spray based the video properties and the pre-mixer pressure readings. Both figures agree with each other as they both show that changing the concentration of the solids had a minimal effect on the stability of the spray. At 0 wt.%, the coefficient of variation is identical to the coefficient of variation at 10 wt.% and 20 wt.% for all solids cases which means that there is a negligible change in stability.

The coefficient of variation obtained from the video properties not only gives information about stability but also takes into consideration intensity of the pixels over the spray area which gives information about the liquid dispersion of the spray. Therefore, it can be deduced that the injected solids have a negligible impact on the stability and liquid dispersion of the spray. It is possible that since the mixture is well mixed, and flow is homogeneous, that the solids resulted in a negligible impact on the pre-mixer pressure readings. Also, from a physical point of view, the size of the particles is so small that in an open-air spray, the sand just follows the water and pixel fluctuations picked up by the camera is mostly caused by the liquid rather than by the solids.

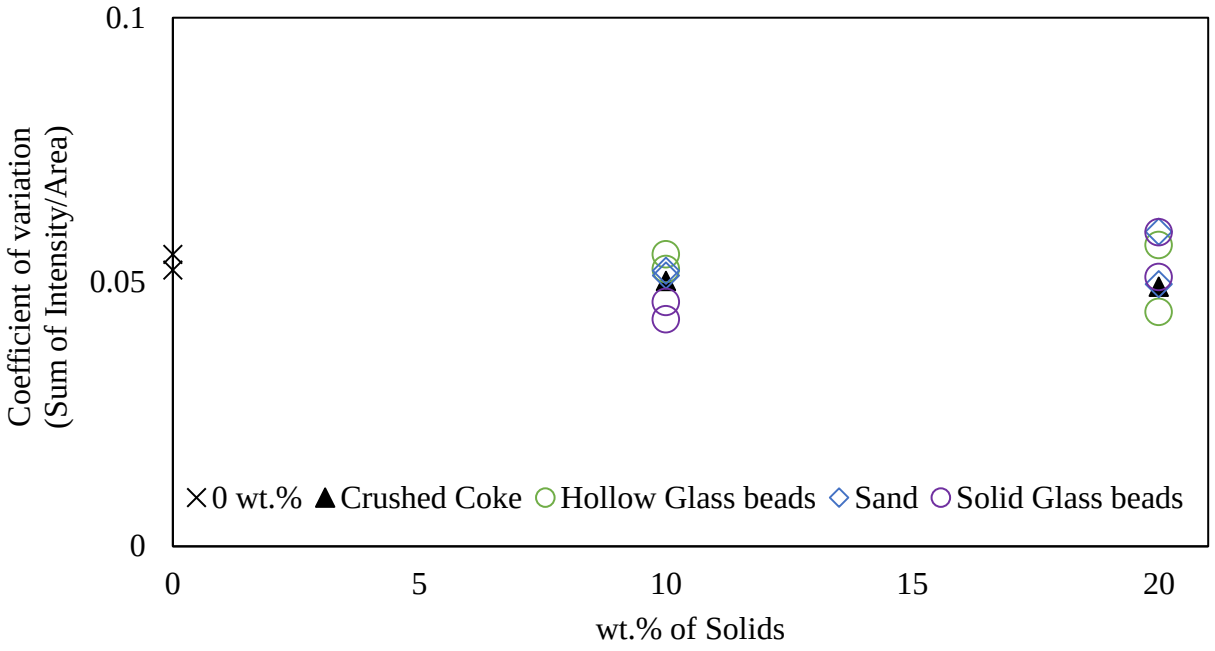

Figure 3.9: Stability of spray based on video analysis

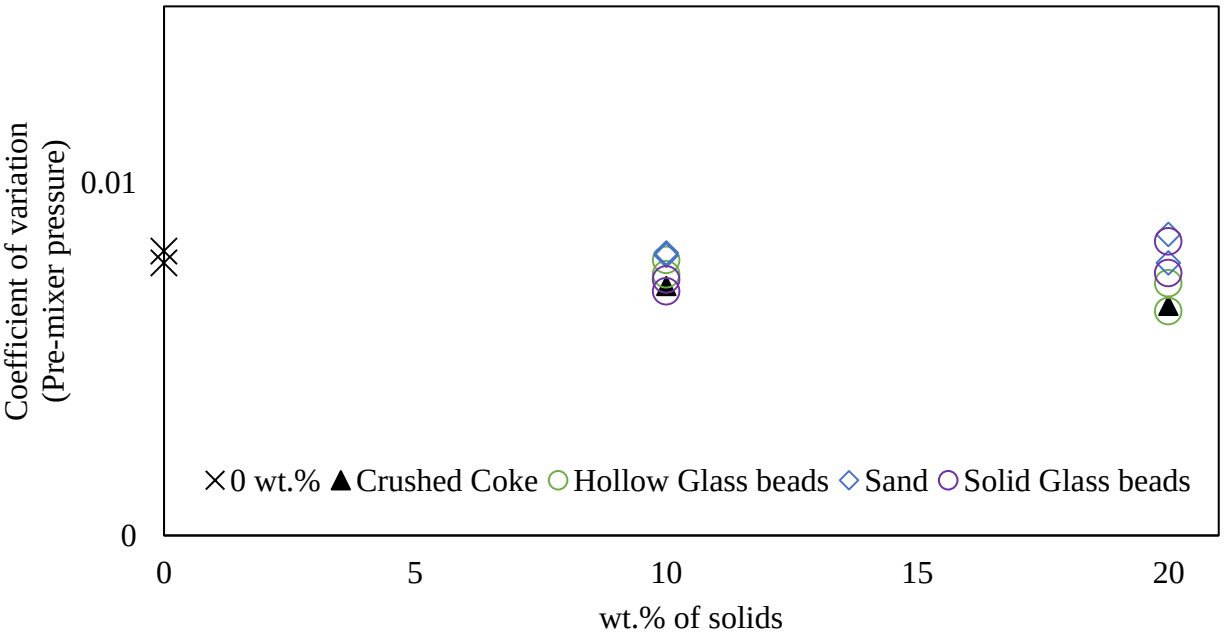

Figure 3.10: Stability of spray based on pre-mixer pressure readings

3.4 Conclusion

In this chapter, open-air experiments were conducted to investigate the effect of a slurry on the spray properties. The addition of solids results in a reduced mass flow rate of the liquid but an increase in the total slurry mass flowrate. Further experiments were carried out to explain these results and it was observed that the mass flowrate of the spray was dependent on the volume of sprayed liquid and the density of the slurry. The change in viscosity due to the addition of the solids had a negligible impact on the slurry flowrate. Also, the presence of the solids resulted in a negligible impact on the spray angle and stability.

Chapter 4

4 Impact of Slurry on Agglomerate Formation and Breakup

4.1 Introduction

Fluidization technology is an effective unit configuration used in a variety of processes such as pharmaceutical granulation, coal gasification, polymerization, fluid catalytic cracking (FCC) and Fluid Coking™ (Hesketh et al. 2002). Agglomeration phenomenon is common to some of these systems. For some systems such as granulation, agglomeration is essential and useful; however, the formation of agglomerates is undesirable for Fluid Coking. The presence of agglomerates in Fluid Cokers™ could lead to poor or reduced heat and mass transfer, resulting in lower yields of valuable products (Darabi et al. 2010), and increased fouling of reactor internals (Sanchez Careaga 2013), reducing operability. As mentioned in chapter 1, the Fluid Coker™ at Syncrude has a recycle stream which can contain fine solid particles. These fines are usually coke particles that have exited from the cyclone gas outlet tube into the bottom of the scrubber. Despite the extensive amount of research done on the Fluid Coker™ technology, the effects of these particles on agglomeration and liquid yield has never been studied. The objective of this chapter is to investigate the impact of the recycled solid particles on agglomerate formation and breakage. As some of the injected liquid gets trapped within agglomerates of different sizes (Knapper et al. 2003), this study focuses on the changes in trapped liquid, mass and size of agglomerates due to the presence of the injected solids.

4.2 Experimental Set-up and methodology

Detailed information regarding the experimental set-up, materials and methodology for the fluidized bed experiments and data analysis is available in chapter 2 of this thesis. The maximum concentration of solids considered was 20 wt.%. Higher concentrations at 30 wt.% and 40 wt.% of sand resulted in plugging of the 1 mm TEB spray nozzle.

To test for initial agglomerate formation, the fluidization velocity during injection (V_{gi}) was 0.44 m/s. After the injection, the fluidization velocity was immediately reduced to a velocity below the minimum fluidization velocity to ensure that there is no break-up of the agglomerates and the drying velocity (V_{gd}) was well below the minimum fluidization velocity (it will be noted as 0 m/s in the rest of this chapter).

Table 4.1 gives a summary of the combinations of fluidization velocities used to study the slurry effects of the injection. Different fluidization velocities during drying and injection were tested. For runs investigating the effect on both agglomerate formation and break-up, the V_{gd} was set to either 0.12 m/s or 0.44 m/s. Other tests were conducted to see the slurry impact with other values of V_{gi}. For each case, the average of the replicates was taken to produce a line graph to show the effects produced for each case.

Table 4.1:Summary of fluidization velocities tested during spray injection and drying of agglomerates

V_{gd} (m/s) / V_{gi} (m/s)	0	0.12	0.44
0.35	N/A	measured	N/A
0.44	measured	measured	measured
0.75 (m/s)	N/A	measured	N/A

4.3 Results and Discussion

4.3.1 Impact of Injected solids on initial agglomerate formation

Figure 4.1 shows the mass of the macro-agglomerates just after the initial agglomerate formation for sand slurry concentrations of 0 wt.%, 10 wt.% and 20 wt.%. Increasing the solids concentration in the slurry from 0 to 10 wt.% slightly reduced the mass of agglomerates, while increasing the solids concentration to 20 wt.% increased the mass of agglomerates. The size distribution of the agglomerates was not greatly affected by the solids' concentration in the slurry.

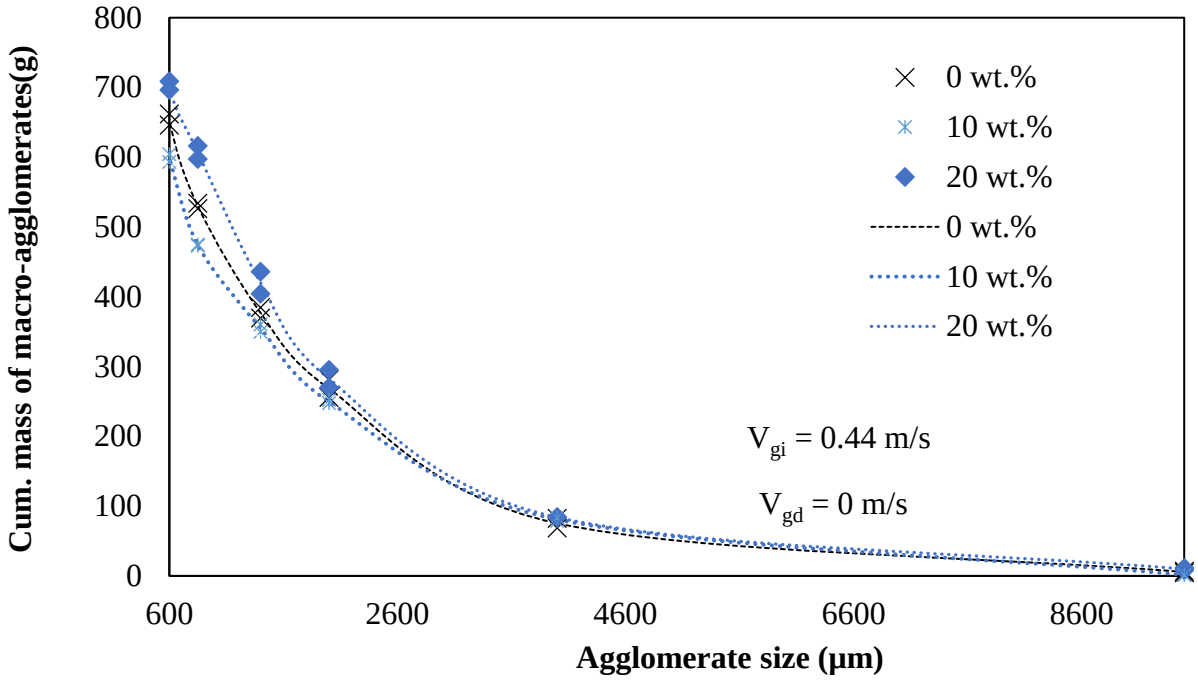

Figure 4.1: Mass of agglomerates after initial agglomerate formation vs. sand slurry concentration: 0 wt.%, 10 wt.% and 20 wt.%

Figure 4.2 shows how the average liquid-solid ratio (L/S) of the agglomerates was affected by the slurry concentration. Increasing the solids concentration in the slurry from 0 wt.% to 10 wt.% sand increased the average L/S ratio by 11.7% while increasing the solids concentration in the slurry from 10 wt.% to 20 wt.% sand produces a difference of 0.8%. This observation suggests that the presence of the particles makes the agglomerates wetter. As a result, it was important to study the fraction of the injected liquid that is trapped within the agglomerates.

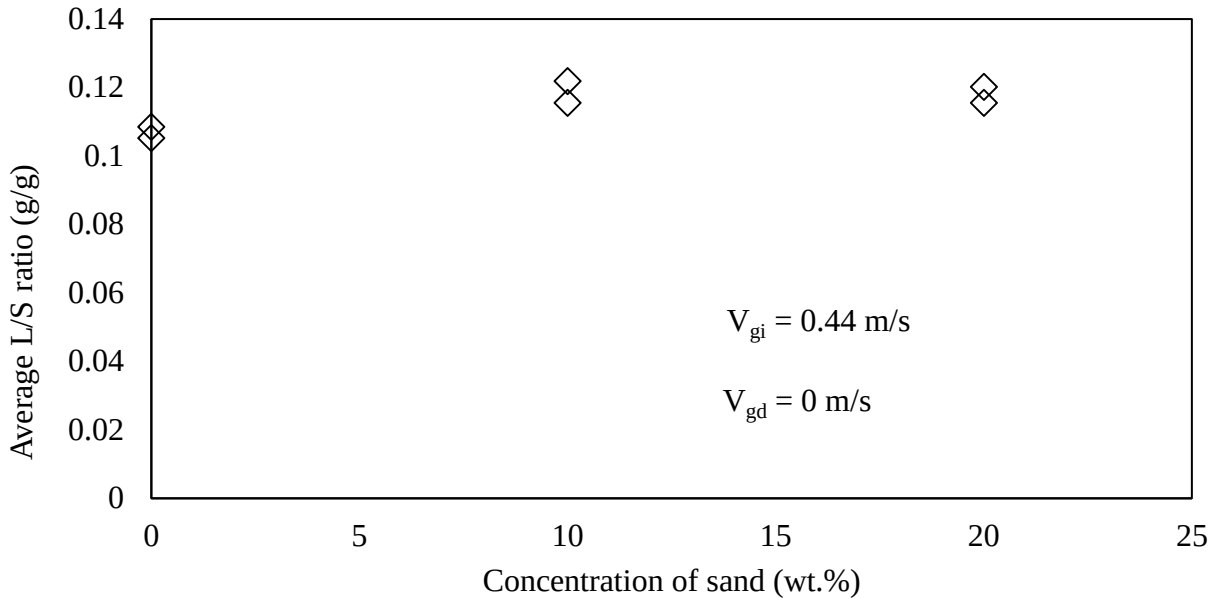

Figure 4.2: Average L/S ratio vs concentration of sand

Figure 4.3 shows the cumulative plot of the fraction of injected liquid that is trapped within the agglomerates against size cuts of the agglomerates at different solids concentrations in the slurry (0 wt.%, 10 wt.% and 20 wt.%). There is a small impact when going from 0 wt.% to 10 wt.%, but a more significant impact can be seen at 20 wt.% sand. The increase occurs over the entire range of agglomerate particle sizes. Going from 0 wt.% to 20 wt.% resulted in a 43.6% increase in the fraction of injected liquid trapped. This proves that the agglomerates are wetter when the fraction of injected solids is increased.

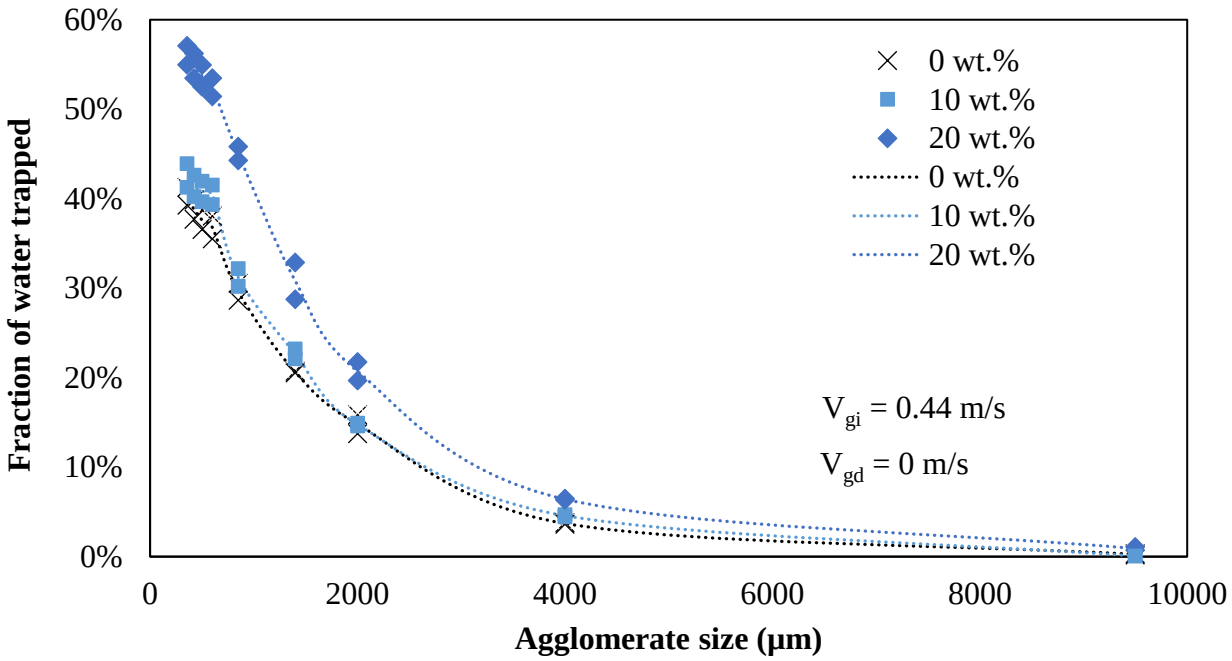

Figure 4.3: liquid trapped after initial agglomerate formation vs. slurry concentration 0, 10, 20 wt.%

Figure 4.4 shows the relationship between the Sauter-mean diameter of the agglomerates and the solids concentration in the slurry. The Sauter-mean diameter appears to have a non-linear increase at higher concentrations of sand suggesting that the sand slurry leads to the formation of larger agglomerates, primarily when the slurry concentration is increased from 10 to 20 wt.%. The increase in Sauter-mean diameter would suggest that the agglomerates are more stable at high solids concentrations in the slurry.

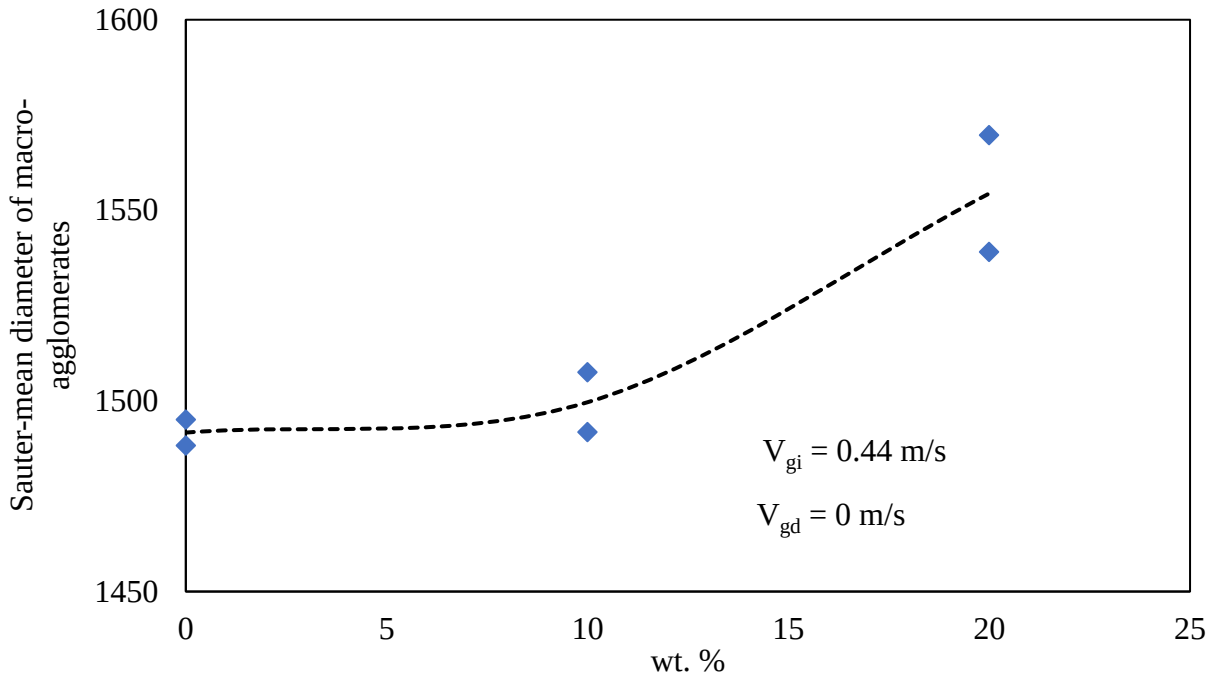

Figure 4.4: Sauter-mean diameter of macro- agglomerates vs. sand slurry concentration 0, 10, 20 wt.%

4.3.2 Impact of Injected solids on agglomerate break-up

After considering the effect of the solids on the initial agglomerate formation, more experiments were conducted to determine the impact after agglomerate break-up. This was achieved by increasing the fluidization velocity during drying, V_{gd} to 0.12 m/s and 0.44 m/s.

Figure 4.5 and **Figure** 4.6 show the impact of drying velocity at 0 wt.% solids and 20 wt.% sand, respectively. For experiments done with a pure solution of gum Arabic, without solids, the fraction of injected liquid trapped reduces with an increase in drying velocity. When the drying velocity was increased from 0 m/s to 0.44 m/s at 0 wt.% solids, the total fraction of injected liquid trapped dropped from 41.3% to 31.7%. Also, going

from a drying velocity of 0.12 m/s to 0.44 m/s resulted in a drop of liquid trapped from 37.1% to 31.7%. This is expected because the shear forces required to break the agglomerates are increased as the fluidization velocity, and hence gas bubble formation, is increased (Weber 2009). Also, Parveen (2013) observed that the breakage probability of agglomerates increases with fluidization velocity as more gas bubbles are formed which help break-up the agglomerates. However, when the injected slurry contained 20 wt.% sand, the fraction of liquid trapped only drops by a factor 1.05 (from 56.02% to 53.2%), much less than in the 0 wt.% case.

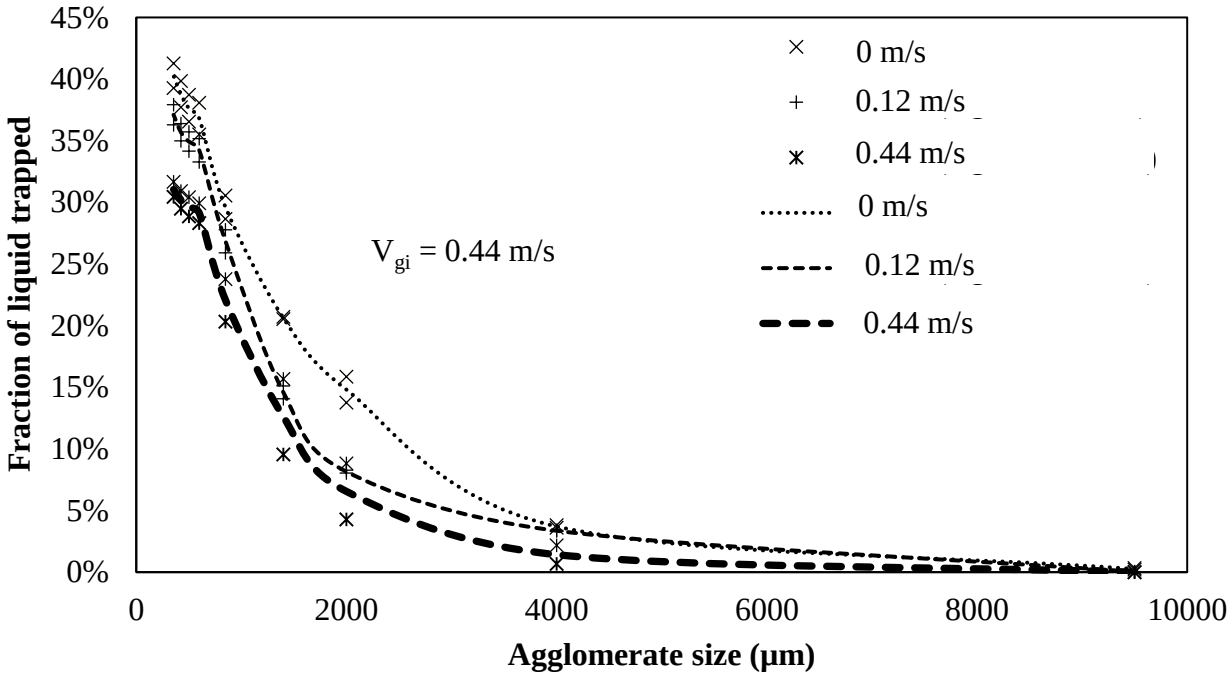

Figure 4.5: Impact of drying velocity at 0 wt.% solids

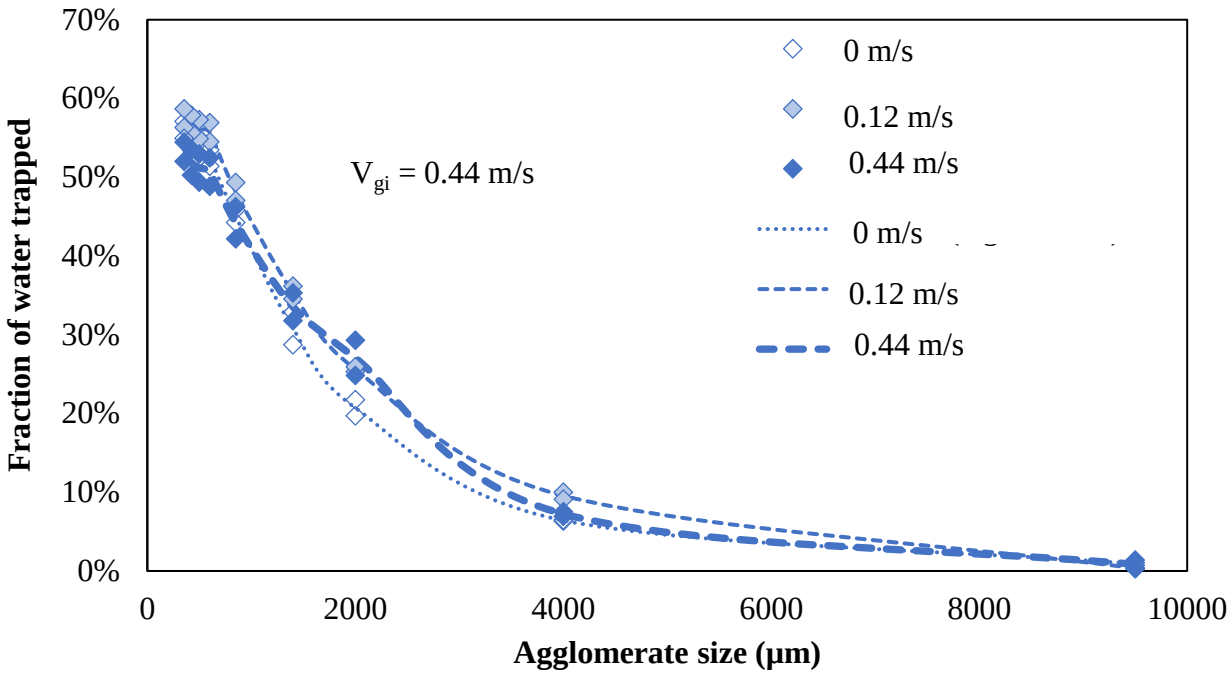

Figure 4.6: Impact of drying velocity at 20 wt.% sand

Figure 4.7 provides a summary of the total percentage of injected liquid trapped in the agglomerates for 0 wt.% and 20 wt.% sand slurry at the different drying velocities. The slope of the graph at 0 wt.% is higher than at 20 wt.%, suggesting that the drying velocity has a weaker effect when the fine particles are injected with the gum Arabic solution. The results suggest that the presence of the fine sand particles make the agglomerates wetter, stronger and more resistant to breakage.

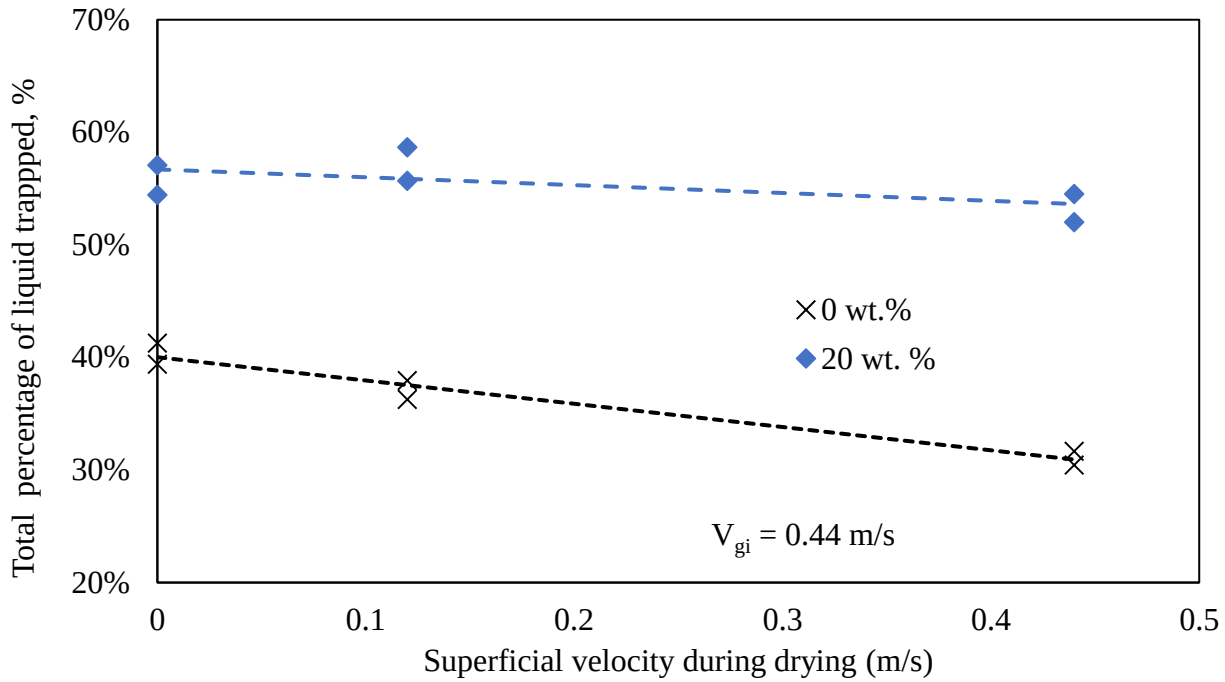

Figure 4.7: Total liquid trapped vs. drying velocity for both 0 and 20 wt.%

4.3.3 Combined impact of fluidization velocity and slurry solids on agglomerate formation and breakup

Figure 4.8 and **Figure** 4.9 show the effect of fluidization velocity during injection at 0 wt.% and 20 wt.% slurry concentrations, respectively. **Figure 4.10** summarizes the data from **Figure 4.8** and **Figure** 4.9 to show the total fraction of liquid trapped against superficial velocity during injection. With respect to both the 0 wt.% and 20 wt.% cases, increasing V_{gi} from 0.35 m/s to 0.44 m/s to 0.75 m/s continuously resulted in drop of the fraction of liquid trapped. This is expected, as increasing fluidization velocity during injection reduces the amount of agglomerates formed (Li 2016). Also, from a physical point of view, increasing fluidization velocity should lead to better contact between bed particles and injected liquid, leading to drier and weaker agglomerates, and hence a lower percentage of injected liquid trapped in the agglomerates.

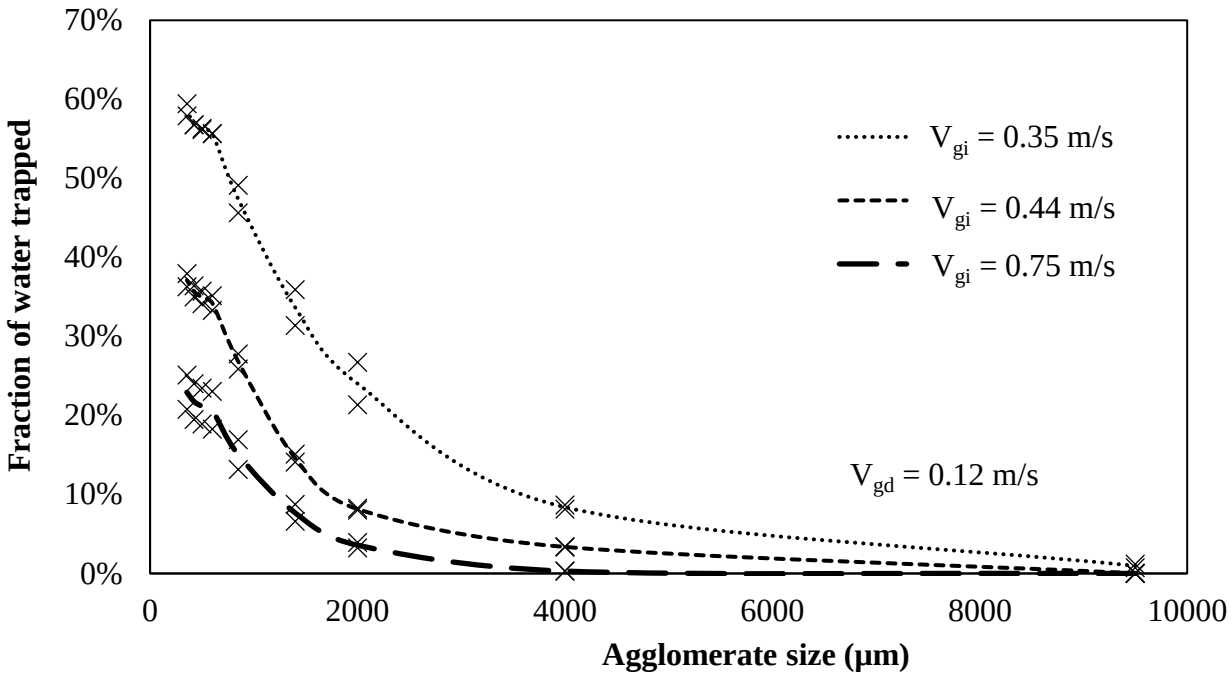

Figure 4.8: Effect of velocity during injection at 0 wt.%

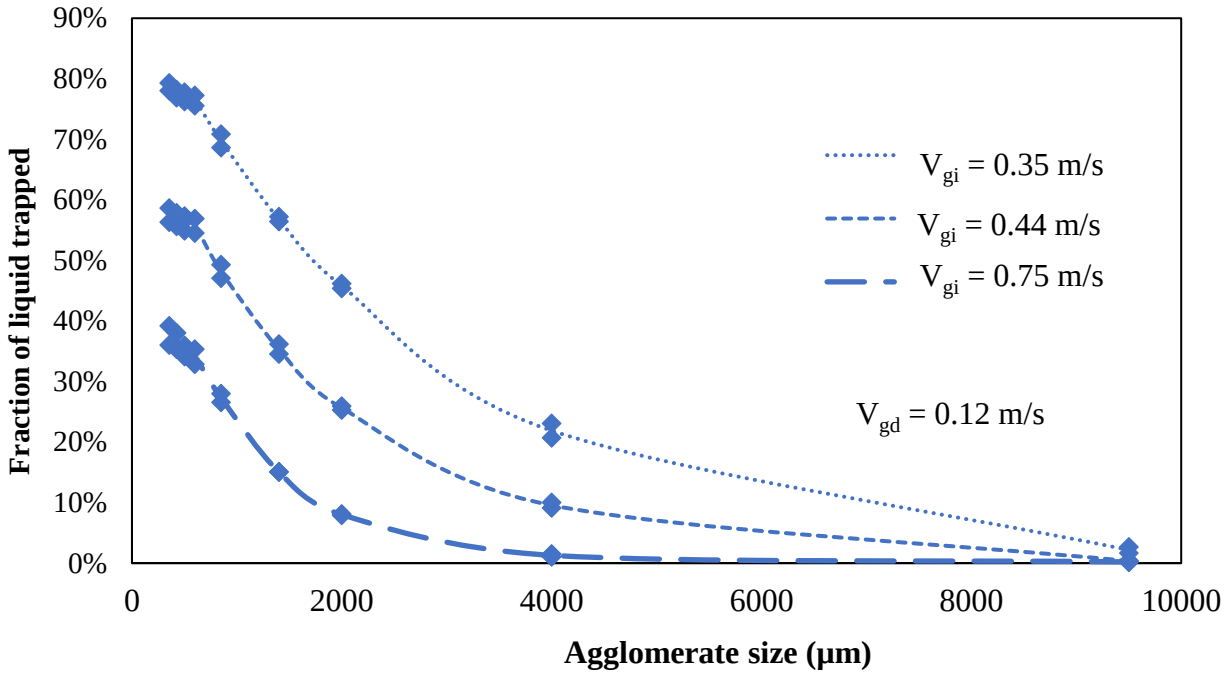

Figure 4.9: Effect of superficial velocity during injection at 20 wt.% sand slurry

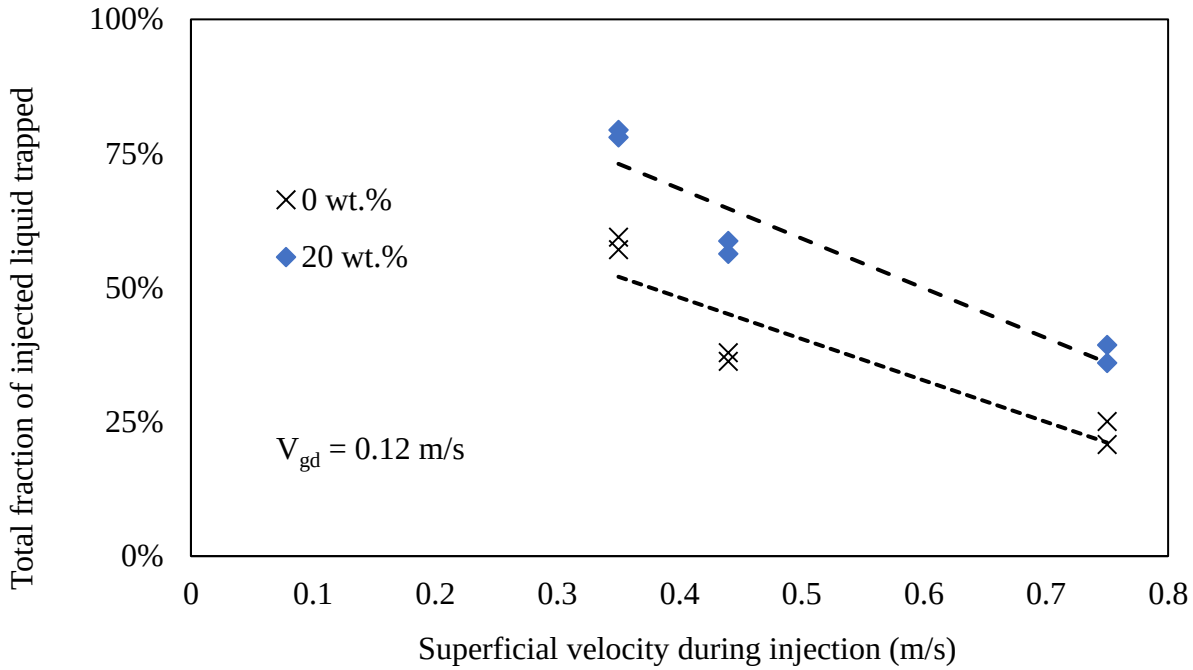

Figure 4.10: Total fraction of liquid trapped vs. superficial velocity during injection

To effectively compare the impact of the slurry the results from the two graphs were summarized into **Table 4.2** which shows that the impact of the solids becomes more pronounced at higher velocities. The ratio of liquid trapped at 0 wt.% to liquid trapped at 20 wt.% increases from 1.34 to 1.64 as the injection velocity increases.

Table 4.2:Effect of slurry concentration with respect to V_{gi}

V_{gi} (m/s)	Total % of liquid trapped at 0 wt.%	Total % of liquid trapped at 20 wt.%	$\frac{\text{Total \% of liquid trapped at 20 wt. \%}}{\text{Total \% of liquid trapped at 0 wt. \%}}$
0.35	58.7	78.7	1.34
0.44	37.1	57.5	1.55
0.75	22.9	37.6	1.64

Figure 4.11 and **Figure** 4.12 show the total mass of macro-agglomerates (600 μm to 9500 μm) and average L/S ratio against V_{gi}, respectively. The total mass of the macro-agglomerates drops with increasing superficial velocity which also accounts for less liquid trapped. The average L/S ratio drops slightly when increasing the superficial velocity. Since both mass of agglomerates and L/S ratio drop with superficial velocity, it can be concluded that the amount of liquid trapped with respect to superficial velocity is dependent on the mass of the agglomerates produced. The higher the velocity, the higher the amount of agglomerate breakage and hence less amount of liquid being trapped. The

results also suggest that the effect of the superficial velocity during injection is more dominant than the effect caused by the presence of solids in the slurry.

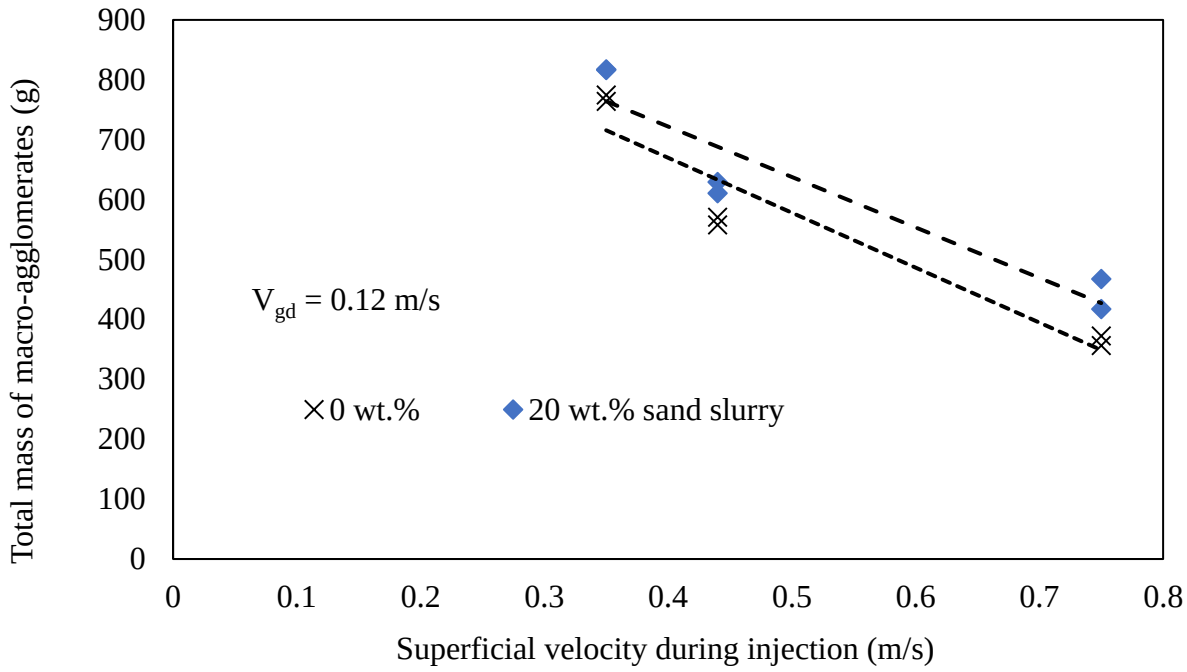

Figure 4.11: Mass of agglomerates vs. V_{gi} for both 0 and 20 wt.% sand slurry

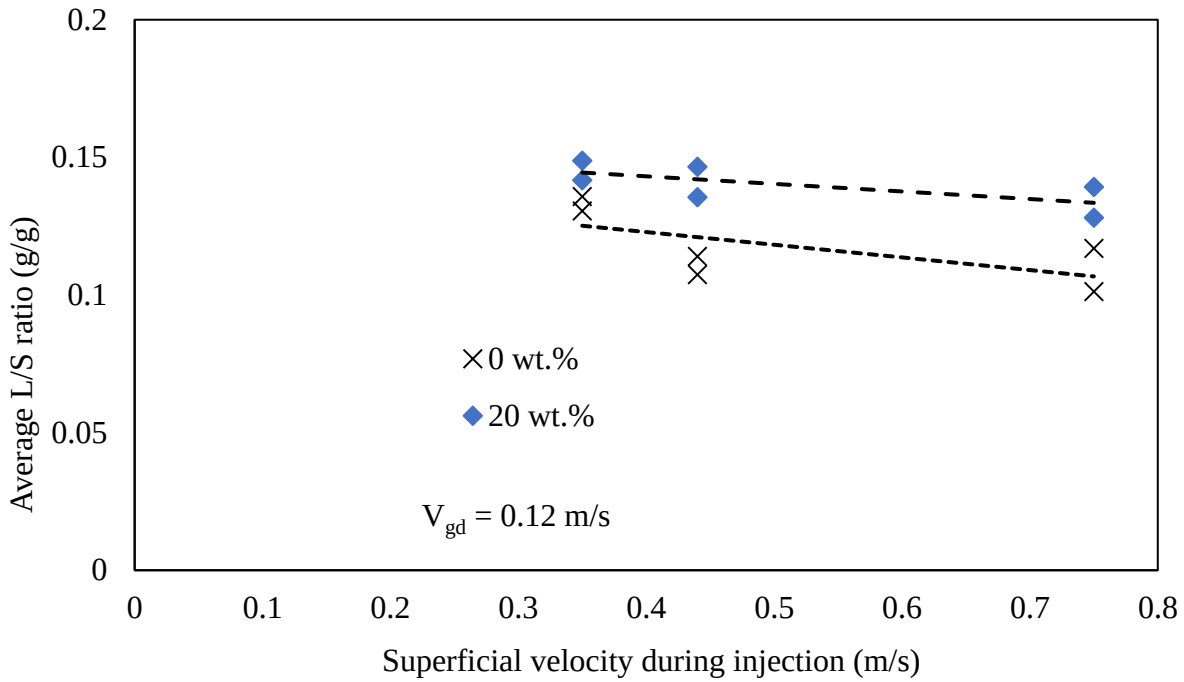

Figure 4.12: Average L/S ratio vs superficial velocity during injection, V_{gi}

Figure 4.13 shows that the Sauter-mean diameter of the agglomerates changed with superficial velocity during injection. The Sauter-mean diameter drops with increasing velocity however the difference in Sauter-mean diameter also drops with velocity. This is physically reasonable, as an increase in the turbulence in the bed should result in smaller agglomerates. The difference between the two cases drops because at higher velocities, breakage of agglomerates occurs more rapidly, and the agglomeration process becomes more dependent on the bed hydrodynamics.

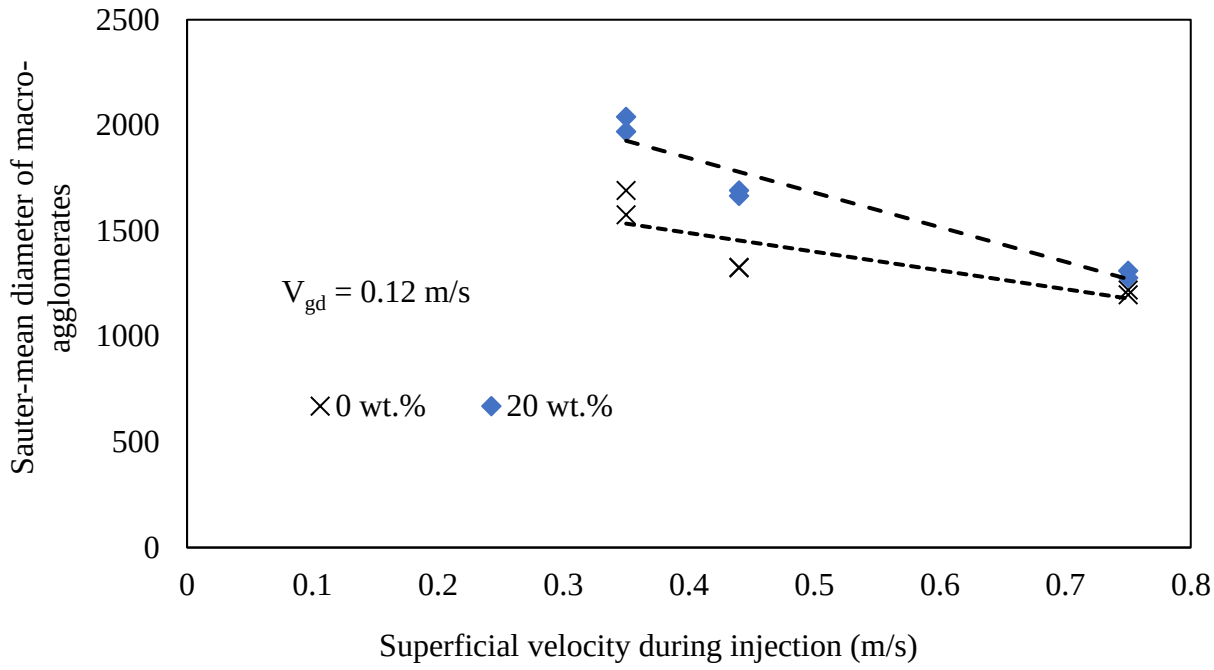

Figure 4.13: Sauter-mean diameter of agglomerates vs. V_{gi} for both 0 and 20 wt.%

4.3.4 Discussion of slurry impact on agglomeration behavior

From the results described, the introduction of the solid particles into the slurry has a significant impact on the formation and breakage of agglomerates. The possible reasons for this impact can be classified into three subsections: impact on spray behavior, impact on drying kinetics, and impact of slurry particles on agglomerate formation and stability.

4.3.4.1 Spray Behavior

Different studies have been carried out to study the effect of spray stability on agglomeration. Li (2016) has shown that pulsating sprays produce more agglomerates than stable sprays. Hulet et al. (2003) has shown that more stable jets lead to an increase in the solids flowrate entrained in the spray jet, leading to better mixing and liquid distribution within the system. A more stable spray has more efficient liquid-solid contact

(Portoghese 2007) which results in a lower fraction of injected liquid trapped inside the agglomerates. However, (Sabouni et al. 2011) showed that sprays with very specific pulsation characteristics can result in better liquid-solid contact than stable sprays. The effect of solids on spray stability was investigated with the open-air results given in chapter 3. The presence of the solids had a negligible effect on the spray stability.

Much like spray stability, the spray angle influences the number of fluidized particles entrained in the spray jet. Ariyapadi (2004) developed a model to calculate the flowrate of solids entrained in the liquid jet which considers the spray angle. According to this model, increasing the spray angle leads to an increase in entrained solids, improves mixing and reduces the L/S ratio in the agglomerates. In chapter 3, it was shown that the presence of the solids resulted in a negligible change in the spray angle, ruling out this option as a reason for the increase in injected liquid trapped.

Figure 4.14 shows the spray jet penetration with and without solids. The method used to obtain the jet penetration in the fluidized bed is available in chapter 2. An increase in jet penetration could mean that the agglomerates develop in a slightly different region of the bed. **Figure 4.14** shows, however, that the presence of the solids appears to have a negligible effect on the jet length and would therefore not have affected the amount of liquid that is trapped in the agglomerates.

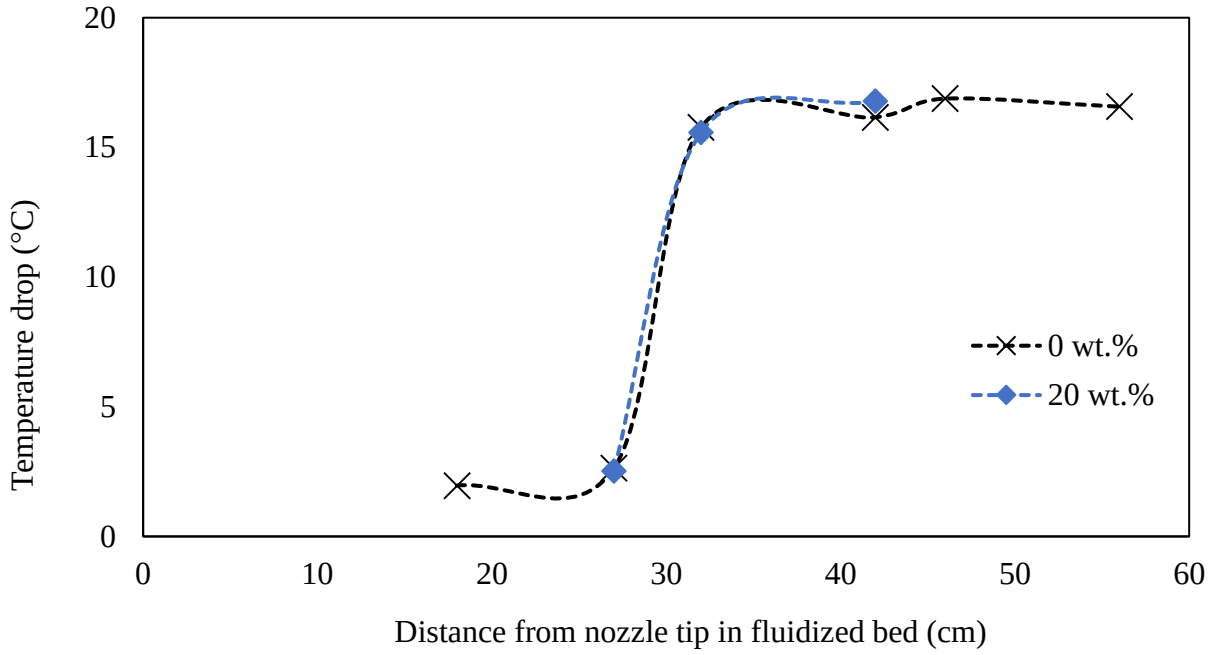

Figure 4.14: Jet penetration vs temperature drop for both 0 wt.% and 20 wt.%

The presence of slurry solids did not produce a significant effect on the spray characteristics that are known to have an impact on liquid-solid contact. Injecting solids with the liquid resulted in a negligible impact on the spray stability, angle and length. Since these spray characteristics remain relatively constant, they cannot account for the slurry impact on the formation and breakage of agglomerates in the bed.

4.3.4.2 Drying Kinetics

The presence of sand particles could affect the drying kinetics of the agglomerates in the fluidized bed. If agglomerates dry faster, their probability of being broken up by gas bubbles should be smaller, resulting in more liquid trapped within the agglomerates. This behavior is in line with what Pardo Reyes (2015) observed, where increasing bed

temperature from 120°C to 130°C to speed up heat transfer dropped the fraction of liquid trapped from 44 wt.% to 74 wt.%.

Table 4.3 compares the thermal properties of sand and water. Sand has a higher thermal conductivity (k) than water, suggesting that replacing water with the 20 wt.% sand slurry case results in faster heat conduction within the agglomerates. The average specific heat capacity (C_p) for the 20 wt.% sand slurry would range between 3496-3545 J/kg·K for temperatures ranging from 25 °C to 99.59 °C. This represents a 16 % C_p reduction compared to the pure gum Arabic solution. Therefore, heating up the same mass of binder to the boiling point of water would take less energy with the 20 wt.% slurry. For the same mass of slurry, the mass of liquid to be evaporated will be less, hence the 20 wt.% slurry will require a lower heat of vaporization from 2257 J/(kg liquid) to 1806 J/(kg slurry). Clearly, the total amount of energy required to dry the liquid bridges for the slurry case is less than it is for the base case, which means the slurry agglomerates dry faster and are thus more likely to solidify before they break up. The total amount of energy required to dry the agglomerates can be calculated using:

$$\Delta H = C_p \Delta T + \Delta H_{\text{vaporisation}} \qquad \textbf{4-1}$$

Using the above equation gives $\Delta H = 257 \times 10^4$ J/ (kg liquid) and 206×10^4 J/ (kg slurry) for base case and slurry case, respectively. This means that the slurry case requires 19.8% less energy for drying than the pure gum Arabic case.

Table 4.3: Thermal properties of sand slurry and water. From Domalski and Hearing (2005) and Thermtest Inc. (2018)

Material	Thermal conductivity, k (W/m·K)	Specific Heat capacity, C_p (J/kg·K) (25 °C – 99°C)	Required energy to evaporate water, $\Delta H_{vap.}$ (J/g of injected mixture)
Sand	6.49	740 - 850	Not Applicable
Water (0 wt.% sand)	0.603	4180 - 4220	2257
20 wt.% Sand slurry	1.78	3500 - 3550	1806

With a higher thermal conductivity, heat transfer by conduction is faster in the slurry agglomerates. Also, the total amount of energy required to dry the agglomerates is reduced, resulting in faster drying and more liquid being trapped inside the agglomerates. Therefore, the change in drying kinetics brought about by the presence of the fines affects the agglomeration process and could result in a higher fraction of liquid trapped in the agglomerates.

4.3.4.3 Agglomerate Formation and Stability factors

The formation and stability of the agglomerates could be affected by different factors such as slurry viscosity and density, as well as the particle properties within the agglomerates, such as size distribution, shape and wettability. For these results, the only factors affected by the presence of the slurry solids are the effective viscosity of the slurry, and the particle size distribution in the agglomerate (i.e., slurry particles and bed particles are sand, with the same wettability and shape, but different sizes) and the packing structure and density of the final agglomerate. Increasing the solids concentration increases the effective slurry viscosity and density from 3 cP to 3.96 cP and from 1000 kg/m^3 to 1140 kg/m^3, respectively (refer to chapter 2). The size distribution of the particles within the agglomerates becomes a bi-modal size distribution, as it is a mixture of bed particles and slurry particles. Also, injecting the fines could result in a filler effect within the structure of the agglomerates.

Prior work investigated the effects of liquid binder properties, especially viscosity, on agglomeration. Pardo Reyes (2015) showed that increasing viscosity from 2.2 cP to 2.6 cP led to an increase in liquid trapped from 35 wt.% to 39 wt.%. Also, Schæfer (2001) performed experiments to understand the effect of binder properties on granulation. The author granulated different calcium carbonate particles using polyethylene glycol (PEG) as the binder and noticed that increasing viscosity led to an increase in the size of the agglomerates until reaching a growth optimum. Increasing viscosity leads to stronger liquid bridges, the agglomerates formed are thus stronger and are more resistant to breakage, leading to wetter and more stable agglomerates.

Table 4.4 shows the different viscosities at different wt.% of sand and their respective fraction of trapped liquid after the initial agglomeration. The effective viscosity was estimated using **equation 2-3** from chapter 2. The viscosity does not increase linearly with respect to the sand weight fraction. This is similar to the behavior of the liquid trapped in the agglomerates, which has a non-linear increase from 0 wt.% to 20 wt.% of sand. This behavior suggests that the change in the fraction of liquid trapped was affected by the increase in the effective slurry viscosity and could explain why the agglomerates are stronger and wetter.

Table 4.4: Change in effective viscosity and liquid trapped with respect to solids concentration in the slurry

wt.% of sand	Effective viscosity (cP)	% of injected liquid trapped
0	3	40
10	3.36	43
20	3.96	56

The introduction of small particles in the injection stream results in a bi-modal distribution of sand within the agglomerates. It has also been found that a wide size distribution of particles in an agglomerate increases its strength (Iveson et al. 2001). According to Rondeau et al (2003), the presence of the fines in the agglomerates makes

them stronger and more stable as the fines fill up interstitial spaces within the agglomerates. Previous research has shown a correlation between bi-modal distribution and an increase in agglomerate size. Lin et al. (2011) have shown that a bimodal size distribution of bed particles resulted in more agglomerates than a narrow size distribution.

In the polymer and construction industry, small particles known as fillers are used to strengthen epoxy composites and cement, respectively. In the design of epoxy composites, Ahmad et al. (2008) showed that addition of silica particulate fillers increased the tensile and flexural strength of polymer composites. Ahmad et al. (2008) also found that increasing the concentration of silica fillers resulted in stronger composites. He et al. (2012), noted that the presence of fillers improves the packing density of concrete as denser micro-structures enhance the mechanical properties and durability of the concrete. Dittanet and Pearson (2012) also showed that increasing the concentration of silica nano-particle fillers significantly improved the toughness of the final composites. In relation to this study, the injected sand particles could act as fillers in the agglomerates making it more stable and resistant to breakage. This means that the agglomerates formed would have a more stable packing structure and higher packing density at 20 wt.% solids than at 0 wt.%. Also, Chen et al. (2003) have shown that the presence and increase in concentration of silica sand as fillers in composites increase the amount of water that the composite can absorb. This is because sand is hydrophilic, and the presence of fillers creates small pores that the water can seep into. This could probably explain the significant difference obtained for liquid trapped produced by the introduction of sand particles as part of the injected slurry. The result from this study

show a consistent increase in the fraction of liquid trapped (from 40% to 56%) with increased concentration of sand in slurry (0 wt.% to 20 wt.%).

Chapter 5

5 Impact of Particle Properties on Liquid distribution in the fluidized bed

5.1 Introduction

In chapter 4, it was observed that the presence of solid particles in the injected mixture led to more liquid trapped and more stable agglomerates. The previous was attributed to the increase in effective viscosity, presence of the fines, and/or a change in drying kinetics. The objective of this chapter is to explore how the slurry impact changes with the properties of the injected slurry solids and to understand which mechanism is responsible for the impact produced by the injected solids. The particle properties studied in this chapter were size, density, shape and wettability. In the industrial case, it is possible to have not only coke but other particles, such as clay, being recycled to the coker. It is thus useful to understand how the change in the injected particle properties could affect the agglomerate stability and liquid distribution within the agglomerates. Changing the particle properties also helps to understand which mechanisms are responsible for the solids' impact on agglomerates and liquid distribution.

5.2 Experimental set-up and methodology

Table 5.1 shows the properties of the slurry solids used for the runs in this chapter. The concentration of the slurry for each experiment was kept constant at 20 wt.% solids. The fluidization velocities during injection and drying were kept constant at V_{gi} = 0.44 m/s and V_{gd} = 0.12 m/s respectively. The method for analysis of agglomerates and calculation

of liquid trapped is described in chapter 2. For each case, the average of duplicates was taken to produce a line graph to compare the observed effects for each case.

Table 5.1: Injected solids and their individual properties. From Weber (2009) and Thermtest Inc. (2018)

Solid material	Properties			
	Particle Density (kg/m^3)	Particle shape	Wettable with water	Sauter-mean diameter (μm)
Sand	2650	angular	Yes	12.8
Hollow glass (H.G.) beads	1000	round	Yes	9.8 61
Solid glass (S.G.) beads	2450	round	Yes	10.2
Coke	1450	angular	No	9

5.3 Results

5.3.1 Impact of particle size of injected solids

Figure 5.1 and **Figure** 5.2 show the impact of particle size on the amount of liquid trapped and the mass of macro-agglomerates (600 μm to 9500 μm), respectively. **Figure**

5.3 shows the change in L/S ratio with agglomerate size for the different cases. Hollow glass beads (H.G. beads) of different particle sizes were used as slurry solids to study the effect of particle size. Increasing the Sauter-mean diameter of the injected solids from 9.8 microns to 61 microns led to a slight increase in the fraction of liquid trapped from 38.3% to 39.7% while the total mass of the macro-agglomerates dropped from 572 g to 464 g. Also, there appears to be differences in the size distribution as the runs with smaller hollow glass beads appear to have formed more of the larger agglomerates, giving a Sauter-mean diameter of 1623 microns than the agglomerates obtained with the larger slurry particles which had a Sauter-mean diameter of 1550 microns. Given that the mass of the macro-agglomerates drops when particle size is increased but the liquid trapped slightly increased, it is likely that the larger particles formed wetter but less stable agglomerates.

Comparing the two hollow glass beads cases to the pure gum Arabic shows an increase in liquid trapped especially for the larger agglomerates. This indicates that the presence of the solid does affect agglomerate formation and break-up. From the L/S ratio graph, there appears to be a slight increase in liquid trapped between the two cases. This is because the agglomerates are weaker when the particle size is increased resulting more breakage and hence a lesser amount of agglomerates.

The results are in accordance with previous research on particle size and agglomeration. In granulation processes, larger particle sizes could result in larger pores within the agglomerates (Weber 2009), leading to larger a separation distance between particles, weaker liquid bridges and hence weaker agglomerates (Simons 1996). Weber (2009) found out that agglomerates made from smaller particle sizes took longer to completely

fragment than agglomerates made from larger particle sizes. Finally, Zhou and Li (1999) explain that the inter-particle cohesion in the agglomerate increases with decreasing size of particles. Hence, it is reasonable that the agglomerates become less stable with increasing particle size.

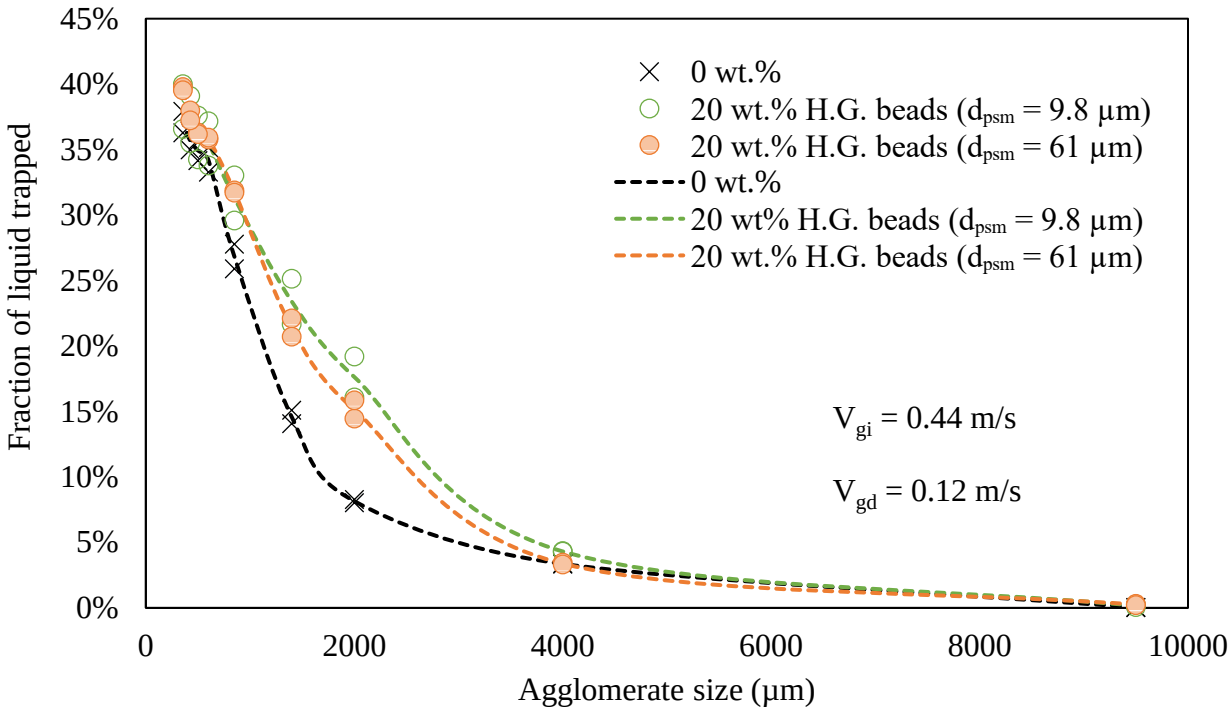

Figure 5.1: Effect of changing particle size on slurry impact on liquid trapped

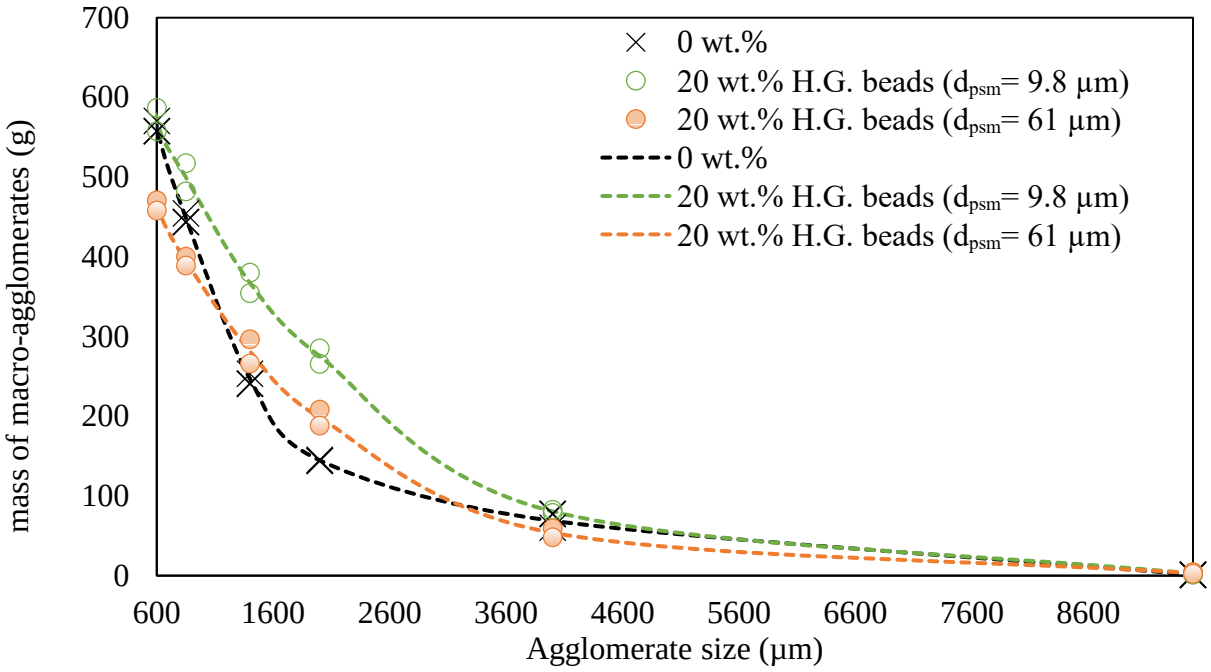

Figure 5.2: The effect of different injected solids particle size on the mass of agglomerates

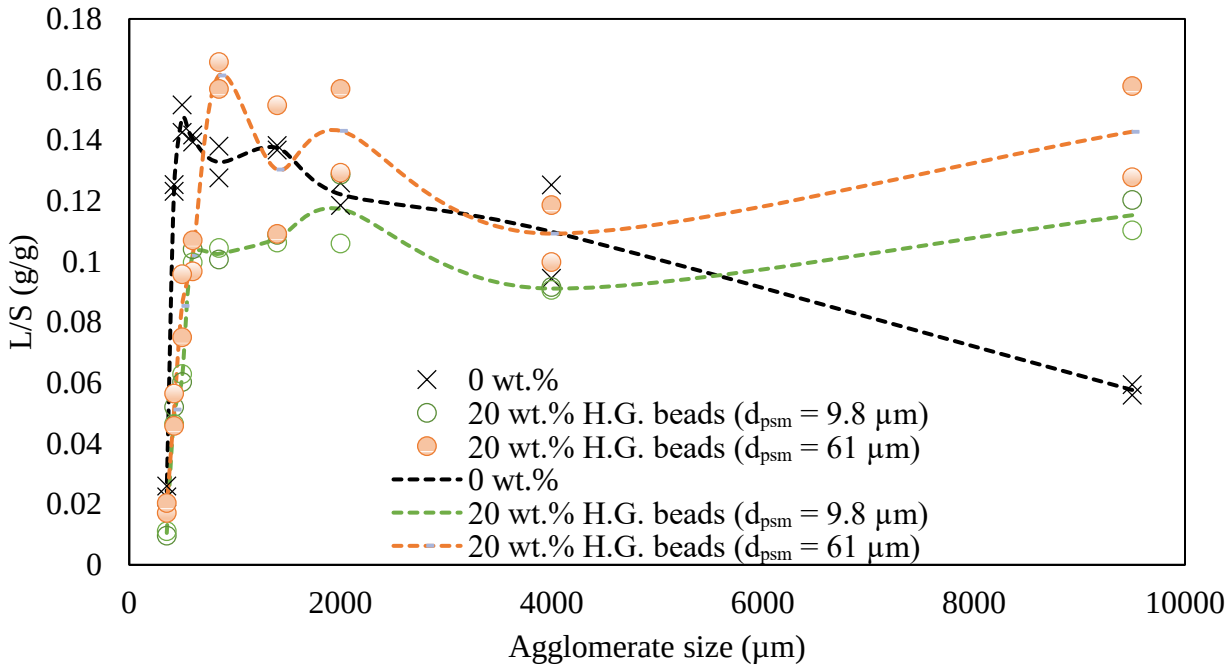

Figure 5.3: L/S ratio vs agglomerate size

5.3.2 Impact of particle density of injected solids

Figure 5.4 and **Figure** 5.5 show the impact of the injected particles density on the fraction of liquid trapped and the mass of macro-agglomerates respectively. **Figure 5.6** shows the change in L/S ratio with agglomerate size cut. The effect of the particle density of the injected solids was examined using hollow glass (H.G.) beads and spherical glass (S.G.) beads as they were both spherical but had different particle densities. When the density of the injected particle is increased from 1000 kg/m^3 to 2450 kg/m^3, there was a significant increase in the fraction of liquid trapped, the mass of the macro-agglomerates, and the L/S ratio. The fraction of injected liquid trapped goes up by a factor of 1.34, from 38.3% to 51.2% and the mass of macro-agglomerates goes up from 572 g to 599 g. This suggests that the heavier beads produce more stable agglomerates and results in an increase in liquid trapped. The size distribution for the two appear to be similar, with the Sauter-mean diameter increasing from 1623 microns to 1691 microns, a difference of 4%, when going from hollow beads to regular beads.

When both runs are compared with the no solids case, there is a significant effect of the solids. It is interesting to note that the density of the gum Arabic solution (at 0 wt.%) and the density of the mixture with 20 wt.% H.G. beads are both 1000 kg/m^3. The 0 wt.% case and the H.G. beads case produce almost the same mass of agglomerates (564 g vs. 572 g), however, the size distribution is different as the H.G. beads produces more of the larger agglomerates. This is probably because the presence of the solids makes the larger agglomerates more stable than they would have been without it.

There has not been any research done to evaluate the effect of changing effective density in agglomeration or filler density in the polymer industry. By increasing the density of the slurry, the density of the resulting agglomerates is likely to be higher resulting in stronger agglomerates. Parveen (2013) has shown that agglomerates with lower densities break faster than denser agglomerates. The author also observed that the lighter agglomerates spend more time in the upper region of the bed where the gas bubbles are larger and are hence more prone to breakage. This suggests that agglomerates formed from the heavier particles (S.G. beads) are less likely to be broken up because they will be located closer to the bottom of the bed than agglomerates formed from the lighter particles (H.G. beads). This was probably the case, as the increase in injected solids` density led to an increase in the mass of agglomerates by 4.7%. Also, it is important to note that despite the volume concentration of the H.G. beads being higher than the volume concentration of the S.G. beads, the S.G. beads are more stable and have a higher amount of liquid trapped.

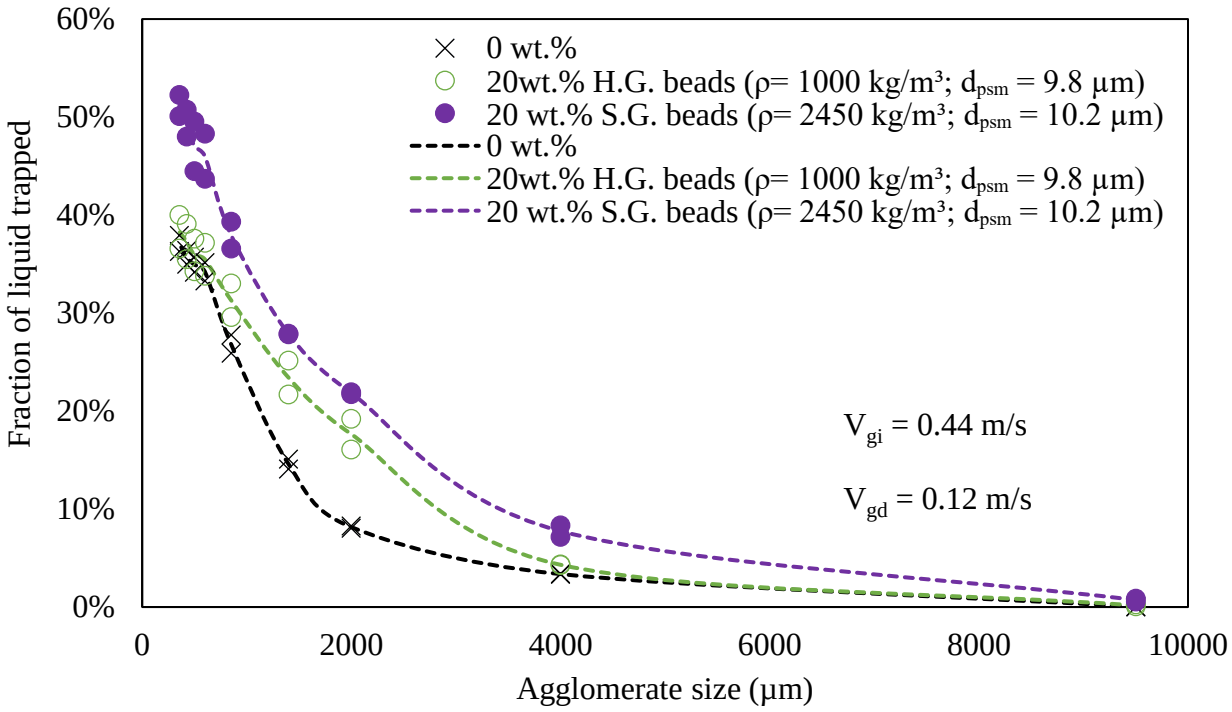

Figure 5.4: Effect of changing slurry particles density on slurry impact on agglomerate formation and breakup

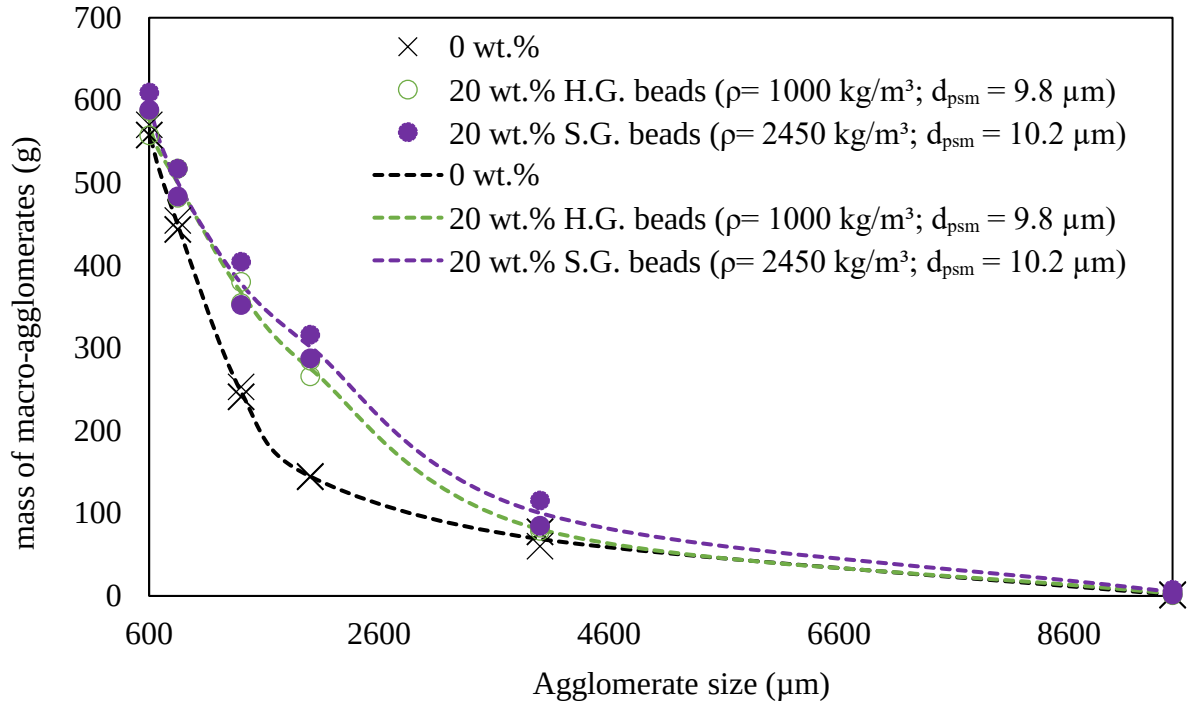

Figure 5.5: Effect of slurry particles density on the mass of macro-agglomerates

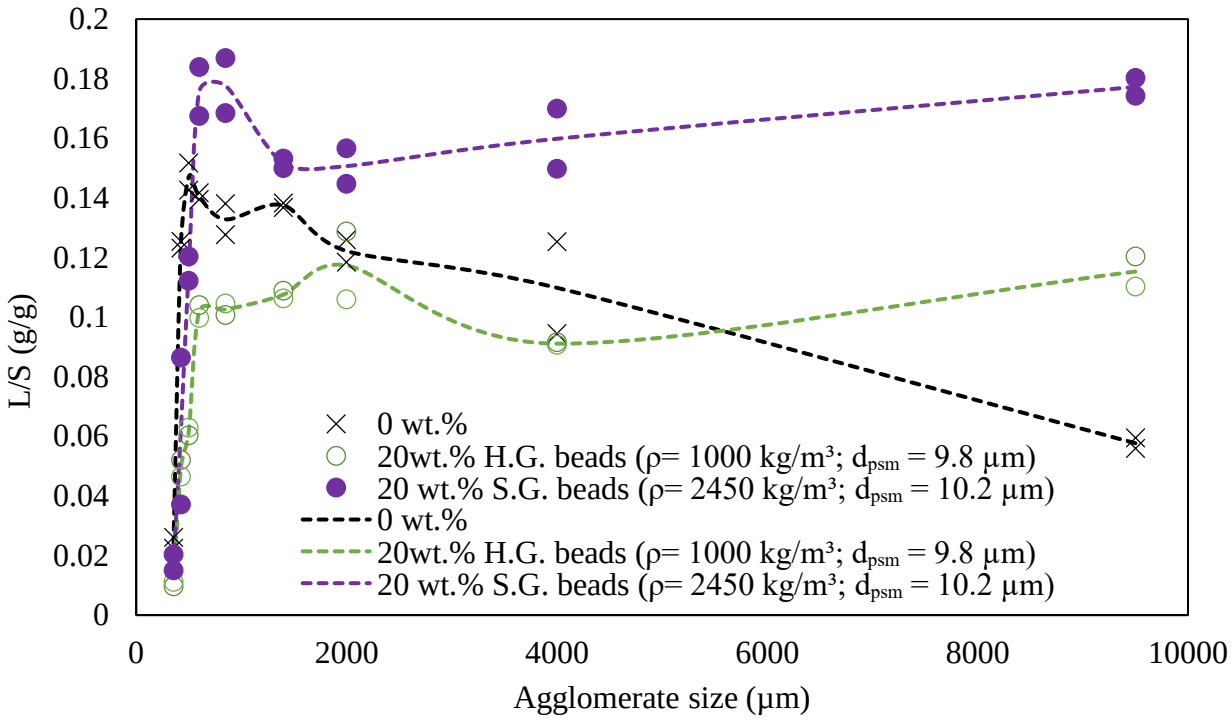

Figure 5.6: L/S ratio vs agglomerate size

5.3.3 Impact of particle shape of injected solids

Figure 5.7 and **Figure** 5.8 show the impact of the particle shape of the injected solids on the fraction of liquid trapped and the mass of macro-agglomerates, respectively. **Figure 5.9** shows the change in L/S ratio with agglomerate size cut. For this study on particle shape, fine sand particles were used as the angular injected particles while the S.G. beads were the round particles. Changing the shape from round to angular resulted in a small increase in the percentage of injected liquid trapped by a factor of 1.12, from 51.3% to 57.5%. There was a small drop in the mass of agglomerates from 628 g to 599 g. There was no significant change in the mass of agglomerates produced or L/S ratio. However, when compared to the base case, both the S.G. beads and sand cases produced significantly more agglomerates, a larger amount of liquid trapped and higher L/S ratios showing again that the presence of the solids does produce a significant effect on agglomerates.

In comparison to previous research, the results obtained from changing particle shape is reasonable as agglomerates made from spherical particles are less stable than agglomerates from angular particles, as a lower compressive force is required to crush the former (Weber 2009). Hemati et al. (2003) showed that sand particles resulted in faster agglomerate growth than spherical glass beads. Also, spherical particles tend to form weaker liquid bridges as there is less surface area compared to angular particles, reducing the fraction of liquid trapped.

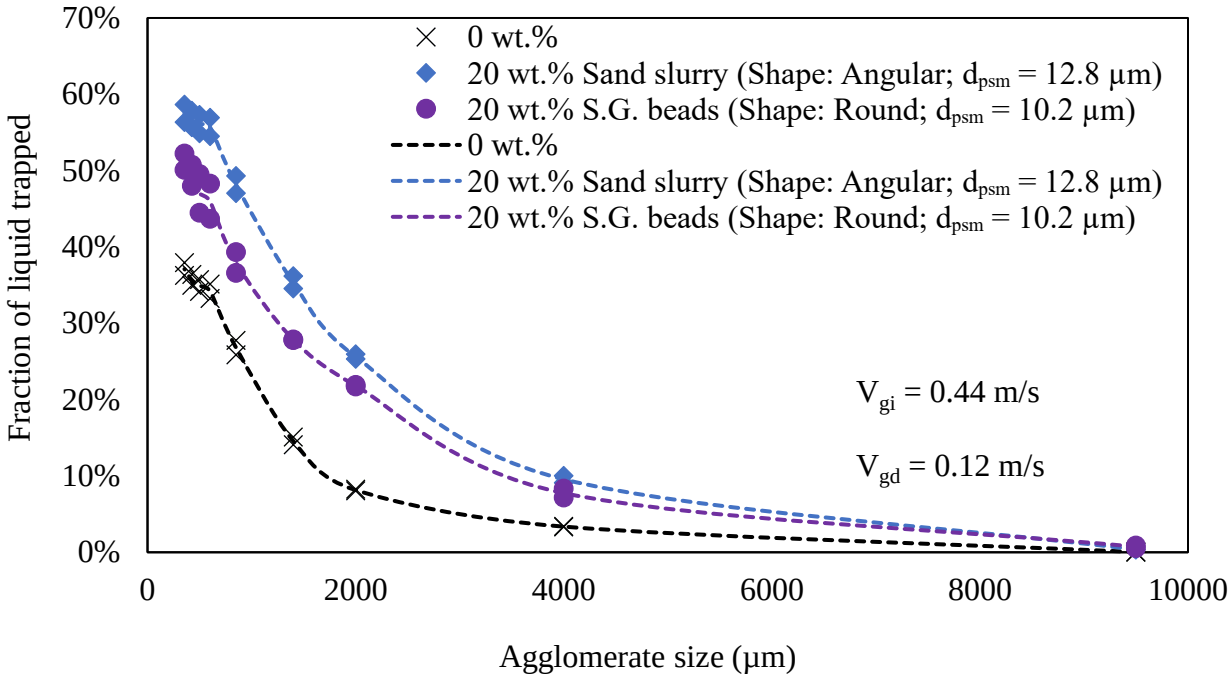

Figure 5.7: Effect of particle shape on the slurry impact on agglomerate formation and break-up

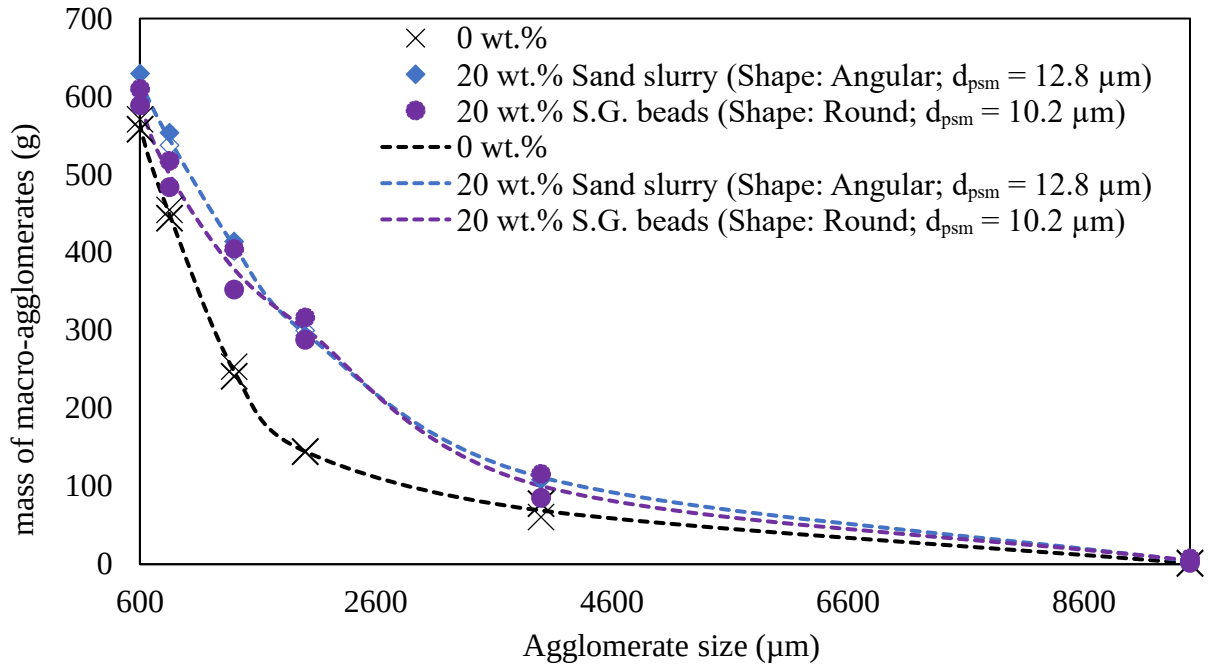

Figure 5.8: Effect of sphericity on slurry impact on the mass of agglomerates

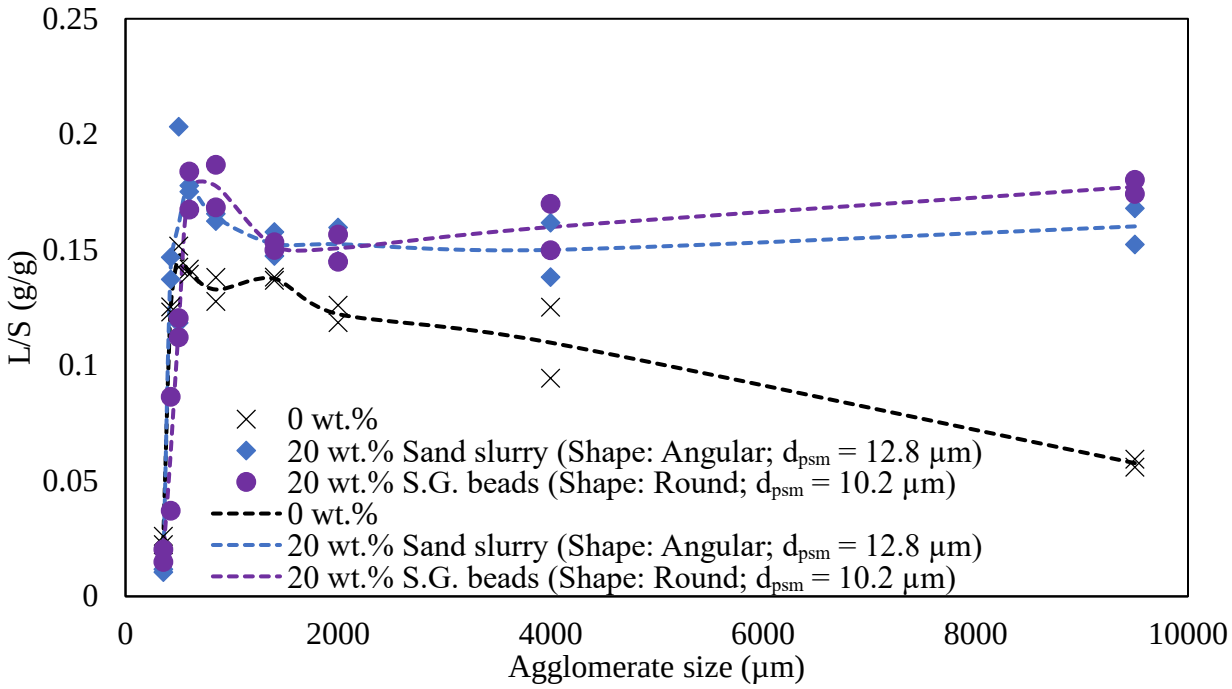

Figure 5.9: L/S ratio showing the effect of sphericity on slurry impact on agglomerate formation and break-up

5.3.4 Impact of wettability of injected solids with water

Figure 5.10 and **Figure** 5.11 show the effect of the injected solids wettability on the fraction of liquid trapped and the mass of macro-agglomerates, respectively. **Figure 5.12** shows the change in L/S ratio with agglomerate size cut. Sand and coke particles were injected separately to investigate the effect of wettability with the gum Arabic solution. Sand is wettable with water while coke is not (Ranji 2014). From **Figure 5.10**, the coke appears to have a reverse effect on liquid trapped when compared with the effect of the sand particles. While the sand particles increase the proportion of the injected liquid that is trapped in agglomerates from 37.1% to 57.5%, coke particles reduce the fraction of liquid trapped to 30.8%. This suggests that the agglomerates are less stable, leading to quicker breakage and hence better distribution of the liquid.

Figure 5.11 shows that the amount of agglomerates formed with the coke particles is less than the amount of agglomerates from the base case and the sand case. The Sauter-mean diameter of the coke macro-agglomerates and sand agglomerates were 1497 microns and 1681, microns respectively. As expected, the coke experiments produced smaller agglomerates than the sand case. These results correspond with previous research showing that agglomerates for non-wettable particles are less stable than agglomerates of wettable particles (Weber 2009). The L/S ratio also shows a trend with the coke having the lowest L/S ratio and the sand case with the highest ratio. It is believed that the water with the injected sand is readily trapped on contact with the fluidized particles; however, with the coke particles, some of the liquid is repelled, causing it spread further into the bed resulting in a lower amount of trapped liquid.

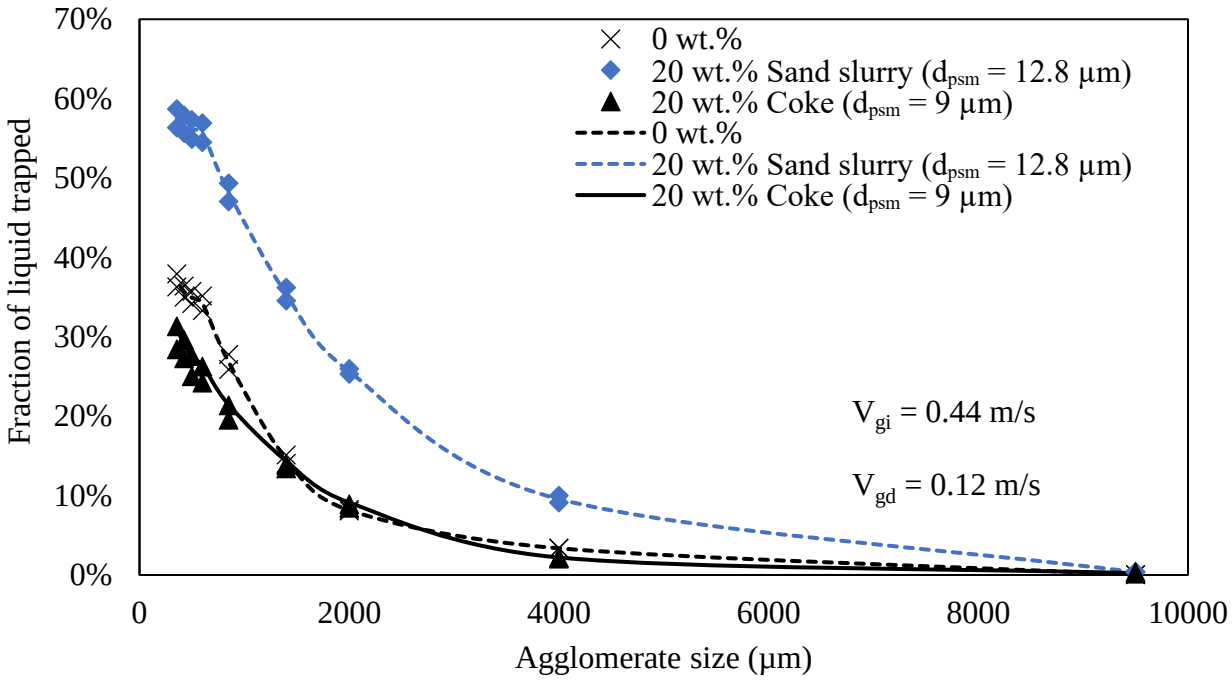

Figure 5.10: Effect of injected solids wettability on the slurry impact on agglomerate formation and break-up

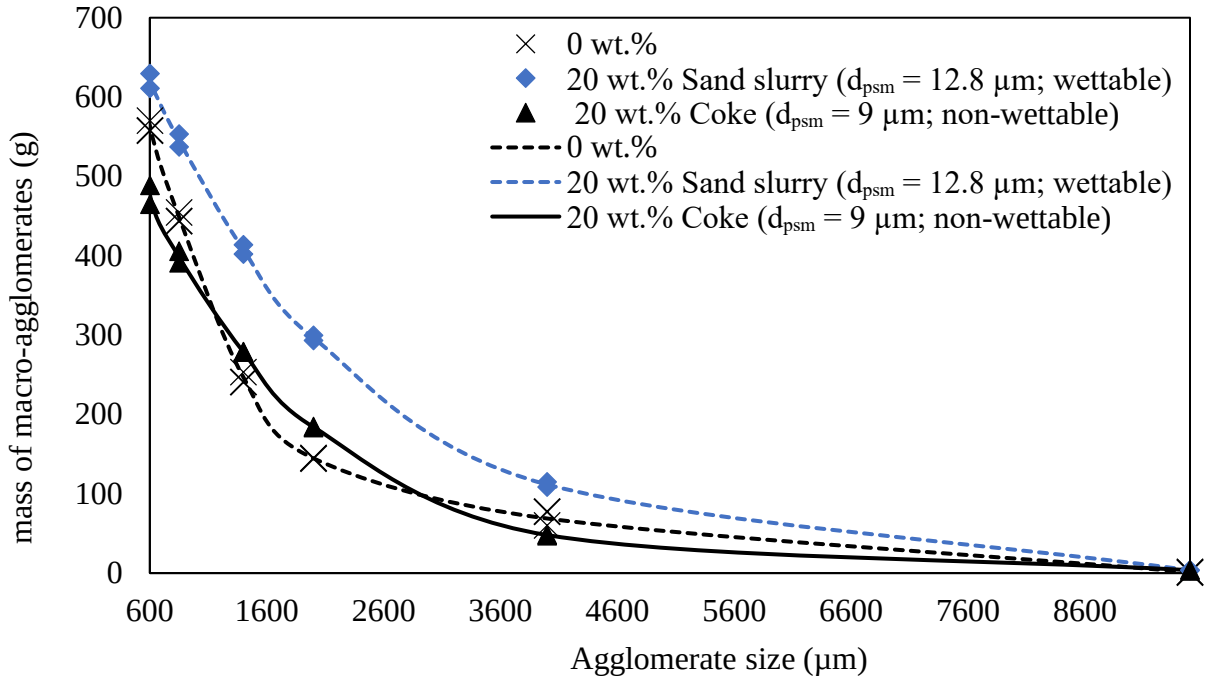

Figure 5.11: Mass of agglomerates vs particle size showing the effect of wettability

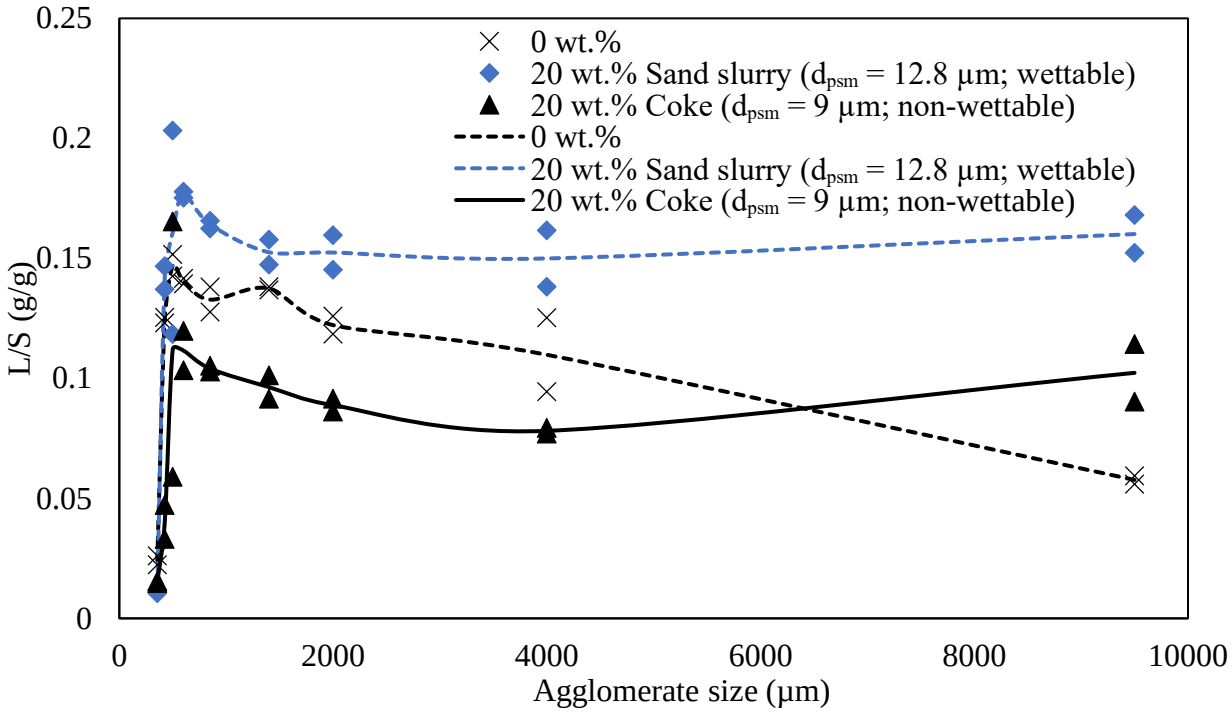

Figure 5.12: Effect of wettability on L/S ratio

5.4 Discussion

Table 5.2 shows a summary of the impact on agglomerates of the different particle properties that were investigated in this study. From chapter 4, the three most likely factors that could account for the impact of injected particles on agglomeration were the change in viscosity, drying kinetics and ability of the solids to provide a filler effect within the agglomerates. In this discussion, the results of chapter 5 are used to identify which of these factors likely dominate.

Table 5.2: Summary of impact from different particle properties

Change in particle properties of injected solids	Percentage change when varying (%):			
	total liquid trapped	total mass of macro-agglomerates	Average L/S ratio	Sauter-mean diameter (d_{psm}) of macro-agglomerates
Changing particle size of from 9.8 to 61 µm	3.7	-18.8	24.7	- 4.5
Changing density from 1000 to 2450 kg/m^3	33.6	4.7	57.0	4.2
Sphericity: angular to round particles	-12.1	-3.4	-6.4	0.6
Wettability: wettable (sand) to non-wettable (coke) with water	-46.3	-23.1	-41.0	-10.9

5.4.1 Effective viscosity

From chapter 4, increasing the effective viscosity may provide an explanation for the effect of the solids on the agglomerates. The effective viscosity of the slurry is dependent on the volume fraction of the solids. The hollow glass (H.G.) beads have a lower density than the solid glass (S.G.) beads, therefore the former would have a higher volume fraction for the same weight fraction of slurry. Going from S.G. beads to H.G. beads changes the solids volume fraction in the slurry from 8.62 vol.% to 20 vol.%, increasing the effective viscosity of the slurry from 3.96 cP to 5.94 cP. The effective viscosities were estimated using **equation 2-3** from chapter 2. As previously discussed in chapter 4.3.4.3, an increase effective viscosity is expected to result in an increase in both the fraction of liquid trapped and mass of agglomerates. However, that is not case here, from **Table 5.2**, the fraction of liquid trapped drops by 33.6% and the mass of agglomerates drops by 4.7% when going from S.G. beads to H.G. beads. Hence, the effective viscosity can be ruled out as a predominant factor for the effect of the injected particles on agglomerates.

5.4.2 Drying kinetics

As seen in chapter 4.3.4.2, the drying kinetics affect the amount of liquid trapped within the agglomerates may be affected by the solids' thermal conductivity, heat capacity, and mass of water to be evaporated. There was no direct comparison to isolate the effect of drying kinetics however, the S.G. and H.G. beads can be used to determine whether the drying kinetics were accountable for the impact produced by the injected solids. Focusing again on the comparison of S.G. and H.G. beads, the effects produced are vastly different. The heat required for liquid vaporization is the same in both cases, since both slurries

contained the same mass of liquid. Both glass beads are expected to have comparable heat capacities, and thus similar drying kinetics. Since they not produce the same results but rather a 33.6% difference in the amount of liquid trapped, the drying kinetics cannot fully account for the impact produced by the solids on liquid trapped and agglomerate stability.

5.4.3 The Filler Effect

In the polymer and construction industry, the use of fillers is useful in making stronger composites and concrete respectively (Ahmad et al. 2008, Soroka and Setter 1977). To optimize the effect of the fillers on the eventual composite, a few factors must be considered such as: size, shape, wettability, and weight/volume fractions of the filler particles. These particle properties have been varied in the experiments to verify whether the injected solids provide a filler effect within the agglomerates.

The effect of changing particle size was studied by using spherical hollow glass beads (H.G. beads) with Sauter-mean diameters of 9.8 μm and 61 μm. In polymer fillers research, studies have been done to understand the effect of filler particle size on the strength of composites and bed particle size on the strength of agglomerates. In making epoxy resins, particle sizes greater than 10 μm are usually avoided as fillers because increasing the particle size of fillers will begin to reduce the mechanical strength of the composite (Ahmad et al. 2008). Bray et al. (2013) used silica nanoparticles with particle sizes 23 nm, 74 nm and 170 nm and found no significant difference for filler particle size much smaller than in our study. However, Ahmad et al. (2008) showed that increasing the particle size of the fillers from 2.18 μm to 10.31 μm reduces tensile strength and the

durability of the composite. Larger particle sizes result in weaker packing structure, leading to weaker composites. From **Table 5.2**, while there is a negligible change in the amount of liquid trapped when the particle size is increased (3.7%), the mass of the macro-agglomerates drops by 18.8%, which is in line with the behavior of fillers in composites.

A variety of research has been conducted on the effect of shape on the formation of agglomerates. The injected particles considered were either round (solid glass beads) or angular (sand). Iveson and Page (2005) showed that irregular-shaped could not be easily compressed to the same extent as spherical particles. Non-spherical powders also produced much stronger pellets as the inter-particle friction and interlocking is more prominent. Ahmad et al. (2008) found that addition of particulate fillers increased the tensile and flexural strength of polymer composites; however, the shape and aspect ratio of the fillers plays a role in determining the strength of the final composite. As reported by Ahmad et al. (2008), anisometric particles are more effective to be used as composite reinforcements, as they provide more contact area than isometric particles. Since spherical particles (S.G. beads) are isometric with an aspect ratio of 1, the literature studies suggest that they are more likely to produce fewer durable agglomerates than the angular sand particles. From **Table 5.2**, using spherical particles instead of angular sand particles resulted in slightly less liquid trapped (12.1%), and the amount of macro-agglomerates reduced slightly (3.4%), but did not affect the L/S ratio of the agglomerates. Changing the particle shape thus mainly affected the strength of the agglomerates and the reduced amount of liquid trapped is due to the smaller amount of agglomerates. This is in

line with the observations made concerning the effect of particle shape on fillers in composites.

From **Table 5.2**, changing the wettability of the injected solids results in a 46.3% change in the amount of liquid trapped and a 23% change in the mass of agglomerates. It appears that the coke particles inhibit the trapping of liquid in the agglomerates resulting in final agglomerates trapping less liquid. This is in line with research done on fillers that show that decreasing the wettability (i.e., increasing the contact angle) of a filler reduces the amount of water the composite can absorb (Gwon et al. 2010).

For most studies, the density of the filler is usually kept constant, as a result, increasing the weight fraction results in a corresponding increasing volume fraction. In this study, the effect of increasing weight fraction and volume fraction were separated and studied differently. Studies on increasing the concentration of fillers in concrete and composites have had varying results (Adams 1993, Urabe et al. 1999, Bleach et al. 2002). Further research shows that the tensile strength of composites actually increases initially with increasing filler concentration until a critical concentration is reached and then it begins to drop (Moosberg-Bustnes et al. 2004), (Fennis et al. 2013), (Fu et al. 2008). This study demonstrated that adding slurry solids generally resulted in bigger and stronger agglomerates. The presence of the solids leads to an increase in liquid trapped from 37% to 57.5%, which is in line with previous research that show a positive correlation with increasing the concentration of fillers in concrete (Moosberg-Bustnes et al. 2004) and composites (Tajvidi and Ebrahimi 2003), (Khalil et al. 2006). When the volume concentration is increased from 8.62 vol.% to 20 vol.%, the amount of liquid trapped drops by 33.6%. This is because for the same mass of injected particles, there are more

than twice the number of individual particles within an agglomerate. As a result, the particles fill in-between the pores that would have been filled with the trapped liquid. With the S.G. beads (8.62 vol.%), the agglomerate pore volume is bigger enabling it to trap more liquid than the less dense H.G. beads (20 vol.%).

Based on the data analysis and discussion, the major mechanism that accounts for the impact of the slurry on the agglomerates is the filler effect of the particles on the agglomerate structure. The results obtained earlier in this chapter ruled out the effect of viscosity changes. The impact of drying kinetics was not able to provide a substantial explanation for the effect of the solids on agglomeration. The filler effect mechanism satisfied the results obtained justifying that the presence of the solids as a filler is responsible for the impact on agglomeration. Thus, the impact produced by the solids is a filler effect within the agglomerates as they not only strengthen the agglomerate but enable it to trap more of the injected liquid.

Chapter 6

6 Conclusions and Recommendations

6.1 Conclusions

The addition of solids in a sprayed liquid from a TEB spray nozzle had no significant observable effect on the spray characteristics, such as length, angle and stability. For the same upstream pressure, the mass flowrate of injected liquid was reduced for a liquid-solid slurry.

When liquid was sprayed into a fluidized bed of sand particles, the addition of solids in the sprayed liquid modified the resulting liquid-particle agglomerate characteristics. It impacted the amount of liquid trapped in the agglomerates and agglomerate stability. Increasing the superficial velocity during injection led to a significant drop in the amount of liquid trapped in agglomerates for both pure gum Arabic and slurry cases. However, increasing the superficial velocity during drying, after the liquid injection, only had a significant effect on the pure case but a negligible impact on the slurry cases. This showed that with 20 wt.% of solids in the injected slurry, the agglomerates were more stable than the pure gum Arabic case. The addition of the solids resulted in wetter, bigger and stronger agglomerates.

Different mechanisms were proposed to explain the change in agglomeration behavior when particles were added to the spray: increased viscosity, spray characteristics, drying kinetics and the solids filler effect. Since there was no effect of the solids on spray properties, a change in spray characteristics was removed as a possible explanation. Experiments that varied the injected solids properties also ruled out the effect of changing

viscosity and drying kinetics. The main contributor to the observed increased agglomeration when adding solids to the liquid spray was thus identified as the filler effect, where fines act as fillers within the agglomerate and increase the agglomerates strength and hence, the mass of liquid trapped.

6.2 Recommendations

- Given that most of the recycled coke particles come from the cyclones, it is essential that the cyclones be properly maintained to minimize the mass of the recycled solids in the injection feed. Also, it can be ensured that the bitumen feed from upstream processes contains a minimal amount of wettable solids to maintain the process efficiency. The introduction of non-wettable solids in the reactor feed should be considered as it could reduce the agglomerate stability.
- Experiments can be conducted by intentionally creating agglomerates containing fines to test the stability of the agglomerates and their ability to trap liquid.
- The fluidized bed experiments conducted in this research were done at 2 wt.% GLR and a liquid flux representative of current industrial practice. Further experiments could be done at different GLRs and spray fluxes to understand the effect of the injected fines over a wider range of conditions.

References

Adams, JM Clay Minerals. 1993. "Particle size and shape effects in materials science: examples from polymer and paper systems." 28 (4):509-530.

Agrawal, Rajesh, and Yadav Naveen. 2011. "Pharmaceutical processing–A review on wet granulation technology." *International journal of pharmaceutical frontier research* 1 (1):65-83.

Ahmad, Farrah Noor, Mariatti Jaafar, Samayamutthirian Palaniandy, and Khairun Azizi Mohd Azizli. 2008. "Effect of particle shape of silica mineral on the properties of epoxy composites." *Composites Science and Technology* 68 (2):346-353. doi: https://doi.org/10.1016/j.compscitech.2007.07.015.

Albion, Katherine J, Lauren Briens, Cedric Briens, and Franco Berruti. 2011. "Multiphase flow measurement techniques for slurry transport." *International Journal of Chemical Reactor Engineering* 9 (1).

Aman, Sergej, Jürgen Tomas, and Haim Kalman. 2010. "Breakage probability of irregularly shaped particles." *Chemical Engineering Science* 65 (5):1503-1512. doi: https://doi.org/10.1016/j.ces.2009.10.016.

Anoop, K. B., S. Kabelac, T. Sundararajan, and Sarit K. Das. 2009. "Rheological and flow characteristics of nanofluids: Influence of electroviscous effects and particle agglomeration." *Journal of Applied Physics* 106 (3):034909. doi: 10.1063/1.3182807.

Antonyuk, Sergiy, Jürgen Tomas, Stefan Heinrich, and Lothar Mörl. 2005. "Breakage behaviour of spherical granulates by compression." *Chemical Engineering Science* 60 (14):4031-4044. doi: https://doi.org/10.1016/j.ces.2005.02.038.

Ariyapadi, Sivakumar. 2004. "Interaction between Horizontal Gas-Liquid Jets and." The University of Western Ontario London.

B.J., Wright, Zevchak S.E., Wright J.M., and Drake M.A. 2009. "The Impact of Agglomeration and Storage on Flavor and Flavor Stability of Whey Protein Concentrate 80% and Whey Protein Isolate." *Journal of Food Science* 74 (1):S17-S29. doi: doi:10.1111/j.1750-3841.2008.00975.x.

Batchelor, George Keith. 2000. *An introduction to fluid dynamics*: Cambridge university press.

Benali, M., V. Gerbaud, and M. Hemati. 2009. "Effect of operating conditions and physico–chemical properties on the wet granulation kinetics in high shear mixer." *Powder Technology* 190 (1-2):160-169. doi: 10.1016/j.powtec.2008.04.082.

Berruti, Franco, Matthew Dawe, and Cedric Briens. 2009. "Study of gas–liquid jet boundaries in a gas–solid fluidized bed." *Powder Technology* 192 (3):250-259. doi: 10.1016/j.powtec.2009.01.005.

Bi, Weidong, William C. McCaffrey, and Murray R. Gray. 2007. "Agglomeration and Deposition of Coke during Cracking of Petroleum Vacuum Residue." *Energy & Fuels* 21 (3):1205-1211.

Bleach, N. C., S. N. Nazhat, K. E. Tanner, M. Kellomäki, and P. Törmälä. 2002. "Effect of filler content on mechanical and dynamic mechanical properties of particulate biphasic calcium phosphate—polylactide composites." *Biomaterials* 23 (7):1579-1585. doi: https://doi.org/10.1016/S0142-9612(01)00283-6.

Boyle, John F, Ica Manas-Zloczower, and Donald L Feke. 2005. "Hydrodynamic analysis of the mechanisms of agglomerate dispersion." *Powder Technology* 153 (2):127-133.

Bray, D. J., P. Dittanet, F. J. Guild, A. J. Kinloch, K. Masania, R. A. Pearson, and A. C. Taylor. 2013. "The modelling of the toughening of epoxy polymers via silica nanoparticles: The effects of volume fraction and particle size." *Polymer* 54 (26):7022-7032. doi: https://doi.org/10.1016/j.polymer.2013.10.034.

Briens, Lauren, Garret Book, Katherine Albion, Cedric Briens, and Franco Berruti. 2011. "Evaluation of the spray stability on liquid injection in gas–solid fluidized beds by passive vibrometric methods." 89 (5):1217-1227. doi: doi:10.1002/cjce.20482.

Bruhns, Stefan, and Joachim Werther AIChE Journal. 2005. "An investigation of the mechanism of liquid injection into fluidized beds." 51 (3):766-775.

Chang, SL, SA Lottes, CQ Zhou, BJ Bowman, and M Petrick Journal of heat transfer. 2001. "Numerical study of spray injection effects on the heat transfer and product yields of FCC riser reactors." 123 (3):544-555.

Chen, Ye-Mon. 2006. "Recent advances in FCC technology." *Powder Technology* 163 (1):2-8. doi: https://doi.org/10.1016/j.powtec.2006.01.001.

Chen, Yung-Chih, Hsueh-Chen Lin, and Yu-Der Lee Journal of polymer research. 2003. "The effects of filler content and size on the properties of PTFE/SiO 2 composites." 10 (4):247-258.

Darabi, Pirooz, Konstantin Pougatch, Martha Salcudean, and Dana Grecov. 2010. Agglomeration of Bitumen-Coated Coke Particles in Fluid Cokers. In *International Journal of Chemical Reactor Engineering*.

Dewettinck, K., and A. Huyghebaert. 1999. "Fluidized bed coating in food technology." *Trends in Food Science & Technology* 10 (4):163-168. doi: https://doi.org/10.1016/S0924-2244(99)00041-2.

Dhanalakshmi, K., S. Ghosal, and S. Bhattacharya. 2011. "Agglomeration of Food Powder and Applications." *Critical Reviews in Food Science and Nutrition* 51 (5):432-441.

Dittanet, Peerapan, and Raymond A. Pearson. 2012. "Effect of silica nanoparticle size on toughening mechanisms of filled epoxy." *Polymer* 53 (9):1890-1905. doi: https://doi.org/10.1016/j.polymer.2012.02.052.

Dunlop, DD, LI Griffin, and JF Moser Chemical Engineering Progress. 1958. "Particle size control in fluid coking." 54 (8):39-43.

Ennis, Bryan J, Gabriel Tardos, and Robert Pfeffer. 1991. "A microlevel-based characterization of granulation phenomena." *Powder Technology* 65 (1-3):257-272.

Farkhondehkavaki, Masoumeh. 2012. "Developing Novel Methods to characterize Liquid Dispersion in a Fluidized bed."

Fennis, SAAM, JC Walraven, and JA Den Uijl Materials and structures. 2013. "Compaction-interaction packing model: regarding the effect of fillers in concrete mixture design." 46 (3):463-478.

Fu, Shao-Yun, Xi-Qiao Feng, Bernd Lauke, and Yiu-Wing Mai. 2008. "Effects of particle size, particle/matrix interface adhesion and particle loading on mechanical properties of particulate–polymer composites." *Composites Part B: Engineering* 39 (6):933-961. doi: https://doi.org/10.1016/j.compositesb.2008.01.002.

Ghosal, Sudeep, T. N. Indira, and Suvendu Bhattacharya. 2010. "Agglomeration of a model food powder: Effect of maltodextrin and gum Arabic dispersions on flow behavior and compacted mass." *Journal of Food Engineering* 96 (2):222-228. doi: https://doi.org/10.1016/j.jfoodeng.2009.07.016.

Gray, Murray R. 2002. "Fundamentals of bitumen coking processes analogous to granulations: A critical review." *The Canadian Journal of Chemical Engineering* 80 (3):393-401.

Gray, Murray R. 2015. *Upgrading oilsands bitumen and heavy oil*: University of Alberta.

Gwon, Jae Gyoung, Sun Young Lee, Sang Jin Chun, Geum Hyun Doh, and Jung Hyeun Kim. 2010. "Effects of chemical treatments of hybrid fillers on the physical and thermal properties of wood plastic composites." *Composites Part A: Applied Science and Manufacturing* 41 (10):1491-1497. doi: https://doi.org/10.1016/j.compositesa.2010.06.011.

He, Huan, Luc Courard, and Eric Pirard. 2012. "Particle packing density and limestone fillers for more sustainable cement." Key Engineering Materials.

Hemati, MRKV, R Cherif, K Saleh, and V Pont. 2003. "Fluidized bed coating and granulation: influence of process-related variables and physicochemical properties on the growth kinetics." *Powder Technology* 130 (1):18-34.

Hesketh, Robert P, C Stewart Slater, Stephanie Farrell, and Michael Carney. 2002. "Fluidized bed polymer coating experiment." *Chemical Engineering Education* 36 (2):138-143.

House, Peter. 2008. *Interaction of gas-liquid jets with gas-solid fluidized beds: Effect on liquid-solid contact and impact on fluid coker operation*. Vol. 69.

Hulet, Craig, Cedric Briens, Franco Berruti, Edward W Chan, and Siva Ariyapadi. 2003. "Entrainment and stability of a horizontal gas-liquid jet in a fluidized bed." *International Journal of Chemical Reactor Engineering* 1 (1).

Iveson, S. M., and N. W. Page. 2001. "Tensile bond strength development between liquid-bound pellets during compression." *Powder Technology* 117 (1-2):113-122. doi: Doi 10.1016/S0032-5910(01)00319-9.

Iveson, Simon M., James D. Litster, Karen Hapgood, and Bryan J. Ennis. 2001. "Nucleation, growth and breakage phenomena in agitated wet granulation processes: a review." *Powder Technology* 117 (1):3-39. doi: https://doi.org/10.1016/S0032-5910(01)00313-8.

Iveson, Simon M., and Neil W. Page. 2005. "Dynamic strength of liquid-bound granular materials: The effect of particle size and shape." *Powder Technology* 152 (1):79-89. doi: https://doi.org/10.1016/j.powtec.2005.01.020.

Jankovic, Jasna. 2005. "Simulation of the Scrubber Section of a Fluid Coker." University of British Columbia.

Khalil, HPSA, SB Sharifah Shahnaz, MM Ratnam, Faiz Ahmad, and NA Nik Fuaad Journal of reinforced plastics and composites. 2006. "Recycle polypropylene (RPP)-wood saw dust (WSD) composites-Part 1: the effect of different filler size and filler loading on mechanical and water absorption properties." 25 (12):1291-1303.

Knapper, Brian A, Murray R Gray, Edward W Chan, and Randy Mikula. 2003. "Measurement of efficiency of distribution of liquid feed in a gas-solid fluidized bed reactor." *International Journal of Chemical Reactor Engineering* 1 (1).

Leach, Aidan, Federica Portoghese, Cedric Briens, and Franco Berruti. 2008. "A new and rapid method for the evaluation of the liquid–solid contact resulting from liquid injection into a fluidized bed." *Powder Technology* 184 (1):44-51. doi: https://doi.org/10.1016/j.powtec.2007.07.037.

Leach, Aidan, Rana Sabouni, Franco Berruti, and Cedric Briens. 2013. "Use of pulsations to enhance the distribution of liquid injected into fluidized particles with commercial-scale nozzles." 59 (3):719-728. doi: doi:10.1002/aic.13872.

Li, Lingchao. 2016. "Effect of Local Bed Hydrodynamics on the Distribution of Liquid in a Fluidized Bed."

Lin, Chiou-Liang, Tzu-Huan Peng, and Wei-Jen Wang. 2011. "Effect of particle size distribution on agglomeration/defluidization during fluidized bed combustion." *Powder Technology* 207 (1):290-295. doi: https://doi.org/10.1016/j.powtec.2010.11.010.

McDonald, James, and CO Rhys. 1959. "28. The Fluid Coking Process–Commercial Experience to Date." 5th World Petroleum Congress.

McDougall, S., M. Saberian, C. Briens, F. Berruti, and E. Chan. 2005. "Effect of liquid properties on the agglomerating tendency of a wet gas–solid fluidized bed." *Powder Technology* 149 (2-3):61-67. doi: 10.1016/j.powtec.2004.09.043.

McDougall, Steven L, Mohammad Saberian, Cedric Briens, Franco Berruti, and Edward W Chan. 2004. "Characterization of fluidization quality in fluidized beds of wet particles." *International Journal of Chemical Reactor Engineering* 2 (1).

Mirgain, Cyrille, Cedric Briens, Mariano Del Pozo, Roben Loutaty, and Maurice Bergougnou. 2000. "Modeling of Feed Vaporization in Fluid Catalytic Cracking." *Industrial & Engineering Chemistry Research* 39 (11):4392-4399. doi: 10.1021/ie000074j.

Mooney, M. 1951. "The viscosity of a concentrated suspension of spherical particles." *Journal of Colloid Science* 6 (2):162-170. doi: https://doi.org/10.1016/0095-8522(51)90036-0.

Moosberg-Bustnes, Helena, Björn Lagerblad, and Eric Forssberg Materials and Structures. 2004. "The function of fillers in concrete." 37 (2):74.

Nares, Hector Ruben, Persi Schachat, Marco Antonio Ramirez-Garnica, Maria Cabrera, and Luz Noe-Valencia. 2007. "Heavy-crude-oil upgrading with transition metals." Latin American & caribbean petroleum engineering conference.

nrcan. 2016. Oil Sands: Economic Contributions. In *Natural Resources Canada*.

Palzer, St. 2011. "Agglomeration of pharmaceutical, detergent, chemical and food powders — Similarities and differences of materials and processes." *Powder Technology* 206 (1):2-17. doi: https://doi.org/10.1016/j.powtec.2010.05.006.

Pardo Reyes, Liliana Andrea. 2015. "Effect of Temperature and Successive Sprays on Liquid Distribution in Fluidized Beds."

Parikh, D.M. 2005. *Handbook of Pharmaceutical Granulation Technology, Second Edition*: Taylor & Francis.

Parveen, Flora, Franco Berruti, Cedric Briens, and Jennifer McMillan. 2013. "Effect of fluidized bed particle properties and agglomerate shape on the stability of agglomerates in a fluidized bed." *Powder Technology* 237:46-52. doi: https://doi.org/10.1016/j.powtec.2012.12.057.

Paul Kamienski, Craig Mcknight, Glen Phillips, Boyd Rumball. 2009. "Upgrading Oil Sands Bitumen with FLUID COKING and FLEXICOKING Technologies." 5th NCUT Upgrading and Refining Conference, Edmonton, Alberta, Canada.

Pietsch, Wolfgang B. 2008. *Agglomeration processes: phenomena, technologies, equipment*: John Wiley & Sons.

Portoghese, Federica. 2007. *Interactions between gas-liquid jets and gas-solid fluidized beds*. Vol. 69.

Ranji, M Mohagheghi Dar. 2014. "Impact of Local Bed Hydrodynamics on Jet-Bed Interaction." Doctoral Thesis, University of Western Ontario, London, ON.

Rondeau, X, C Affolter, L Komunjer, D Clausse, and P Guigon. 2003. "Experimental determination of capillary forces by crushing strength measurements." *Powder technology* 130 (1):124-131.

Sabouni, Rana, Aidan Leach, Cedric Briens, and Franco Berruti. 2011. "Enhancement of the liquid feed distribution in gas-solid fluidized beds by nozzle pulsations (induced by solenoid valve)." *AIChE Journal* 57 (12):3344-3350.

Sanchez Careaga, Francisco J. 2013. "Hydrodynamics in Recirculating Fluidized Bed Mimicking the Stripper Section of the Fluid Coker."

Schuchmann, Harald. 1995. "Production of instant foods by jet agglomeration." *Food Control* 6 (2):95-100. doi: https://doi.org/10.1016/0956-7135(95)98912-K.

Schæfer, Torben. 2001. "Growth mechanisms in melt agglomeration in high shear mixers." *Powder Technology* 117 (1):68-82. doi: https://doi.org/10.1016/S0032-5910(01)00315-1.

Simons, S. J. R. 1996. "Modelling of agglomerating systems: from spheres to fractals." *Powder Technology* 87 (1):29-41. doi: https://doi.org/10.1016/0032-5910(95)03078-6.

Soroka, I., and N. Setter. 1977. "The effect of fillers on strength of cement mortars." *Cement and Concrete Research* 7 (4):449-456. doi: https://doi.org/10.1016/0008-8846(77)90073-4.

Stanlick, Clayton. 2014. "Effects of Mixing and Vapor Residence Time on the Thermal Cracking Performance of Fluidized Beds."

Subudhi, Nirmalkumar. 2006. "Simulation of pressure drop and coke deposition in the grid of a scrubber." University of British Columbia.

Tafreshi, Z. M., D. Kirpalani, A. Bennett, and T. W. McCracken. 2002. "Improving the efficiency of fluid cokers by altering two-phase feed characteristics." *Powder Technology* 125 (2-3):234-241. doi: 10.1016/S0032-5910(01)00511-3.

Taitel, Yemada, and A. E. Dukler. 1976. "A model for predicting flow regime transitions in horizontal and near horizontal gas-liquid flow." *AIChE Journal* 22 (1):47-55. doi: doi:10.1002/aic.690220105.

Tajvidi, Mehdi, and Ghanbar Ebrahimi. 2003. "Water uptake and mechanical characteristics of natural filler–polypropylene composites." 88 (4):941-946. doi: doi:10.1002/app.12029.

Thomas, David G. 1965. "Transport characteristics of suspension: VIII. A note on the viscosity of Newtonian suspensions of uniform spherical particles." *Journal of Colloid Science* 20 (3):267-277. doi: https://doi.org/10.1016/0095-8522(65)90016-4.

Urabe, H, Y Nomura, K Shirai, M Yoshioka, and H Shintani Journal of Materials Science: Materials in Medicine Shintani. 1999. "Effect of filler content and size to properties of composite resins on microwave curing." 10 (6):375-378.

Vervaet, Chris, and Jean Paul Remon. 2005. "Continuous granulation in the pharmaceutical industry." *Chemical Engineering Science* 60 (14):3949-3957. doi: https://doi.org/10.1016/j.ces.2005.02.028.

VIBEKE, ANDERSSON, and GUDMUNDSSON JÓN STEINAR. 2000. "Flow Properties of Hydrate-in-Water Slurries." *Annals of the New York Academy of Sciences* 912 (1):322-329. doi: doi:10.1111/j.1749-6632.2000.tb06786.x.

Wang, Wuchang, Yuxing Li, Haihong Liu, and Pengfei Zhao. 2015. "Study of agglomeration characteristics of hydrate particles in oil/gas pipelines." *Advances in Mechanical Engineering* 7 (1):457050.

Wangen, Espen Standal, William C. McCaffrey, Steven Kuznicki, Anne Hoff, and Edd A. Blekkan Topics in Catalysis. 2007. "Cracking of vacuum residue from Athabasca bitumen in a thin film." 45 (1):213-217. doi: 10.1007/s11244-007-0268-x.

Weber, Sarah C. 2009. "Agglomerate stability in fluidized beds."Ph D, School of Graduate and Postdoctoral Studies, University of Western Ontario,

University of Western Ontario (Graduate Program in Engineering Science, Department of Chemical and Biochemical Engineering).

Zhou, Tao, and Hongzhong Li. 1999. "Effects of adding different size particles on fluidization of cohesive particles." *Powder Technology* 102 (3):215-220. doi: https://doi.org/10.1016/S0032-5910(98)00211-3.

Appendix A: Cumulative size distribution of tested solids

Table A. 1: Cumulative size distribution of solids tested in this research

Size (μm)	Percentage (%)				
	Sand	Coke	Solid Glass Beads	Hollow Glass beads (d_{psm} = 9 μm)	Hollow Glass beads (d_{psm} = 61 μm)
4.5	9.7	8.3	0	9.6	1.00
5.5	11.3	11.4	3.7	12.7	1.3
6.5	12.6	15.0	9.7	16.0	1.7
7.5	13.5	22.0	17.2	19.6	2.0
9	14.7	35.8	30.0	25.1	2.6
11	16.1	55.5	47.4	32.5	3.3
13	17.7	73.2	63.7	39.6	4.0
15.5	20.5	89.0	80.4	47.8	4.7
18.5	25.3	97.1	93.8	56.6	5.3
21.5	31.7	97.7	99.9	64.3	5.8
25	40.8	97.7	100	72.2	6.1
30	54.8	97.7	100	81.9	6.6
37.5	74.5	97.7	100	93.0	7.7
45	88.9	97.7	100	99.1	9.2
52.5	96.8	97.7	100	100	11.3
62.5	100	97.7	100	100	15.2
75	100	98.3	100	100	21.6
90	100	99.4	100	100	31.0
105	100	99.9	100	100	41.0
125	100	100	100	100	53.7
150	100	100	100	100	67.5
180	100	100	100	100	80.5
215	100	100	100	100	91.0
255	100	100	100	100	97.6
305	100	100	100	100	100

Curriculum Vitae

Name:	Joshua Idowu
Post-secondary Education and Degrees:	University of Alberta Edmonton, Alberta, Canada 2011-2015, BSc. The University of Western Ontario London, Ontario, Canada 2016-2018, MSc.
Honors and Awards:	University of Western Ontario Graduate Student Scholarship 2017-2018
Related Work Experience	Teaching Assistant University of Western Ontario Sept. 2017 – Dec. 2017